Universitat Autònoma de Barcelona

Glutamatergic vestibular neurons sustain motion-induced autonomic and aversive responses

Pablo Machuca Márquez

Universitat Autònoma de Barcelona

INc Institut de Neurociències

Glutamatergic vestibular neurons sustain motion-induced autonomic and aversive responses

PhD Program in Neuroscience

Supervisors

Dr. Albert Quintana Romero

Dr. Elisenda Sanz Iglesias

Academic tutor

Dr. Juan Hidalgo Pareja

PhD Thesis 2020

Pablo Machuca Márquez

Institut de Neurociències
Facultat de Medicina
Departament de Biologia Cel·lular, Fisiologia i Immunologia
Universitat Autònoma de Barcelona

Glutamatergic vestibular neurons sustain motion-induced autonomic and aversive responses

Pablo Machuca Márquez
2020

Memòria de Tesi Doctoral presentada
per **Pablo Machuca Márquez** per tal d'optar al grau de
Doctor en Neurociències amb Menció Doctor Internacional
per la Universitat Autònoma de Barcelona.

Aquest Projecte Doctoral s'ha dut a terme sota la supervisió
del Doctor **Albert Quintana Romero**, Investigador Principal del
Laboratori de Neuropatologia Mitocondrial,
i de la Doctora **Elisenda Sanz Iglesias**,
investigadora postdoctoral RETOS-JIN.

Director de Tesi	Directora de Tesi	Tutor acadèmic	Doctorand
Dr. Albert Quintana Romero	Dra. Elisenda Sanz Iglesias	Dr. Juan Hidalgo Pareja	Pablo Machuca Márquez

A loh que m'han hecho crecé

Caminante no hay camino,
se hace camino al andar

Antonio Machado
i cançó de Joan Manuel Serrat

This PhD Thesis received funding from the following entities:

- European Research Council (ERC-2014-StG-638106),
- Ministerio de Economía y Competitividad (SAF2014-57981P and SAF2017-88108-R),
- Agència de Gestió d'Ajuts Universitaris i de Recerca (2017SGR-323),
- FENS – Federation of European Neuroscience Societies (NENS Exchange Grant for an international stay at Prof. Carmen Sandi Laboratory – Behavioral Genetics Laboratory, École Polytechnique Fédérale de Lausanne, Lausanne, Switzerland).

CONTENTS

LIST OF ACRONYMS

5-HT	5-hydroxytryptamine (serotonin)
5-HT2A	5-hydroxytryptamine (serotonin) type 2A receptor
5-HT3	5-hydroxytryptamine (serotonin) type 3 receptor
AAV	Adeno-associated viral vectors
AAV1	Anterograde, neurotrophic type 1 adeno-associated viral vector
ACh	Acetylcholine
Adcyap1	Pituitary adenylate cyclase-activating peptide (gene)
Agrp	Agouti-related protein (gene)
AM	Anteromedian nucleus
AP	Antero-posterior
Apo AIV	Apolipoprotein AIV
BNST	Bed nucleus of the stria terminalis
bp	Base pairs
Camk2a	Calcium/calmodulin-dependent protein kinase II alpha (gene)
CAV2	Retrograde canine adenovirus type 2
Cbln1	Cerebellin 1 precursor (gene)
Cbln2	Cerebellin 2 precursor (gene)
Cbln3	Cerebellin 3 precursor (gene)
Cck	Cholecystokinin (gene)
CCK	Cholecystokinin (protein)
CCK-1R	CCK 1 receptor
CeA	Central amygdala
Calca	Calcitonin gene-related peptide (gene)
ChAT	Choline acetyltransferase
ChR2	Channelrhodopsin-2
CNO	Clozapine-N-oxide
Cnp	2',3'-Cyclic-nucleotide 3'-phosphodiesterase (gene)
CNS	Central nervous system
Coch	Cochlin (gene)
CRE	CRE-recombinase (protein)
Cre	CRE-recombinase (gene)
Crh	Corticotropin releasing hormone (gene)
CRH	Corticotropin releasing hormone (protein)
Crhbp	Corticotropin releasing hormone binding protein (gene)
CS	Conditioned stimulus
CsCl	Cesium chloride
CTA	Conditioned taste aversion

DIO	Double floxed inverted open reading frame
DMSO	Dimethyl sulfoxide
DREADDs	Designer Receptors Exclusively Activated by Designer Drugs
DV	Dorso-ventral
DVN	Descending vestibular nucleus
E	Efference
EA	Excitatory aminoacids
Ea	Ex-afference
Ec	Efference-copy
EF1α	Elongation factor 1 alpha
eNpHR3.0	Halorhodopsin 3.0
Floxed	*loxP*-flanked DNA sequence
FMH	α-fluoromethylhistidine
fMRI	functional magnetic resonance imaging
GABA	Gamma-aminobutyric acid
$GABA_BR$	Gamma-aminobutyric acid B receptor
Gad1	Glutamate decarboxylase 1 (gene)
Gad2	Glutamate decarboxylase 2 (gene)
Gal	Galanin and galanin message-associated peptide (GMAP) prepropeptide (gene)
GFAP	Glial fibrillary acidic protein
Gfap	Glial fibrillary acidic protein (gene)
GFP	Green fluorescent protein
GOI	Gene of interest
HA	Hemagglutinin
HBSS	Hanks Balanced Salt Solution
HDC	Histidine decarboxylase
HEK293T	Human embryonic kidney cells 293T
hM3Dq	Human M3 muscarinic receptor-derived DREADDs (Gq-coupled)
hM4Di	Human M4 muscarinic receptor-derived DREADDs (Gi-coupled)
I	Input sample
IHC	Immunohistochemistry
i.p.	Intraperitoneal
IP	Immunoprecipitate
IRES	Internal ribosome entry site
KO	Knock out
KORD	Kappa opioid receptor-derived DREADD
Lc	Lower center (eye muscle)
LiCl	Lithium chloride

LPS	Lipopolysaccharide
LVN	Lateral vestibular nucleus
LVST	Lateral vestibulospinal tract
ML	Medio-lateral
MS	Motion sickness
MVN	Medial vestibular nucleus
MVNmc	Medial vestibular magnocellular nucleus
MVNpc	Medial vestibular parvicellular nucleus
MVST	Medial vestibulospinal tract
NDS	Normal donkey serum
NTS	Solitary Tract nucleus
OF	Open field
PACAP	Pituitary adenylate cyclase-activating peptide
PBel	External lateral part of the parabrachial nucleus
PBN	Parabrachial nucleus
PCR	Polymerase chain reaction
PVN	Paraventricular nucleus of the hypothalamus
Ra	Re-afference
RiboTag	Ribosome tagging
Rpl22	Ribosomal Protein L22 (gene)
RTC	Re-afference–efference combination
SalB	Salvinorin B
scA	Anterior semicircular canal
scL	Lateral semicircular canal
Scn4b	Sodium channel β-subunit 4 (gene)
scP	Posterior semicircular canal
Slc17a6	Vesicular glutamate transporter 2 (gene)
Slc17a7	Vesicular glutamate transporter 1 (gene)
Slc6a5	Chloride-dependent glycine transporter 2 (gene)
SVN	Superior vestibular nucleus
Syn-GFP	Synaptophysin-green fluorescent fusion protein
TTS	Transdermal therapeutic system
US	Unconditioned stimulus
Veh	Vehicle
VGLUT1	Vesicular glutamate transporter 1
***Vglut2*VGLUT2**	Vesicular glutamate transporter 2
VN	Vestibular nuclei
VOR	Vestibulo-ocular reflex
VTA	Ventral tegmental area
WT	Wild-type

ABSTRACT

Motion sickness (MS) is an autonomic physiological alteration occurring in individuals undergoing passive movement. It is currently believed that MS is encoded in the brain as a “toxic shock”, mirroring key aspects of toxic-induced nausea. Consistently, MS is characterized as an unpleasant feeling, accompanied by reduction in spontaneous ambulatory activity, appetite suppression, hypothermia and the establishment of conditioned taste aversion (CTA) –an association between a novel flavor and nausea-related gastrointestinal malaise–. It is widely accepted that MS develops with the occurrence of neural mismatches between the integrated input of motion-related sensory information and correlated past memory. In the brainstem, vestibular nuclei (VN) are classically associated with MS. Provocative motion activates VN neurons, recapitulating MS-related signs. However, the genetic identity of VN neurons mediating MS-related autonomic regulation and aversive learning, and their MS-relevant downstream projections remain largely unknown. In this PhD Thesis, we find that targeted inhibition of glutamatergic vestibular ($VGLUT2^{VN}$) neurons during provocative motion prevents MS-like autonomic alterations and CTA response, revealing that *Vglut2*-VN neurons are necessary for MS establishment. Moreover, through cell type-specific neuronal tracing and optogenetic approaches, we identify a cholecystokinin-expressing, glutamatergic VN (CCK^{VN}) subpopulation that projects to the parabrachial nucleus (PBN), dissecting a functionally-relevant circuit selectively controlling MS-related CTA. Together, these findings provide ground-breaking insights into MS neurobiological regulation, untangling key genetically-defined neural substrates and a vestibulo-parabrachial circuit.

1. INTRODUCTION

1.1. Motion sickness

Motion sickness (MS) is an unpleasant autonomic physiological alteration that occurs in healthy individuals undergoing passive or even illusory motion (Bertolini & Straumann, 2016). MS signs include pallor, cold sweating, yawning, retching and vomiting, among others, while referred MS symptoms include headache, increased salivation, stomach awareness or discomfort, dizziness or vertigo, a warmth sensation, anorexia, drowsiness and even pain (Graybiel et al., 1968; Oman, 1991).

The first known reference of MS comes from the Ancient-Greek physician Hippocrates, who more than 2000 years ago described that sailing-associated motion causes some kind of body disorder. Throughout History, ships have been the main source for MS, explaining why it is still referred as seasickness or nausea. Indeed, the word nausea stems from the Greek word “naûs”, meaning ship. In this sense, Julius Caesar and Charles Darwin are great examples of historical references especially susceptible to seasickness (Money, 1970).

In spite of being disabling, MS is surprisingly common among species, including humans, monkeys, sheep, some birds, codfish, horses (Treisman, 1977), rats, musk shrews (Ngampramuan et al., 2014), mice (Wei et al., 2011), unlike rabbits, guinea pigs (Treisman, 1977) and lower invertebrates (Lychakov, 2012). Stressing why an apparently non-beneficial, motion-triggered nausea has been evolutionarily conserved is a relevant question. We need to consider that being disabling does not preclude MS

may have adaptive significance, as it is possible that MS is a neutral consequence of another beneficial biological function. Treisman in 1977 focused on that evolutionary perspective, specifically on the fact that species have been strongly selected throughout evolution to protect themselves against toxins, from prevention of ingestion to vomiting. The “toxic theory” of MS (Treisman, 1977) describes that MS may be an effective early warning system to get rid of ingested toxins. It is assumed that toxins are likely affecting the central nervous system centers for sensory input and motor coordination, thus producing nausea-inducing input-output mismatches.

Interestingly, young mammals are considered not susceptible to MS (Treisman, 1977), which may be beneficial as they are experiencing passive unexpected motion when they are carried. Moreover, albeit not having a functioning toxic defense system yet, as young mammals are fed on select food or milk, the mother may act as a proxy for toxic defense.

Nevertheless, we may still wonder why nausea and malaise are features of MS. A logical explanation is suggested by this toxic theory — toxic defense is not only about toxic expulsion but toxic avoidance in the future, that is to say, aversive learning.

Overall, Treisman’s theory (1977) supports an evolutionary and logical explanation for MS as a neutral byproduct accidentally created in the context of a complex system for toxin defense, that relies on the highly-skilled body orientation system as an early warning system.

With the advent of novel means of transportation (i.e. plane, train, ship, car), MS has become a common issue. Daily activities performed during commuting and transportation, such as reading a book, using a smartphone or doing computer work, can initiate or aggravate MS. Besides civil relevance, MS also impacts current military activities, including air, naval and space industries, highlighting the relevance of this physiological alteration.

Since different sources of movement lead to a similar distress, drowsiness, nausea and in some occasions vomiting, this syndrome is currently referred as “motion” sickness. However, the etiology of MS has been —and still is— largely discussed. Today, with the appearance of modern variants of MS involving normal or absent motion such as flight simulator sickness, space sickness (when experiencing weightlessness) or spectacle sickness (when using new glasses), it needs to be clarified that “motion” sickness denomination still does not appropriately reflect its nature. In fact, the mechanisms governing MS remain poorly understood. For the purposes of this Thesis, the compelling knowledge concerning MS etiology building on different theories will be addressed.

1.1.1. Etiological theories of MS

MS was originally believed to be provoked by acceleration-related cerebral ischemia or acceleration influence on the abdominal visceral organs (as reviewed in Reason & Brand, 1975). However, in the 1880s, these hypotheses lost consensus once the role of the vestibular system in body balance was revealed, with MS attributed to altered vestibular function (Irwin, 1881), especially

after James (1881) noted that deaf-mute people —which lack vestibular function— are not susceptible to MS. The relevant inner ear vestibular (or vestibular apparatus) anatomy is summarized in Box 1.

Irwin (1881) referred that the endolymph filling the semicircular canals is a liquid whose transient, inertial movement along the opposite sense of head rotation would continue for a certain time beyond head motion cessation, causing a “mistaken message” or MS-triggering conflict. Additionally, visual information itself can create a similar discrepancy. Overall, these disagreements would lead to a “confusion” in the abdomen that “passes into consciousness as a distressing feeling of uncertainty, dizziness and nausea”.

Subsequently, James (1881) linked the inner ear function loss with MS immunity, positing the assumption that MS was induced by vestibular overstimulation. Nevertheless, it is now clear that the overstimulation hypothesis is not consistent with the fact that drivers of vehicles do not tend to suffer from MS as opposed to their passengers, exposed to the same motion stimulation. Daily activities also include a variety of intense motions that does not induce MS. Furthermore, this hypothesis also fails to explain why astronauts suffer MS when returning to Earth, why sailors get habituated and eventually resistant to MS, or why head fixation in an MS-inducing environment reduces MS susceptibility (Oman & Cullen, 2014). These open questions shifted the attention away from the vestibular overstimulation hypothesis. However, during the 1880s, beyond the existence of a somehow vestibular-related

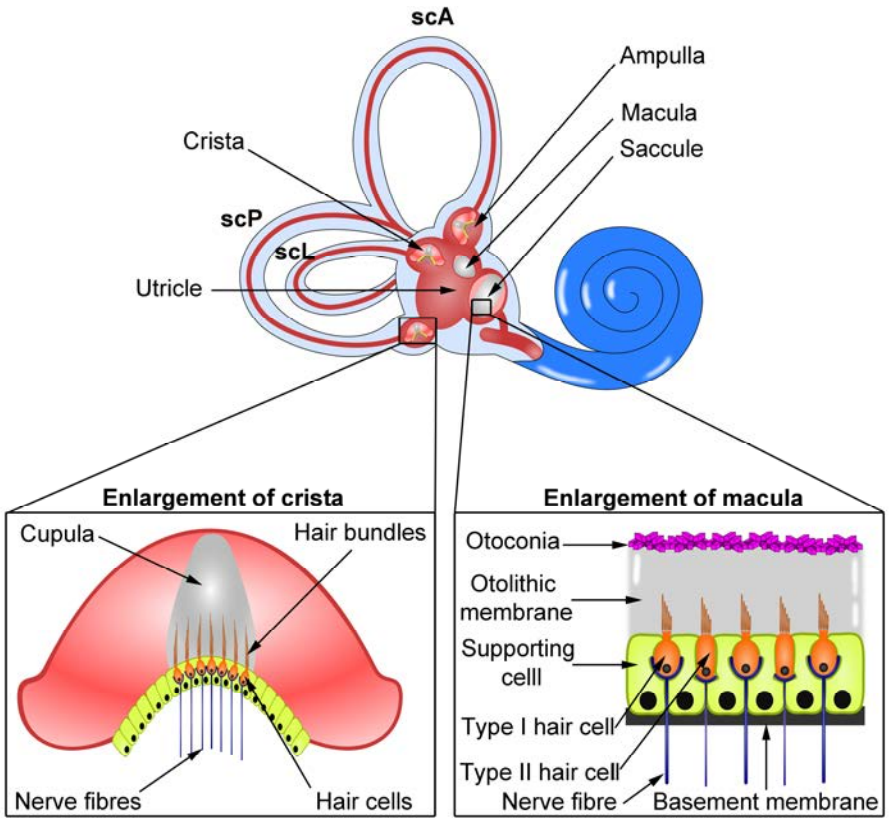

The vestibular inner ear comprises of two main components:

The three semicircular canals or labyrinths

- sense **angular accelerations**, reporting head rotations in a direction dependent-manner (as a gyroscope)
- each canal presents one crista (a widening) containing an ampulla with sensitive hair cells
- the endolymph is a liquid filling each semicircular canal (describes inertial motion in opposite direction of head rotation, leading to hair cell bundle deflection)

The otolith organs (the maculae of the saccule and utricle)

- detect **linear accelerations** to inform head position compared to gravity or to a sum resulting from overall linear accelerations
- cilia of maculae hair cells are sensitive to head tilting-related forces exerted on the otolithic membrane

Box 1.- Inner-ear vestibular apparatus comprises the semicircular canals and otolith organs. scA stands for anterior semicircular canal; scP, posterior semicircular canal; scL, lateral semicircular canal.

conflict for eliciting MS, the mechanisms by which the vestibular system governs MS were not understood. In this regard, some 70 years later Von Holst and Held remarkably contributed to shape the knowledge in conflict processing, with some of their terms still used today. First, Von Holst (1954) proposed that the brain differentiates active from passive motion through comparing expected versus ongoing inputs, through information obtained from the same receptors. Second, Held (1961) built on Von Holst's theory to posit that this comparison is undertaken in a multiple-cycle, feedback process of learning.

Specifically, Von Holst proposed his so-called re-afference principle (1954). According to this model, the brain distinguishes visual input (afference) from self-propelled motion (re-afference) versus the one produced by passive motion (ex-afference) through the superposition of the "efference copy" —a signal produced by the efference or motor command— against the re-afference (Box 2). This superposition implies a positive or negative, single-cycle feedback resulting in the nullification or summation of both signals, which in case of self-propelled, active movements leads to the cancellation of the efference-copy against the re-afference.

This principle is exemplified with the Von Holst model, consisting of an eye with narcotized muscles to reveal the properties of the principle (Box 2). When voluntarily an efference is sent to turn the eye to the right, due to the narcotization, no self-propelled movement takes place and no re-afference is produced. Therefore, in this case, the efference-copy remains unmatched,

resulting in a misleading perception of the surroundings moving to the right (Box. 2A). In another situation with absence of voluntarily movement but rather an exogenously-controlled movement towards the right, no efference and no efference-copy are produced. However, the image motion in the retina produce an ex-afference unmatched by the efference-copy, leading to a false perception of surrounding motion to the left (Box. 2B). The third situation, which is a combination of the two previous ones, the narcotized eye is mechanically moved to the right (producing an afference) at the same time and magnitude as the voluntary intention (efference and efference-copy). Interestingly, then, the cancellation takes place as if it were a self-propelled motion, revealing the feedback component (Box. 2C). Nevertheless, the Von Holst principle is focused only in visual input, restricted to the perception of surrounding movement and lacks a specific scope for MS.

Subsequently, Held introduced the concept of rearrangements and exposure-history (1961), highlighting the role of the central nervous system in the adaptation to changing surroundings, by storing, comparing and selecting the appropriate sensory information. Based on his results on spatial coordination experiments with prism glasses that shift the retinal image, Held proposed a model for ex-afference-related adaptation (or rearrangement). This rearrangement does not take place (or is resolved) when motor command matches the re-afference. Unlike the single-cycle re-afference feedback proposed by Von Holst, Held stated that rearrangements imply a flexible learning process

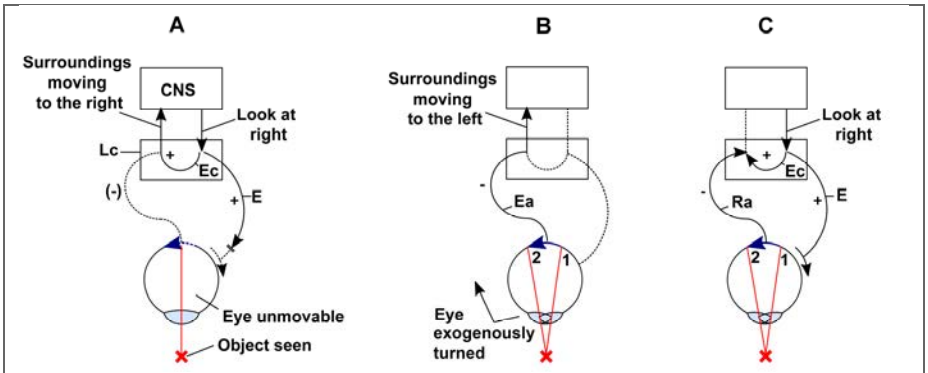

	Afference	Visual input
Ra	Re-afference	Visual input from self-propelled motion
Ea	Ex-afference	Visual input from passive motion
E	Efference	Motor command
Ec	Efference copy	Signal produced by the efference
Lc	Lower center	Eye muscle (effector)

Box 2. — The von Holst's terminology and principle exemplified in narcotized human eye experiments (adapted from von Holst, 1954). Numbers 1 and 2 represent changes in eye position. A) Situation of unmatched efference-copy. B) Situation of absence of efference and efference-copy. C) Situation designed for revealing the cancellation. A detail explanation of each experiment can be found in the text.

—rather than summation or nullification of signals— towards the changing environment, involving multiple feedbacks for signal correlation and comparison. For instance, if prism glasses are maintained during several hours, a rearrangement takes place resulting in habituation to the ex-afference; again, if glasses are subsequently removed, another rearrangement initiates following the new ex-afference. Likewise, an involuntary eye movement (or movement of surrounding image) results in an ex-afference that leads to a rearrangement, since the afference is not cancelled

against the re-afference (because of lack of motor command and efference-copy).

Noteworthy, Held's model is not restricted to visual information but rather introduced the concept of a comparator that matches present re-afference (present input from any sensory source) with a stored re-afference signal. To do so, a correlation store retrieve the stored re-afference guided or selected by the efference-copy. This is possible due to the proposed ability of the correlation store to retain traces of re-afference–efference combinations (RTC) from previous situations. The model includes an external loop, connecting the effector (i.e a muscle) and a source of re-afference (i.e. an eye), which enables the correlation storage to be executed multiple times (Fig. 1). In turn, this multiple feedback loop represents a proposed mechanism for explaining rearrangement-related adaptation, with the correlation store biasing its selection towards a more recent and more similar RTC, leading to the acquisition of new RTCs.

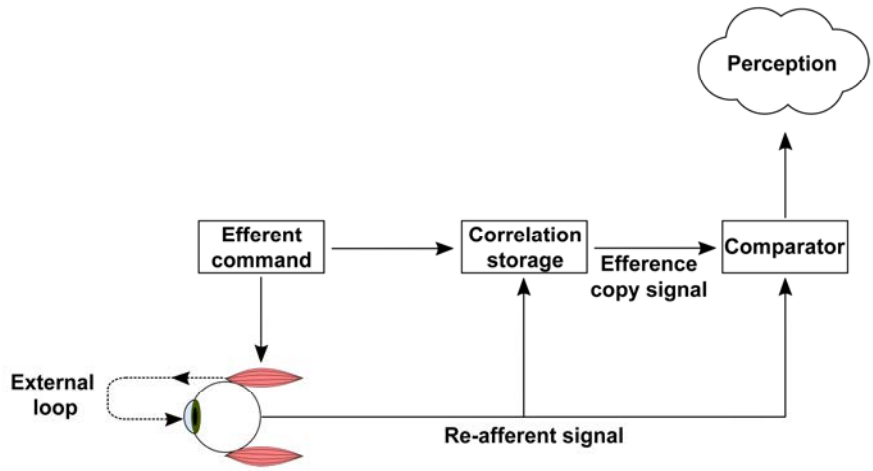

Fig. 1. Held's model (adapted from Held, 1961).

Although Held did not propose a specific approach for MS, he theorized that, in a changing environment, the external loop works multiple times leading to motor discoordination ("disarrangements") with an excess of equivalent trace combinations. However, a clear link of the MS-eliciting conflict with the vestibular system was still missing in a model. In this sense, Money (1970) widely reviewed the signs and symptoms involved in MS, including the role of the acceleration-sensitive, vestibular inner input in MS. Labyrinthine-defective animals —i.e. humans, dogs, cats, cows, squirrel, monkeys and chimpanzees with the semicircular canals removed— are incapable of experiencing MS following provocative movement, even so after a visual stimulus that otherwise would elicit MS. These evidences reveal that the vestibular system, and specifically its semicircular canals, are necessary to elicit MS.

Additionally, Money (1970) reviewed that vestibular stimulation itself is sufficient to provoke an MS-inducing conflict in healthy animals. Head movements in a rotating environment (known as Coriolis/cross-coupled accelerations) are classical examples of conflicting vestibular-restricted stimulus inducing MS with high efficiency, even during blindfolding. Noteworthy, another currently well-known stimulus sufficient to induce MS is the unilateral vestibular caloric stimulation — the irrigation of hot or cold water relative to body temperature into the external auditory canal, thought to affect selectively the semicircular canals to elicit ocular spasmodic movements (nystagmus) and vertigo. The caloric

stimulation was discovered by Robert Bárány, who in 1914 received his Nobel prize for this contribution. However, despite the association between the vestibular apparatus, nystagmus and vertigo, it was not until the 1960s that nystagmus started to be recognized as an MS sign (Lidvall, 1962; Money, 1970). At the time, although the specific contribution of the vestibular components to MS remain —and still is— unclear, the vestibular system was definitely agreed to be critically required in MS regulation (Money, 1970).

A unifying theory explaining MS is still lacking. Nevertheless, Reason (1978) established what still is considered the most accepted theory, an iteration of the very same Irwin's principle built on Von Holst's, Held's major contributions — the existence of a conflict between the integrated input of sensory information and the memory from a similar previous body orientation situation, that is to say, a conflict between current versus anticipated sensory information. It was also the first time the MS-related conflict was clearly linked to the CNS component of the vestibular system. It is referred as the neural mismatch theory and includes a specific scope for the so-called force environments, environments where the subjects are exposed to accelerations (Reason, 1978).

To better understand the neural mismatch producing MS, it is relevant to address the proposed mechanisms for rearrangements (Reason, 1978). Reason defined in his neural mismatch theory two main types of sensory rearrangements by which the vestibular system controls body orientation or position in space, namely the visual-vestibular (inertial) rearrangement and the intravestibular

(canal-otolith) rearrangement. Normally, all rearrangements are in consonance, conveying consistent information of body orientation in space. However, this relationship can be disrupted in three ways, driving a sensory rearrangement conflict, that is, the two sensory rearrangements are sending contradicting inputs each other, one rearrangement does not receive confirmation from the other one, or the other way around. Because of rearrangement conflict, a mismatch signal arises, whose signal strength depends on the following:

- The higher the intensity of discordance in one single sensory channel as opposed to the others, the higher the mismatch signal strength.
- The higher the number of discordant sensory channels, the higher the rearrangement and mismatch signal strength.
- The higher the consolidation of an RTC, the lower the mismatch signal strength.

Under Reason's view, RTCs are re-afferent combinations associated with a common efference command signal, where each one of those are representations of rearrangements of the same motor under different force environments. Thus, each RTC is composed of sensory inputs governing the rearrangements: visual, canal and otolith inputs. The consolidation of each RTC is directly proportional to the exposition of the motor command to the same force conditions. Under these premises, a neural comparator has the role of matching these motion-associated rearrangements with a pattern (RTC) from the neural store (selected by the efference-copy), acquired through past sensory

experience. Along this iterative process, when the mismatch signal exceeds certain threshold, MS responses are elicited (Fig. 2).

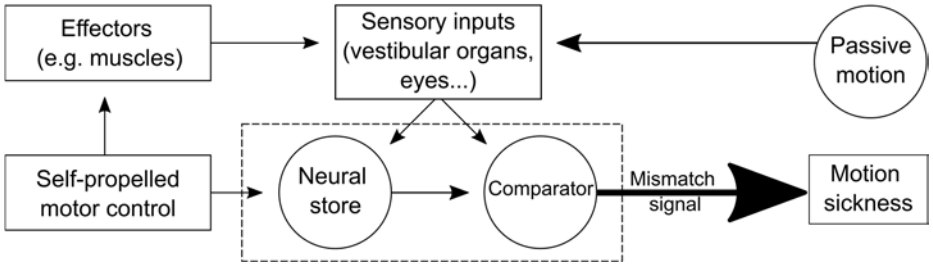

Fig. 2.— The premises of the neural mismatch model.

It is hypothesized —and still accepted— that, if a discordance arises, a neural mismatch signal appears, and the neural store selects another consolidated pattern to be compared to. If, again, another mismatch results, the step is repeated in an iterative manner until a match is found, with the neural store retrieving each time the next highest consolidated RTC associated to the efferent signal. If the conflict persists, then the neural store biases the selection of the stored pattern (RTC) towards a more recent and less consolidated pattern, which in turn reinforces the validity of this new pattern (for instance, RTCs from a new force environment), ultimately leading to adaptation and both conflict and MS extinctions. Therefore, Reason's theory focuses on adaptation to MS. However, as previously discussed, its views on active and passive movement sensory processing are still accepted.

Applying the model to the case of active or self-propelled movement, it is unlikely to elicit a discordance in the first place, as

the RTCs have been repeated and calibrated throughout the development of the individual, reporting consistent and correlated information associated to body orientation in space. On the contrary, passive or illusory movement lacks a corresponding motor command. The lack of efference-copy is proposed to impede the selection of a consolidated RTC from neural store, hence leading to MS and starting an adaptation process through biasing towards recent RTCs that, upon iteration, ultimately becomes consolidated with MS termination (Fig. 3). Furthermore, the more predictable a passive motion is, the faster the adaptation.

Although it is limited to a qualitative approach, Reason's model (1978) represented the first theory to provide mechanistic insight to explain the efficiency of classical MS-inducing stimuli (Money, 1970).

More recently, Oman (1991) proposed a mathematical model based on Reason's theory, from the assumption that the central nervous system (CNS) acts as an observer, managing multiple inputs and outputs. In Oman's model, the CNS generates the so-called orientation state vector. The model implies, analogous to the neural store concept, that the CNS holds an internal dynamic model for continuously interpreting body orientation and related sensory inputs, calculating an error between expected feedback (analogous to the efference-copy) and actual orientation. Likewise, when the efference-copy vector does not subtract present sensory afference, a sensory conflict vector is presumed to compensate and improve model predictions.

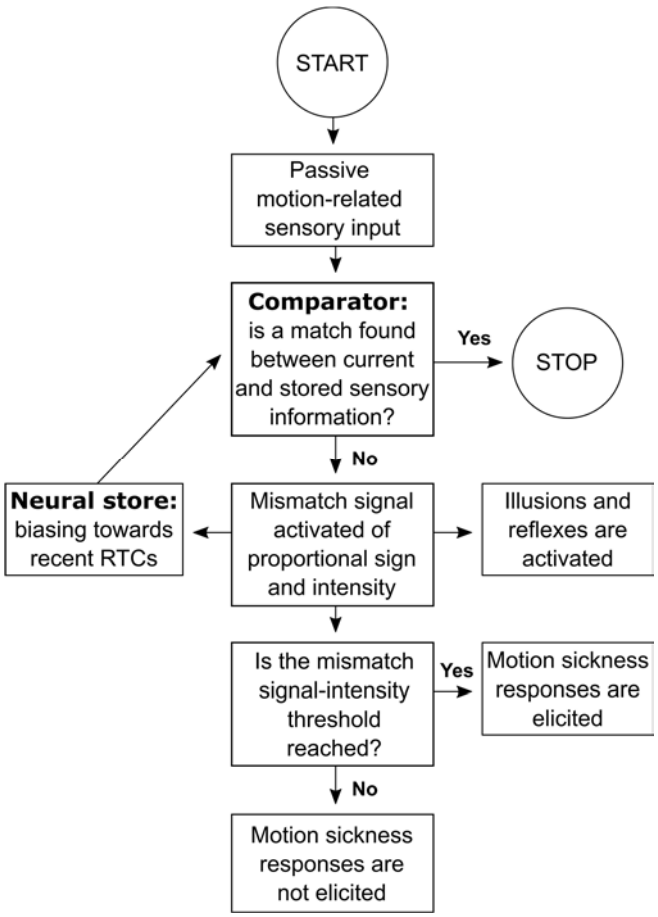

Fig. 3.— Chart flow describing the proposed mechanism of passive motion-triggered neural mismatch signal in the context of Reason's mismatch theory.

Oman's model recognizes the need of daily-life corrections of motor commands to deal with mild external forces, with the vestibular input playing a prominent role compared to visual and proprioceptive inputs. Key features of MS were still not represented in Reason's model, such as changes in nausea susceptibility upon re-exposition to MS-inducing stimulus. In this sense, Oman's model posits that in case of sustained sensory

conflict, the CNS is presumed to need a significant modification of the observer internal model, implying sensory-motor learning.

Since MS physiologic responses are boosted with nausea, appearing faster and stronger if a previous provocative motion has already been experienced, and since MS responses like skin pallor and reduced skin temperature are sustained even after provocative motion cessation (Oman, 1990), Oman's model incorporated two mathematical components mimicking this behavior, a fast and a slow dynamic components, both conveying neural mismatch information that is in turn regulated by a set threshold, ultimately providing nausea intensity estimation. The fast pathway response mimics neuronal mediation, while the slow one involves humoral or hormonal processing. The dynamics of these pathways qualitatively follow a leaky integrator processing, in the sense that both signals can accumulate and when sustained conflict reaches the slow path, the fast path output is boosted, leading to increases in nausea intensity (Fig. 4).

This mathematical approach would more appropriately model the fact that once MS-related signs are well elicited (sensitized period), including discomfort and nausea, individuals are susceptible to develop several temporal spikes in nausea intensity despite not undergoing additional provocative motion. Under this state, humans can find problems to avoid vomiting if a longer resting period is not provided. Despite the model does not explain the sudden decrease in nausea that follows emesis, these two dynamic pathways provide the first model addressing the relationship between spatial orientation and emesis.

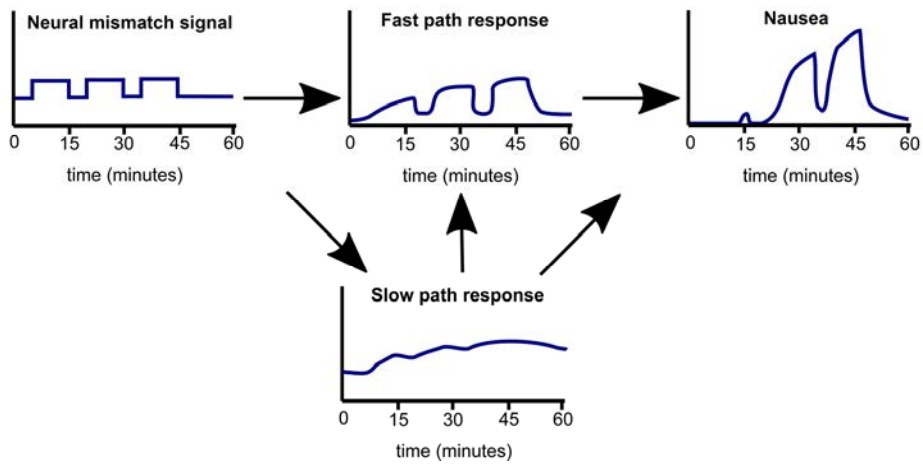

Fig. 4.— Proposed leaky integration processing in MS-associated nausea (adapted from Oman, 1990). Oman's model involves a mathematical definition of two components, a fast path response for mimicking the neuronal, CNS aspect mediating MS-related nausea, and a slow path response for mimicking MS the hormonal mediation. When an MS-eliciting conflict signal is repeated, the slow path response steadily accumulates, subsequently boosting the fast path response. The slow path response modulates both the fast path and nausea responses, ultimately leading to increases in nausea intensity.

Noteworthy, this model also highlights the putative existence of vestibular conflict neurons and the relevance of the poorly known vestibular connectome in regulating nausea and vomiting. Given the proposed leaky integration processing, it is even projected that in case that these vestibular conflict neurons are excitatory, their neuronal depolarization should extend to ~1 min.

Hence, conflict signals are projected to be neurally computed, albeit the mechanism to elicit MS signs is expected to be also contributed by humoral, undefined mechanisms. However, besides anatomical and electrophysiological approaches defining a general description of the vestibular connectome (which will be

addressed in subsequent sections), the vestibular neural substrates mediating MS neurobiological regulation remain poorly understood.

Nowadays, it is accepted both sensory-motor (Reason's and Oman's neural mismatch) theories and Treisman's toxic theory (Treisman, 1977). Thus, briefly, it is believed that MS is developed by a neural mismatch-eliciting, vestibular-mediated sensory input that leads to MS-like autonomic regulation and aversive learning, mimicking key aspects of toxic-induced nausea.

There are, however, persistent uncertainties, such as the relative contribution of linear (otolith-mediated) versus angular (semicircular canal-mediated) movement in MS development. To this end, an intravestibular imbalance theory has been recently proposed (Previc, 2018). In light of this theory, MS would be the result of an imbalance between the different autonomic regulation exerted by otoliths in opposition of semicircular canals. In this regard, it has been described that canal stimulation is more effectively producing MS (pro-nauseogenic) than otolith stimulation. This is consistent with the event of severe MS-related nausea and vertigo by a semicircular canal stimulation through caloric vestibular stimulation (Lidvall, 1962). Conversely, a decreased canal input through triple canal plugging confers protection to Meniere's disease-related vertigo (Zhang et al., 2016). Furthermore, drugs like the $GABA_B$ agonist baclofen or the anticholinergic scopolamine, that diminish primarily canal inputs (Weerts et al., 2015; Weerts et al., 2013), are considered treatments for MS.

Conversely, Previc's theory consistently predicts that a reduced otolith activity compared to semicircular canals normally leads to MS, like in a microgravity environment (space sickness), in an otolith dysfunction situation, in vertical oscillation (named otolith unloading) or in Coriolis angular accelerations —where, beyond intravestibular conflict, angular accelerations and velocities from head tilts in rotating environment are positively correlated with MS severity—. Despite these evidences, otolith input cannot be universally seen as the anti-nauseogenic input, as its targeted activation by sinusoidal vertical movements or rotation about an Earth-horizontal axis are indeed pro-nauseogenic and, after bilateral otolith lesion, these stimulations cannot establish MS (Previc, 1993, 2018). However, the more prominent pro-nauseogenic role of semicircular canal input vs. otolith input is clear.

Altogether, Previc's intravestibular imbalance theory is the latest effort to find a unified and consistent explanation for the varied range of existing MS-eliciting motions. It addresses a truly complex sickness, involving autonomic alterations, apparently both parasympathetic- and sympathetic-mediated (Previc, 1993, 2018). However, there is not a consensual, unifying theory for MS yet. Still, the etiological basis and neurological mechanisms underlying MS are poorly understood. Nevertheless, the involvement and necessity of the vestibular system in MS neurobiological regulation is a major consensus in the accepted MS theories, with the conflict proposed to be computed by vestibular neurons (Oman, 1990).

1.2. The vestibular nuclei

Movement-related information processed by the vestibular organ in the inner ear is relayed directly to the vestibular nuclei (VN). The vestibular nuclei (VN) consist of different structures in the medulla and pons areas classically associated with the control of the body orientation system (Highstein & Holstein, 2006).

Compelling evidence demonstrate that VN neurons are particularly crucial in MS neurobiological regulation. Accordingly, provocative motion activates VN neurons, reproducing MS-like autonomic alteration in rats and mice (Abe et al., 2010; Murakami et al., 2002). There is additionally a variety of diseases sharing VN affectation and autonomic dysregulation. That is the case for Meniere's disease, with vestibular inner ear affectations producing vertigo and nausea, as well as other diseases such as Wallenberg's syndrome patients with unilateral ischemic infarcts including specifically the VN area showing vertigo and vomiting in the acute infarct phase (Dieterich et al., 2005).

1.2.1. Anatomy of the vestibular nuclei

The etymology of "vestibular nuclei" and "vestibular system" comes from the word "vestibule", from the latin term for "entrance" or "hall", used to describe a small bony anatomic hollow close to the cochlea in the inner ear, where the otoliths and semicircular canals are located (Watson et al., 2010).

The VN area is defined by the brainstem afferent terminals of the eighth cranial nerve coming from the otoliths and semicircular

canals of the labyrinths (Highstein & Holstein, 2006; Watson, Paxinos, & Puelles, 2012). The VN is located ventrally from the fourth ventricle, representing a large brainstem portion along the anteroposterior axis, sharing intense connections with the spinal cord, the cerebellum and the ocular motor control system. The anatomy of the VN is accepted to follow a common design in mammals (Paxinos, Xu-Feng, Sengul, & Watson, 2012; Watson et al., 2012).

The vestibular system is assumed to be governed under the influence of the cerebellum, to refine head position and trunk rotation movements (Watson et al., 2010). In agreement with that, the murine vestibular nerve and VN send projections to the cerebellum via mossy fiber axons, specifically to the paraflocculus, flocculus and the lobules I, II, III, IX and X, to mediate at least body position, balance and eye movement (Sillitoe & Fu, 2012). The rostral region of the medial cerebellar nucleus, in turn, is thought to regulate body position, balance and autonomic functions through projections to the VN and reticular areas (Sillitoe & Fu, 2012).

The cytoarchitectonic features of the VN have classically been used to delimit the region into 4 distinct VN subnuclei —the superior, the medial, the lateral and the descending or spinal VN— and distinct cellular groups —the nucleus X, nucleus Y, group F and the vestibulocerebellar group— (Paxinos et al., 2012; Watson et al., 2012). Anatomical and cytoarchitectural details of each vestibular nucleus will be reviewed below.

1.2.1.1. Superior vestibular nucleus

In mice, the superior VN (SVN) is composed by a wide group of cells, broadening rostrocaudally from the caudal portion of the parabrachial nuclei (PBN) to the rostral pole of the cerebellar lobule 10. Mostly, the SVN is located dorsal to the lateral VN (LVN), except rostrally, where is dorsal to de medial VN (MVN). The SVN lies ventral to the superior cerebellar peduncle and lateral to the inferior cerebellar peduncle. The caudal tip of the SVN is bounded laterally by the lateral cerebellar nucleus and medially by the vestibulocerebellar nucleus (Watson et al., 2012).

1.2.1.2. Lateral vestibular nucleus

The murine and human LVN is constituted by multipolar, large size, dark neurons (Dieters' neurons) that get strongly labelled by acetylcholinesterase staining (Paxinos et al., 2012; Watson et al., 2012). The LVN receives input from both the saccules and utricles. The LVN is limited dorsally by the SVN and ventrally by MVN. The rostral tip of the LVN is at the same level as the rostral tip of the dorsal cochlear nucleus, which is the same situation between the caudal pole of the LVN and the rostral pole of the nucleus Y. At the caudal level, the LVN merges with the SVN, with mildly acetylcholinesterase-positive, slightly-smaller cells (Watson et al., 2012).

1.2.1.3. Descending vestibular nucleus

In humans and mice, the descending VN (DVN), also named as inferior or spinal VN, can be considered a prolongation of the LVN containing multipolar and medium-to-large cells which, when compared to the LVN, are slightly smaller and not as intensely labelled for acetylcholinesterase. The DVN is a fasciculated region, delimited rostrally by the LVN and caudally by the rostral pole of the cuneate nucleus (Paxinos et al., 2012; Watson et al., 2012).

1.2.1.4. Medial vestibular nucleus

The MVN represents the largest vestibular subnucleus, both in humans and mice. Likewise, in both species the MVN can be subsequently divided into two portions, a dorsomedial parvicellular nucleus (MVNpc) and a ventrolateral magnocellular nucleus (MVNmc). As can be inferred by their names, the MVNmc includes mildly acetylcholinesterase-positive, scarcer, bigger cells. In contrast, the MVNpc, consists of strongly acetylcholinesterase-labelled, compact, small-medium-sized cells. The MVNpc is the largest part of the MVN, mostly defined dorsally by the ventral limit of the fourth ventricle, limited medially by the prepositus nucleus in mice. The MVN receives input from the semicircular canals and sends outputs to the cervical cord through the medial vestibulospinal tract. In humans, the MVN is abutted dorsomedially by the ventral limit of the fourth ventricle, dorsolaterally by the SVN, rostrally between the locus coeruleus and the SVN and also rostrally abutting the caudal part of the

medial parabrachial nucleus, whereas the MVN and SVN draw input from semicircular canals constituting the vestibulospinal tract, reaching the cervical cord (Paxinos et al., 2012; Watson et al., 2012).

1.2.1.4.1. Cell-type diversity of the medial vestibular nucleus

Clasically, neurochemical markers have been used to identify the neuronal populations in the MVN. Accordingly, the MVN has been shown to contain glutamatergic, glycinergic, GABAergic as well as cholinergic neurons, among others, being the glutamatergic population more abundant (Balaban, 2016). Given the remarkable neuronal heterogeneity in the region, genetic identification of specific cell types is fundamental for dissecting functionally-relevant vestibular circuits. Recent studies using a single-cell transcript profiling approach in MVN cells, have identified 6 groups of functionally-relevant MVN cell types have been recently categorized into 3 inhibitory and three excitatory populations in mice (Kodama et al., 2012). Excitatory subpopulations were genetically defined as *Crh/Vglut2-* (encoding corticotropin releasing hormone and the vesicular glutamate transporter 2), *Vglut1-* (*Slc17a7*, a glutamatergic marker encoding the vesicular glutamate transporter 1), or *Adcyap1* (Adenylate cyclase-activating peptide, or PACAP). On the other hand, inhibitory subpopulations were defined by either *Gad1 or Gad2* expression (inhibitory neurotransmitter marker encoding glutamate decarboxylase 1) as well as *Crhbp-* (encoding corticotropin releasing hormone binding protein), *Coch* (encoding cochlin) or

Scn4b/Slc6a5 (encoding respectively sodium channel β-subunit 4 or sodium- and chloride-dependent glycine transporter 2). Interestingly, *Cck* expression was found present in both excitatory and inhibitory cell types. Anatomically, several populations showed distinct distributions. In this regard, *Crh*-expressing neurons are located in the central part of the MVN, whereas *Adcyap1*- or *Crhbp*-expressing ones are located along the 4th ventricle (Kodama et al., 2012).

1.2.2. Vestibular pathways

As mentioned previously, Balaban (2016) comprehensively reviewed the knowledge on neurochemical and circuitry characterization of the neurovestibular system. In the VN, a plethora of different neurotransmitters are involved, including excitatory aminoacids (EA), gamma-aminobutyric acid (GABA), acetylcholine (ACh), histamine, serotonin, melatonin, glycine, dopamine, endocannabinoids, norepinephrine, neuropeptides.

Classically, the research on the vestibular circuitry has been focused in the vestibular reflexes, such as the vestibulo-ocular (VOR), vestibulospinal and vestibulocollic reflexes.

1.2.2.1. Vestibulo-ocular pathways

VORs serve as gaze stabilizers in context of motion. To that end, the reflex seeks to stabilize images in the retina of the eye during head movements. As reviewed by Balaban (2016), the VN and the

group y receive input from semicircular canals to process the angular VORs. Biomarkers of EA or glutamate, GABA and glycine have been found in these vestibular regions (Bagnall et al., 2007). Excitatory and glycinergic murine MVN cells, including interneurons, show different electrophysiological features, like maximum firing rate, and receive different inhibitory input from the cerebellar flocculus being denser in for excitatory neurons (Shin et al., 2011). Subsequently, the VN send projections to the choline acetyltransferase (ChAT)-positive neurons of the anteromedian nucleus (AM) and the adjacent ventral tegmental area (VTA), which may mediate eye (lens and pupilla) accommodation during VORs and changes in force environments or body posture (Balaban, 2003).

1.2.2.2. Vestibulospinal pathways

The vestibulospinal reflexes involve changes in the activity of body muscles in response to movements of the head in space in order to stabilize posture. To that end, labyrinthine inputs reaching the VN are processed and projections sent to the spinal cord in two direct pathways, the medial (MVST) and the lateral (LVST) vestibulospinal tracts. The MVST constitutes bilateral excitatory and inhibitory vestibular connections to neck-related motoneurons (for vestibulocollic reflex), under the control of inhibitory cerebellar zone A Purkinje cells. On the other hand, LVN sending ipsilateral, excitatory projections to limb muscles constitute the LVST, which is under inhibitory control from cerebellar zone B Purkinje cells (Balaban, 2016).

1.2.2.3. Motion sickness-relevant vestibular circuitry

As opposed to the classical vestibular reflexes, the knowledge of the vestibulo-autonomic circuitry is comparatively more limited, focused in its vestibulo-sympathetic aspect (blood-pressure and cardiovascular compensations), rather than the parasympathetic component (sweating, drowsiness, temperature drop, nausea and vomiting), which are hallmark of MS (Money, 1970; Nalivaiko, 2018; Previc, 2018).

As described, vestibulo-sympathetic regulation comprises the reflexes that control blood pressure-related cardiovascular compensations to body posture. Vestibular stimulations have been shown to induce variations in blood pressure (Yates et al., 1994). Conversely, bilateral transections in the eighth cranial nerves hinder proper adaptations of blood pressure along posture changes (Yates et al., 2000). In this regard, it has been suggested that the vestibulo-sympathetic reflexes are mediated by connections between the caudal MVN, the DVN and the subretrofacial rostral ventrolateral medulla (Porter et al., 1997). However, both sympathetic and parasympathetic autonomic regulation are thought to be governed under vestibular influences given that clinical correlations are clear between acute vertigo and nausea, gastrointestinal malaise and alterations in breathing and heart rate (Balaban et al., 1994; Money, 1970).

To identify the neural substrates of MS physiologic responses, several studies have carried out provocative rotations, in order to reveal consequently activated, *Fos*-expressing brain regions, indicative of neuronal activity. In mice lacking functional vestibular

hair cells and subjected to a continuous 2G force environment for 21 days, MS-like autonomic responses are prevented, correlating with abolishment of *Fos* expression in MVN, SVN, PBN, central amygdala (CeA), solitary nucleus (NTS), dorsal raphe nucleus, locus coeruleus and paraventricular nucleus of the hypothalamus (PVN) (Murakami et al., 2002). In rats, a provocative stimulation of 3G for 14 days revealed *Fos* expression in MVN, NTS, PVN, CeA, area postrema and raphe nucleus (Abe et al., 2010).

Among the different areas, the NTS and PBN are the most promiment since both nuclei are known to process visceral sensory input in the brainstem. A direct anatomical link between the neurovestibular circuitry and autonomic brainstem circuitry has been described, with the discovery of vestibulo-solitary connections in the rabbit, specifically caudal MVN and DVN projections to the NTS, the ventrolateral medullary reticular formation and less densely to the dorsal motor nucleus of the vagus nerve, suggesting a vestibular contribution in autonomic functions (Balaban et al., 1994). A similar study in rabbits additionally unravelled vestibular projections to the nucleus raphe magnus, lateral medullary tegmentum, ventrolateral caudal aspect of the Kölliker-Fuse nucleus, nucleus ambiguous, ventrolateral medulla, and more intense projections from the caudal MVN, DVN, SVN and rostral LVN to the medial and lateral PBN (Balaban, 1996).

Furthermore, histological reviews in rabbit, rat and cat have identified the existence of a common pattern of vestibulo-autonomic pathways, supporting the hypothesis of a conserved

vestibulo-autonomic system in mammals (Porter et al., 1997). In rats, there are remarkably denser NTS and area postrema terminals in the lateral PBN (Herbert, Moga, & Saper, 1990). The PBN in turn receives input from amygdala and cerebral cortex (Moga et al., 1990) and the PBN projects to autonomic- or aversive learning-associated nuclei, including the infralimbic prefrontal cortex, the insular, the hypothalamus and CeA among others (Balaban, 1996). Noteworthy, anatomical studies in rats and rabbits established that the VN and the PBN are bidirectionally connected (Balaban, 1996, 2004). The rostral, gustatory-related region of the NTS sends direct projections to the medial PBN, and also the dorsomedial, visceral-related NTS and the area postrema send axons to the outer part of the external lateral PBN (Herbert et al., 1990). Altogether, the PBN is in a unique position to integrate vestibular, emotional and visceral inputs. Noteworthy, the PBN has been proposed as a center for vertigo and panic association, consistent with clinical reports correlating panic disorder-related and agoraphobia-related anxiety with space and motion discomfort (Jacob et al., 1996).

Accordingly, provocative stimulus activates excitatory VN neurons projecting to the NTS and PBN, as revealed by FOS and phosphate-activated glutaminase histochemistry (Cai et al., 2007; Kaufman et al., 1992). This is in agreement with recent data from Blue Brain Cell Atlas (Erö, Gewaltig, Keller, & Markram, 2018) showing that the main neuronal source in the VN is excitatory. Furthermore, optogenetic activation of excitatory, *CamK2a*-expressing MVN neurons in anaesthetized mice, coupled to functional magnetic resonance imaging (fMRI) has shown an

activation in motor, somatosensory, visual and auditory thalamic nuclei along with their associated sensorimotor cortices, also high-order cortices and hippocampal regions, further supporting excitatory VN neurons as major sensory mediators (Leong et al., 2019).

MS is characterized by changes in autonomic responses, including hypolocomotion, appetite suppression, loss of body temperature, and aversive learning, with the acquisition of a conditioned taste aversion (CTA) (Braun et al., 1973; Money, 1970). Hence, taken together, the existence of the reviewed vestibular network indicates that both the NTS and the PBN, with a highlighted role for the latter, may be key circuits accounting for the VN-mediated, MS-like autonomic (Porter et al., 1997) and/or aversive processing.

1.3. MS-related physiological responses

Despite MS being evolutionarily highly conserved in animal species (Lychakov, 2012; Ngampramuan et al., 2014; Treisman, 1977; Wei et al., 2011), the study of the physiologic role of the VN in autonomic functions is still mostly limited to the anatomic level. Furthemore, a link between the VN and MS-related aversive learning has not been yet defined (Abe et al., 2010; Murakami et al., 2002). Its unclear parasympathetic-sympathetic nature, the lack of standardization for MS behavioral correlates and the absence of vomiting reflex in rodent preclinical models, have certainly hindered the elucidation of the etiology and neural

mechanisms of MS (Foubert et al., 2005; Ngampramuan et al., 2014; Previc, 1993, 2018; Singh et al., 2016).

Although nausea normally precedes vomiting, nausea does not always conclude in vomiting. It is being increasingly clear that the physiology and pharmacotherapy of vomiting (a reflex) is distinct from those of nausea (a more subjective experience) (Singh et al., 2016). Widely used drugs effectively reducing chemotherapy-provoked vomiting, including 5-HT_3 and neurokinin-1 antagonists (Di Maio et al., 2013; Eliasen et al., 2020), are not so effective in nausea amelioration. Nausea has classically being the neglected symptom during MS research in favor of vomiting (Foubert et al., 2005; Navari, 2013), further hindering progression in the understanding of MS.

As mentioned, limited physiologically-relevant models have been another cause impeding a swift progress in the field. Typical research models, such as rats or mice, does not possess the vomiting reflex. In this regard, the Musk shrew (*Suncus murinus*) a species that possesses vomiting reflex, has been widely used. However, as stated before, the different neurobiology between nausea and vomiting makes it inappropriate the study of vomiting as a proxy to specifically understand nausea. In this light, and taking into account the well-defined biology and the availability of state-of-the-art molecular tools, it is best to better establish and validate physiological correlates of nausea in common rodents. As such, reduced spontaneous locomotor activity, appetite suppression, drop in body core temperature and acquisition of CTA are typically assessed as common outcomes of nausea in

preclinical studies (Abe et al., 2010; Fuller et al., 2002; Murakami et al., 2002; Ngampramuan et al., 2014).

1.3.1. MS-related autonomic regulation

Typical autonomic-related MS responses include reduced willingness to move, appetite suppression and loss of body core temperature, both in humans (Money, 1970) and other mammals, including mice, rats and musk shrews (Abe et al., 2010; Fuller et al., 2002; Murakami et al., 2002; Nalivaiko, 2018; Nalivaiko, Rudd, & So, 2014; Ngampramuan et al., 2014).

It is widely known that in susceptible mammals acute hypolocomotion follows after MS-inducing provocative stimuli. In an experiment in rats assessing the role of acute bilateral vestibular inner ear hair cell lesion —which in terms of sensory conflict is considered as vestibular stimulation—, acute hypolocomotion was observed 24h after bilateral vestibular chemical damage as compared to controls (Pan et al., 2016). Furthermore, rats subjected to rotation show decreased spontaneous locomotor activity, and decreased body temperature, which are absent in labyrinthectomized rats subjected to the same rotation (ruling out vestibular surgery-related sensory conflict) (Ossenkopp, Rabi, Eckel, & Hargreaves, 1994). Other experiments in rats revealed that serotonin (5-HT) is key in the MS-like decreased food intake, as evidenced by the facts (1) that 5-HT concentrations in cerebrospinal fluid are increased under provocative conditions, (2) ketanserin (a 5-HT_{2A} antagonist) partially ameliorate appetite suppression during

provocative motion as well as (3) ketanserin significantly decrease *Fos* expression in the MVN (Abe et al., 2010).

On the other hand, mice subjected to provocative motion subsequently show a drop in locomotion, appetite suppression, and a severe loss of body temperature (Fuller et al., 2002; Murakami et al., 2002). However, in mice subjected to the same stimulus but lacking macular otoconia —a component of the vestibular inner ear organs utricle and saccule sensing linear accelerations or gravitational load—, the decrease in temperature is prevented, while MS-related drop in spontaneous locomotion and appetite suppression are not, or mildly, ameliorated (Fuller et al., 2002). These data suggest that, at least for MS-related thermoregulation, sensing the gravitational load is required, while MS-like hypolocomotion and appetite suppression are mediated by vestibular inner ear organs sensing both linear (saccule and utricle) and angular (semicircular canals) accelerations.

Recent efforts have highlighted the relevance of thermoregulation as an excellent real-time correlate of nausea across species. MS-induced temperature response presents a differential signature — hypothermia despite the stressfulness of provocative motion. This constitutes an exception for temperature response to stressors, like physical restriction or novelty, which generally induce increases in core body temperature. This singular physiological signature of MS has been proposed to be engrained into a more broad anti-toxic defensive response, as a defensive hypothermia, consistent with Treisman evolutionary theory (Nalivaiko et al., 2014; Treisman, 1977). In this context, vomiting would be a

response to evacuate toxics, and nausea would be more oriented towards immediate defense (appetite suppression to avoid toxic ingestion, hypothermia to fight against neurotoxins already ingested altering the vestibular system) and towards learning avoidance of future risking situations. Thus, these conditioned responses would be elicited in MS, as commented before, as an accidental secondary byproduct derived from the toxic defense system. Thus, these responses are in agreement with the accepted etiological theories of MS (Oman, 1990; Reason, 1978; Treisman, 1977).

Of interest, hypothermia perhaps might not only be a defensive response in intoxication, but also crucial for survival since it reduces tissue oxygen demand, as seen after lipopolysaccharide (LPS, a component of infective, gram-negative bacteria) intoxication (Romanovsky, Shido, Sakurada, Sugimoto, & Nagasaka, 1997). Noteworthy, LPS or cisplatin (anticancer therapeutic) also activates PBN neurons, specifically calcitonin gene-related peptide-expressing, glutamatergic neurons in the lateral PBN, known to be involved in malaise (Alhadeff et al., 2015), appetite suppression (Carter et al., 2013) and even CTA (Carter et al., 2015). While, on the other hand, NTS is more classically associated with vomiting (Horn, 2008; Hornby, 2001; Singh et al., 2016), these evidences strongly underscore the vestibulo-parabrachial circuit as a potential candidate for relaying MS-inducing conflict and MS-elicited nausea.

1.3.2. Taste aversion learning as an MS response

In 1927, Pavlov established what is now seen as the classical conditioning association between an unconditioned stimulus (US) with a conditioned stimulus (CS), through repeated pairing sessions (Pavlov, 2010). The acquisition of the conditioned response is assessed after the conditioning sessions, testing the emergence of the conditioned response in absence of US.

It is widely known that gastrointestinal malaise within short time (hours) after ingestion of a novel flavor can elicit a conditioned taste aversion (CTA) response (Bernstein, 1978). Accordingly, the lateral PBN has been shown to be required to acquire a CTA (Agüero, Arnedo, Gallo, & Puerto, 1993). Interestingly, MS-evoking rotations can establish a CTA (Braun & McIntosh, 1973). And conversely, if the PBN is lesioned, MS-evoking rotations are unable to establish the MS-related CTA (Gallo, Marquez, Ballesteros, & Maldonado, 1999), indicating that the PBN mediates MS-triggered CTA. This mechanism, consistent with Treisman theory, would be largely adaptive for avoiding toxic food in the future.

The specific necessity of the area postrema in general CTA acquisition was discarded since its lesions lead to the abolishment of toxin-induced CTA but enhancement of MS-induced CTA (Ossenkopp, 1983), again supporting the role of the PBN in VN-mediated, MS-triggered aversion learning. At the cellular level, Compelling evidence demonstrates that *Calca*-expressing neurons in the external lateral part of the PBN are mediating the establishment of a CTA when using several challenges as US,

including LPS or lithium chloride (LiCl) or CCK, a neuropeptide that has been associated to appetite suppression and lipid-induced nausea, and that is interestingly produced by MVN neurons (Carter et al., 2015; Essner et al., 2017; Feinle et al., 2000; Kodama et al., 2012; Pilichiewicz et al., 2006). These results, in conjunction with the known existence of an anatomical vestibulo-parabrachial pathway and the *Fos* expression in both nuclei after provocative motion (Cai et al., 2007), suggest a common pathway to integrate vestibular, gustatory and gastrointestinal inputs through the PBN for both intoxications and MS, providing anatomical basis for the Treisman's toxic theory of MS (Ngampramuan et al., 2014; Treisman, 1977). However, the genetic identity of the vestibulo-parabrachial circuit ─both VN-projecting neurons and PBN-receiving neurons─ mediating MS-like CTA has not been elucidated.

1.4. Neuronal interrogation of the vestibular system

1.4.1. Pharmacological dissection of vestibular role on MS

Several pharmacological interrogation approaches have been performed to support many aspects of current MS sensory-motor theories, providing relevant insight in the neural mechanisms governing the vomiting-like aspect of MS, (Takeda et al. 2001).

A thorough pharmacological interrogation in rats was applied using the so-called pica behavior ─the consumption of non-nutritive substances as kaolin clay─ as a measure of vomiting-like behavior or MS correlate in rats (Takeda et al. 1993). Daily rotations around one (single rotations) or two axes (double

rotations) for 10 days lead to a significant increase in kaolin intake, consistent with MS-associated, vomiting-like behavior, in the double-rotation group (Morita et al., 1988).

Using this model, three anti-MS drug classes have been described depending on their influence over MS habituation, which in turns correlates with the level at which MS is being tackled, such as through a blockade of the sensory input that elicit the neural mismatch —class A drugs—; through a decrease in the neural mismatch signal intensity via modification of the neural store —class B drugs—; or through the suppression the subsequent neural mechanisms leading to MS-related autonomic alteration and MS-related aversive learning —class C drugs—. Regarding habituation, class A drugs would delay habituation, while class B drugs would boost, and class C drugs would not alter habituation, respectively (Fig. 5) (reviewed in Takeda et al. 2001).

Antihistamines antagonizing histamine H_1-receptor, such as diphenhydramine (clinically used in humans as an anti-MS drug), are efficiently suppressing pica in double-rotated rats. As diphenhydramine also exhibit anticholinergic activity, it cannot be claimed only with this drug effect that MS is mediated by histaminergic mechanisms. Nevertheless, α-fluoromethylhistidine (FMH), that irreversibly inhibits the histidine decarboxylase enzyme (HDC), specifically suppressing histaminergic transduction, is likewise effectively inhibiting pica in rats (Takeda et al., 2001). Together, these results strongly suggest that MS is mediated through histamine H_1-receptors.

Accordingly, the pons medulla oblongata and the hypothalamus are regions known to concentrate histaminergic neurons. In particular, the caudal part of the MVN concentrates the majority of the afferent histaminergic fibers present in the brainstem vestibular nuclei (Steinbusch, 1991). Furthermore, double rotations in rats boosted histamine content in both pons medulla oblongata and hypothalamus, which did not take place in single rotated rats; similarly, vestibular caloric stimulation with hot or ice water irrigation potentiates histaminergic hypothalamic activity (Horii et al., 1993). Furthermore, in Takeda's model (daily stimulation for 10 days), FMH administration on days 4 to 6 matched with a reduction in kaolin consumption in double rotated rats, that was followed by a kaolin intake rebound replicating the same habituation pattern observed in double rotated rats without FHM administration (Fig. 5C). Therefore, FMH fits in the category of class C drug. Conversely, intracerebroventricular infusion of histamine has been shown to induce vomiting through H_1-receptors. Consistently, the emetic center —which is thought to include the NTS, nucleus ambiguus, parvicellular reticular formation and the dorsal motor nucleus of the vagi (Mehler, 1983)— contains H_1-receptors and histaminergic fibers. That is why H_1-antagonists clinically ameliorate MS signs either if administered before or during nausea or vomiting onset, as these class C drugs intervene in the signs and symptoms of MS (Takeda et al., 2001). In global, these findings suggest that a neural mismatch-induced increase in the histaminergic transmission via H_1-receptors is stimulating the emetic center, thus mediating MS signs.

As for the pharmacological modulation of the mismatch signal itself, acethilcoline has shown a pivotal role. In this regard, scopolamine administration is a known and effective treatment for MS antagonizing acetylcholine muscarinic receptors (Brand et al., 1966; Graybiel et al., 1975; Wood et al., 1970). However, it has a reduced efficacy when administered after initiation of the sensory conflict. Scopolamine administration led to a reduced kaolin consumption in double rotated rats, consistent with MS amelioration. Furthermore, this reduction was maintained after removal of scopolamine (Fig. 5B) (Morita et al., 1990). Given that there is an acceleration effect in MS habituation, scopolamine is considered a class B drug, affecting the neural store. A conversed approach increasing acetylcholine content in the brain by the cholinesterase inhibitor physostigmine showed a retardation in habituation. On the contrary, the use of neostigmine, a cholinesterase inhibitor that take action in the brain, did not had any effect (Morita et al., 1990), which reproduces a similar situation as per the use of scopolamine buthylbromide in humans, a drug unable cross the blood-brain barrier (Brand et al., 1966). Overall, these evidences support that a decrease in acetylcholine transmission is correlated with MS habituation.

Pharmacological interrogation of the cholinergic system has revealed mechanisms underlying MS, in agreement with Reason's and Treisman's MS theories. It has been suggested that the hippocampal cholinergic system, specifically the septo-hippocampal pathway, is key, as electrical vestibular stimulation enhances acetylcholine transmission from the hippocampus (Horii et al., 1994). The hippocampus *per se* is known to process

sensory information, including spatial and non-spatial information (Barnes, 1988). Nevertheless, despite the anatomic source of the neural mismatch remains still unknown (Kohl, 1983; Kohl et al., 1983), the activation of the cholinergic system is known to promote associative-memory acquisition via integration of a new input pattern vs. suppression of stored patterns (Hasselmo et al., 1992; Hasselmo et al., 1993). This mechanism is analogous to the one proposed in the neural mismatch theory, making the hippocampus a strong candidate for the source of the neural mismatch. Accordingly, unilateral vestibular caloric stimulation, both with hot or cold water irrigation in the middle ear, increases acetylcholine release in the hippocampus (Horii et al., 1994). These evidences point that the neural mismatch signal promotes hippocampal cholinergic transmission. Ultimately, it has been proposed that scopolamine may prevent MS via decreasing the signal intensity through modification of the neural storage, as in absence of neural mismatch signal the acquisition of a new pattern in the neural store is facilitated (Takeda et al., 2001). Recently, the MVN, which receives fibers mainly from the semicircular canals, has been proposed as the CNS substrate for the anti-MS action of scopolamine. Interestingly, the MVN presents a high density of muscarinic receptors, while stimulation of these receptors increases neuronal activity (Schwartz, 1986; Aurélie P. Weerts et al., 2015). It has been suggested that scopolamine decreases muscarinic receptors in the MVN (Weerts et al., 2015), highlighting a potential role of the MVN in MS.

Finally, the catecholaminergic system has been suggested to play a key role modulating MS-inducing sensory inputs. Accordingly,

amphetamines are clinically effective against MS (Brand et al., 1966; Graybiel et al., 1975; Wood et al., 1970). Amphetamines are known to increase noradrenergic transmission. Thus, the noradrenergic system was been suggested to antagonize MS (Wood et al., 1970). However, this hypothesis was not consistent with the fact that the use of amphetamines produced an enhancement in both single rotated and double rotated rats. Hence, the boost in noradrenergic activity in the brainstem is rather consistent with the presence of a sensory input, regardless if it sufficient to induce MS (Takeda et al., 2001). Additionally, other authors (Nishiike et al., 1996) have pointed that a noradrenergic activity suppression in the locus coeruleus in rats is correlated with MS signs. Vestibular caloric stimulation, both with ice or hot water, produce a suppression of noradrenergic tone, correlating with MS (Nishiike et al., 1996). Thus, it is proposed that if an increase in noradrenergic activity in the brainstem due to a sensory input is sufficient to create a neural mismatch that in turns suppresses locus coeruleus noradrenergic activity, leading to MS. Therefore, amphetamines are proposed to mediate the suppression of sensory processing via locus coeruleus noradrenergic increase, thus antagonizing MS. These substances are to be considered class A drugs given that in absence of the sensory conflict, no learning/habituation can take place (Fig. 5A). In agreement with this, administration of the $GABA_A$-receptor antagonist, bicuculline blocked the inhibition of noradrenergic locus coeruleus neurons after vestibular caloric stimulation (Nishiike et al., 1996), revealing that the neural mismatch suppresses noradrenergic locus coeruleus neurons via $GABA_A$

receptors. Anatomically, it is known that lesions in the ventrolateral medulla (VLM) lead to an amelioration in locus coeruleus activity suppression, indicating that the neural mismatch promotes activation of VLM which in turn inhibits noradrenergic locus coeruleus neurons through $GABA_A$ receptors (N Takeda et al., 2001).

Besides MS-induced nausea and vomiting, the drowsiness (the so-called sopite syndrome) is a long-lasting relevant aspect of MS, remaining for a certain period of time after nausea or vomiting have remitted (Graybiel et al., 1976). Given that locus coeruleus plays a role in arousal (Foote et al., 1991) and that a long-lasting inhibition of locus coeruleus neurons is promoted by caloric stimulation, the noradrenergic locus coeruleus neurons are proposed to mediate drowsiness (Nishiike et al., 1996). Accordingly, central nervous system psychostimulants, as amphetamine, methylphenidate and pemoline, and even unspecific arousal stimulants, are all effective against MS and its associated drowsiness (Kohl et al., 1986). In conclusion, these stimulants may prevent conflict-induced noradrenergic locus coeruleus suppression, highlighting the role of locus coeruleus as a key neural center for sensory processing and revealing the relevance of the arousal state in the neurobiological regulation of MS.

However, despite being useful for unravelling some neurobiology of MS, classical pharmacological approaches lack spatial and cell-type specificity, which have been widely overcome with new genetically-defined neuronal manipulation techniques, such as

optogenetics and chemogenetics. Specifics and targeted advantages of these new approaches are relevant for this Thesis, thus reviewed below.

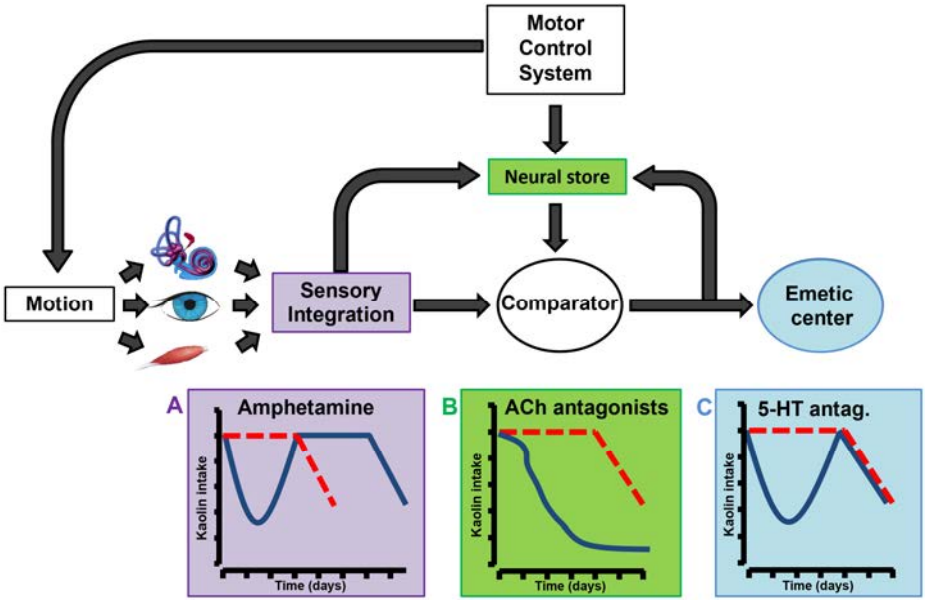

Fig. 5. — Projected pharmacological effects on MS habituation (according to and adapted from Takeda et al., 2001). Solid blue line in the graphs represents expected kaolin intake as a measure of MS-related vomiting in rotated rats treated with different drugs, dashed red line indicates expected kaolin intake in rotated rats treated with vehicle. A) Class A drugs such as amphetamine are thought to block the MS-eliciting sensory input, leading to habituation delay. B) Class B drugs such as ACh antagonists modulate the neural store decreasing the neuronal mismatch signal intensity, leading to boosted habituation. C) Class C drugs such as 5-HT antagonists inhibit MS-related autonomic responses, leading to unchanged MS habituation.

1.4.2. Functional manipulation of genetically-defined neural circuits

Classically, galvanic electrical stimulation has been widely applied. While this type of stimulation provides great temporal resolution, it lacks cell-type specificity (Fenno et al., 2011). Although it has undoubtedly contributed to the understanding of the nervous system in general, and the vestibular circuitry in partical, electrical manipulation is not efficient for neuronal inhibition and lacks cell-type resolution. On the other hand, genetic and pharmacological approaches can provide cell-type specificity, although they lack temporal resolution. Therefore, novel tools to modulate the activity of genetically-defined neuronal populations with sufficient (ms) temporal range are needed to unequivocally untangle the vestibular circuitry underlying MS.

1.4.2.1. Cre-loxP system

A key step forward for improving neural interrogation techniques has come precisely from genetics, specifically from understanding the fundamental mechanism of the P1 bacteriophage CRE-recombinase activity (Sternberg & Hamilton, 1981). The CRE-recombinase protein (CRE) possesses the ability to recognise specific DNA sequences (named *loxP* sequences) and recombine any *loxP*-flanked (floxed) DNA sequence. LoxP sequences consist of two symmetric 13-bp sequences with a central (core) asymmetric 8-bp sequence. The orientation of the core of *loxP* sequences determines the result of recombination: when both of them are in the same orientation (cis), the floxed sequence get

excised; on the contrary, when *loxP* sequences are opposed (trans orientation), the floxed sequence will undergo inversion. For the purposes of expressing tools for neural activity manipulation, anti-sense sequences flanked by opposed *loxP* sites are ideal, as the presence of CRE would lead to the inversion of the floxed sequence and thus activation of the expression of the tool. However, although this recombination is specific –it requires both CRE and *loxP* presence in the same cell–, this inversion is reversible, leading to a mix of forward and reverse orientations, which makes the strategy inefficient.

To improve the expression strategy, the simultaneous use of both inversion and excision capabilities of the Cre-loxP system turned out to be essential. Atasoy adapted in 2008 (Atasoy, Aponte, Su, & Sternson, 2008) the original Schnütgen's switch strategy (FLEX) (Schnütgen et al., 2003), which uses both CRE-mediated inversion and excision. The original FLEX switch used double pairs of opposing *lox* sequences that, in the presence of CRE, drive a first reversible inversion of the flanked sequence followed by a subsequent irreversible excision of two *lox* sites, one of each *lox* variant. Schnütgen system however showed heterotypic recombination. Hence Atasoy adapted his system with the *loxP* and *lox2272* sites, known to exert only homotypic recombination, that is to say, efficient recombination only with the same *lox* variant (Lee & Saito, 1998). This way, the resulting sequence contains opposed, incompatible *lox* sites that cannot undergo further recombination, obtaining the desired orientation of the flanked sequence (Fig. 6). Today this adapted strategy is named doubly

floxed inverted opsin –for its first use with an optogenetic opsin tool– or doubly floxed inverted open reading frame (DIO).

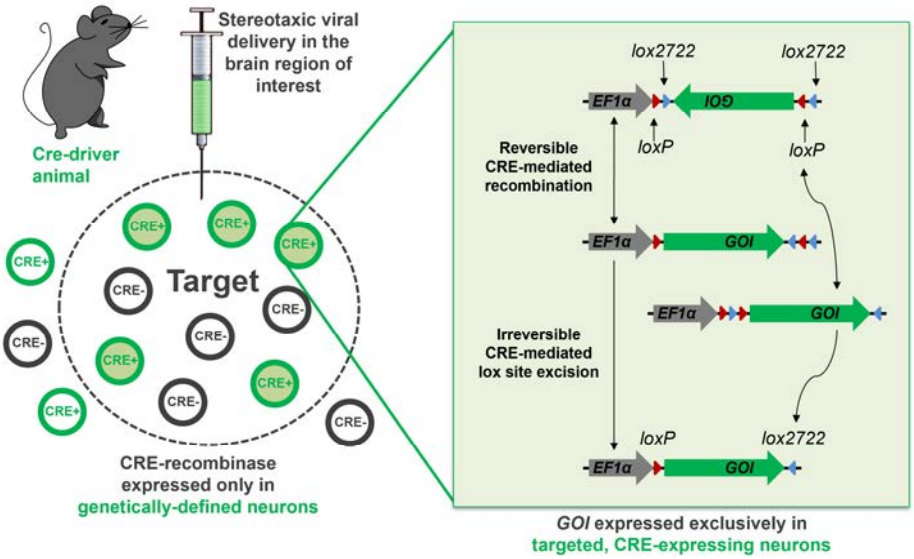

Fig. 6.– Cre-loxP system-based strategy for achieving gene of interest (GOI) expression exclusively in targeted, CRE-expressing neurons (adapted from Fenno et al., 2011).

Hence, delivering DIO-flanked, anti-sense sequences encoding tools for neural activity manipulation into animal lines driving CRE expression in a cell-type specific manner leads to the specific expression of gene of interest (GOI) with cell-type resolution.

To add anatomic resolution to the expression of a neuronal modulation tool in genetically-defined neurons, the above-described Cre-loxP technology is combined with stereotaxic delivery of viral vectors aiming at the brain region of interest. Typically, adeno-associated viral vectors (AAV) containing strong promoters such as human elongation factor 1 alpha (EF1α) promoter are commonly used for expression in neurons, being

available anterograde or retrograde ones. These viral vectors are conveniently engineered to contain DIO-flanked, inverted sequences encoding a GOI such as a tool for neural activity manipulation, and stereotaxically delivered into the brain region of interest of animal lines driving CRE expression in the desired neuronal cell-type. Although other cells are transduced, this strategy restricts the expression of the viral vector-encoded GOI exclusively in CRE-positive neurons of the targeted region of interest (Fig. 6).

Manipulation of genetically-defined neuronal subsets has proven to be essential for dissecting neuronal contribution in the control of select behavioral responses. Currently, there are two main functional neuronal manipulation techniques that allow both activation or inhibition with cell-type and spatial resolution: optogenetics and chemogenetics. These techniques are chosen, under several approaches, on the basis of their differences in temporal resolution, being optogenetics in the millisecond (operated by ion channels) and chemogenetics the minute range (based on second messenger signaling) (Vlasov et al., 2018).

1.4.2.2. Optogenetics

Optogenetics allows the modulation of the activity of genetically-defined neuronal populations with the fastest temporal resolution (milliseconds) (Deisseroth, 2011). It relies on light-operated transmembrane channels called opsins expressed along the whole cell membrane of the desired neurons. We distinguish two types of opsins regarding their origin. On the one hand, we can

find type I opsin genes in prokaryotes, algae and fungi (Sharma et al., 2006; Spudich, 2006). On the other hand, type II opsin genes are exclusive of higher eukaryotes in vision-related organs (Shichida et al., 2003). Both of them require retinal —a vitamin A-related cofactor— to result functional, as it acts as an antenna when attached to the opsin for the light-triggered conformational changes of the channel. The resulting functional retinal-opsin complex is named rhodopsin. Unlike type II opsins, type I opsins do not dissociate from its retinal. The covalently-bound retinal is recycled in every photocycle (Haupts et al., 1997)

After discovering type I opsins, optogenetics developed with channelrhodopsin, a blue-sensing channel from the green alga *Chlamydomonas reinhardtii*. Since then, the optogenetic toolbox has grown vastly, including a variety of opsins with different light wavelengths and ion conductance regulated over a great range of speeds (milliseconds to several minutes). Fortunately, they work as a single-component system, which made rhodopsin suitable for its use in all vertebrates, as they naturally contain retinal (Fenno et al., 2011).

Concerning its capacity to activate or inhibit neurons, we classify opsins into two main groups: channelrhodopsins and halorhodopsins. Whereas channelrhodopsins —with ChR2 being commonly used in Neuroscience (Boyden, Zhang, Bamberg, Nagel, & Deisseroth, 2005)— trigger inward cation currents upon illumination of blue light, depolarizing the neuronal membrane and initiating an action potential firing, on the contrary halorhodopsins (eNpHR3.0) (Gradinaru, Thompson, & Deisseroth, 2008;

Gradinaru et al., 2010; Zhao et al., 2008) are chloride pumps that produce inward anion currents to hyperpolarize neurons when yellow light is applied, thus preventing firing (Fenno et al., 2011).

For the light delivery, right after injection of a viral vector encoding the CRE-dependent (DIO-controlled) optogenetic tool gene in the Cre-driver animal line of interest, a fiber optic-containing cannula implantation is required over the desired region. Since the expression of the optogenetic tool take place over the whole cell membrane, the regional resolution of the technique is provided by the illumination cone. While somata manipulation modulate the activity of whole neurons, projection manipulation provides a further resolution to dissect specific circuits in behaving animals. Thus, the location of the fiber optic tip determines the genetically-defined somatic or circuit manipulation.

After opsin expression (normally 3 weeks suffice), behavioral tests can start. Typically, ChR2 are illuminated with 473 nm blue light (Vlasov et al., 2018), while eNpHR3.0, 593nm (Gradinaru et al., 2008). Light intensity, frequency and pulse duration are the three light-pulse-related parameters to be set for specific experiments.

For activation, the usual approach is to reproduce the physiologic firing, where ChR2 is the typical choice if 20-40 Hz firing rate is desired (Boyden et al., 2005). Normally, 5-10 ms light pulses of 1-10 mW intensity suffice (Vlasov et al., 2018). On the other hand, for optogenetic silencing, the use of eNpHR3.0 has been standardized, being activated by green or yellow wavelengths (Gradinaru et al., 2010).

1.4.2.3. Chemogenetics

Chemogenetics is a technique that relies on designer receptors exclusively activated by designer drugs (DREADDs) to manipulate, via G protein-related signalling cascades, the activity of genetically-defined neurons in a CRE-dependent manner. DREADDs can be activating or inhibiting receptors, both modifications from G protein-coupled human muscarinic receptors engineered to show high affinity for a designer drug called clozapine-N-oxide (CNO) while having reduced affinity for their original ligands. The activating DREADD is designed from human M3 muscarinic Gq-coupled receptor (hM3Dq), that in presence of CNO lead to action potentials (Alexander et al., 2009). On the other hand, the inhibiting DREADD has been engineered from human M4 muscarinic Gi-coupled receptor (hM4Di), that silences neuronal activity when CNO is present (Armbruster et al., 2007).

Given their drug-operated nature, DREADDs are exerting their neuronal modulation during several hours, unlike the millisecond temporal resolution from optogenetics. Mice administered intraperitoneally (i.p.) with CNO show effects 10-15 min after injection, with a maximum peak at 45-50 min that during 9 h is gradually reduced to baseline (Alexander et al., 2009). Usually the CNO dose i.p. injected is 0.3–3 mg/kg (Roth, 2016). Nevertheless, microinfusions of CNO with a cannula implantation in a brain region of interest is also a possibility, allowing targeted local terminal modulation. Alternatively, DREADDs expression can be restricted to a select circuit through a combination of a retrograde canine adenovirus encoding CRE (CAV2-Cre) injected in the

projection site with another injection in neuronal somas of an AAV encoding a DREADD gene in a CRE-dependent fashion, in non-transgenic animals (Urban & Roth, 2015). Therefore, a systemic or local CNO administration or the use of a CAV2-Cre-mediated genetic strategy determine the regional resolution of this technique (Vlasov et al., 2018).

There is however a recent concern regarding the dose that needs to be considered. It has been discovered that DREADDs are not activated directly by CNO itself but its metabolized clozapine, which is an antipsychotic with sedative effects. In fact, CNO cannot cross the blood-brain barrier and does not show affinity for DREADDs whereas CNO is rapidly metabolized *in vivo* to clozapine, which can cross the blood-brain barrier and binds to DREADDs with strong affinity. Hence, a reduced dose of CNO is encouraged (Gomez et al., 2017; Roth, 2016; Vlasov et al., 2018).

Interestingly, chemogenetics allows bidirectional manipulation of the same neurons as besides clozapine-operated DREADDs, there are another type of DREADDs that can be simultaneously utilized: salvinorin B (SalB)-operated kappa opioid receptor-based DREADD (KORD). KORDs are activated by SalB and no other endogenous opioids, being recommended for behavioral multiplexing with hM3Dq. However, the pharmacodynamics of SalB are significantly faster than CNO, appearing behavioral changes minutes after i.p. injection up to a maximum of 1 h. Therefore, for a long-lasting neuronal silencing, the CNO-based hM4Di suits best (Vardy et al., 2015).

In general, compared to optogenetics, chemogenetics is more suitable for long-lasting neuronal modulation in vast brain areas, as it does not require fiber optic implantation (Vlasov et al., 2018).

1.4.2.4. Novel tools for genetic identification and interrogation of neural substrates and circuits

Novel neural interrogation techniques open an unprecedented room for understanding the brain. These techniques can be applied for testing hypothesis related to the genetic identity of neural substrates and circuits controlling select MS responses. Under several behavioral assays, optogenetics and chemogenetics approaches are chosen on the basis of the excitatory or inhibitory nature of the neurons to be assessed and their technical features concerning temporal and spatial resolution. Whereas optogenetics allows the fastest temporal resolution, chemogenetics possesses the slowest one. On the other hand, chemogenetics is more suitable for neuronal activity modulation of extensive areas, as it is not limited by an illumination cone.

In global, both techniques can be adapted to probe genetically-defined neurons and circuits. Therefore, to dissect the role of excitatory glutamatergic vestibular neuronal subsets in the regulation of MS-related behavioral responses, it is necessary to address optogenetic and chemogenetic techniques, providing a level of resolution not attained, to date, in the MS field.

As above described, to achieve expression of an optogenetic or chemogenetic tool in genetically-defined neurons of a region of interest, it is required the combination of both Cre-loxP technology with region-targeted stereotaxic AAV injections, using a *Cre*-driver animal line expressing CRE in the neuronal population to be interrogated.

Finally, the identification of specific markers of neuronal (sub)populations is critical for an in-depth dissection of the functional connectome of the VN. To this end, genetic identification of neuronal populations can be achieved by cell-type-specific transcriptomic profiling of ribosome-associated transcripts in the cell types of interest. As such, the RiboTag approach relies on the CRE-dependent expression of a virally-delivered construct encoding the ribosomal subunit *Rpl22* tagged with hemagglutinin A (HA), allowing the immunoprecipitation of ribosome-bound transcripts (Sanz et al., 2009; Sanz et al., 2019; Sanz et al., 2015). The subsequent gene expression analysis yields the identity of the genes enriched in the neuronal population of interest . Hence, the use of mouse lines expressing CRE under the control of this select markers, combined with optogenetics or chemogenetics provides a unique and extremely powerful platform to dissect at the anatomical, genetic, and temporal level, the contribution of discrete VN neuronal populations in MS responses.

2. HYPOTHESIS

The vestibular system is classically associated to spatial orientation and MS. Furthermore, excitatory vestibular neurons are the main neuronal source in the VN. Therefore, glutamatergic vestibular neurons and their subsets and circuits constitute excellent sensory conflict-processing neural candidates, key to elicit MS-like responses.

Hence, we hypothesize that genetically-defined glutamatergic neuronal populations and circuits in the VN are crucial and/or necessary in governing select MS-like responses, namely autonomic regulation and/or aversive learning.

3. OBJECTIVES

Given that excitatory neurons are the main cell type in the VN (Erö et al., 2018) and that provocative stimulus are sufficient to activate glutamatergic VN neurons that in turn project to nuclei such as the PBN (Cai et al., 2007), we proposed the following objectives:

1. Defining if glutamatergic vestibular neurons are sufficient or necessary to eliciting MS-related autonomic responses and CTA, through the combination of a chemogenetic inhibition of glutamatergic vestibular neurons with a physiologic rotational mouse model of MS, in provocative motion or control conditions.

2. Identifying potential genetic markers of glutamatergic vestibular subsets in the VN, through a ribosomal tagged-immunoprecipitation (RiboTag) approach from *Vglut2*-expressing vestibular (VGLUT2^{VN}) neurons.

3. Validating an optogenetic approach for interrogating the *in vivo* function of VGLUT2^{VN} neurons and their subsets in regulating defined MS-related autonomic responses and CTA.

4. Dissecting a genetically-defined, glutamatergic vestibular circuit controlling specific MS responses.

4. METHODS

4.1. Mice

Three mouse strains were acquired from Jackson Laboratory, all of them with C57Bl/6 background:

- *Vglut2*^{iCre} mouse line (MGI:4881727; http://www.informatics.jax.org/allele/MGI:4881727), expressing CRE-recombinase (CRE) only in glutamatergic neurons, through the control of *Slc17a6* promoter that drives the expression of the endogenous vesicular glutamate transporter 2 (Borgius et al., 2010),
- *Cck*^{Cre} mouse line (JAX stock #012706; https://www.jax.org/strain/012706), expressing CRE only in *Cck*-expressing cells, by using the internal ribosome entry site (IRES) following the *Cck* locus (Taniguchi et al., 2011).
- *Crh*^{Cre} mouse line (JAX stock #012704; https://www.jax.org/strain/012704), expressing CRE specifically in *Crh*-expressing cells, relying on an IRES sequence downstream the *Crh* locus (Taniguchi et al., 2011).

Mice were maintained group-housed with a 12:12h light:dark circadian cycle at 22°C, with *ad libitum* access to rodent normal-chow No. 2014 diet (HSD Teklad Inc) and water, unless otherwise stated. For experimental procedures, heterozygous mice for their respective *Cre* allele were selected. To obtain these animals, *Vglut2*$^{iCre/+}$, *Cck*$^{Cre/+}$ or *Crh*$^{Cre/+}$ males were bred to C57Bl/6 females, producing 50% heterozygous *Vglut2*$^{iCre/+}$, *Cck*$^{Cre/+}$ or

Crh$^{Cre/+}$ animals (from now on, Vglut2-cre, Cck-cre or Crh-cre mice). The remaining 50% homozygous wild-type (WT) animals were used specifically for establishing a rotation-based model of MS (as explained in "Behavioral assays") or euthanized by CO_2 overdose.

Sex-balanced mouse groups were established all across experimental procedures, aged 2-7 months-old. Animals were single-housed after surgery and until the end of all experimental procedures. Both experimental and control mice were randomly assigned and simultaneously tested all along behavioral approaches to ensure no session-related differences take place. Sample sizes were determined using power analysis. Animals used per experiment are detailed in figure legends.

Animal husbandry and all animal experiments were carried out in agreement with the Autonomous University of Barcelona-Ethics Committee/Generalitat de Catalunya guidelines and approvals.

4.2. Genotype identification

A 0.5 cm tail snip was obtained from each animal and genotyping identification was run using a polymerase chain reaction (PCR) kit (Phire Tissue Direct PCR Master Mix, F170S, Thermo Scientific), including all reagents required from DNA extraction to electrophoresis gel loading. DNA from tail cut was extracted mixing 0.5 µL of DNA Release Additive and 20 µL Dilution Buffer, heating at 98°C for 2 min and resting at room temperature (RT) for 5 min. Afterwards, a PCR mix was prepared (see Table 1),

including specific primers and thermocycler programs (see Table 2). For Vglut2-cre genotyping, TCTGATGAAGTCAGGAAGAACC forward sequence and GAGATGTCCTTCACTCTGATTC reverse sequence were used; for Cck-cre or Crh-cre genotyping, ATTGCTGTCACTTGGTCGTGGC forward sequence and GGAAAATGCTTCTGTCCGTTTGC reverse sequence were used.

Table 1.- PCR mix conditions for all genotyping.

PCR mix reagents	Volume (µL)
PCR-grade H_2O	7
2X Phire Tissue Direct PCR Master Mix	10
Primer forward (10uM)	1
Primer reverse (10uM)	1
DNA extracted	1
Total	20

Table 2.- PCR conditions for Vglut2-cre, Cck-cre or Crh-cre genotyping.

	Vglut2-cre genotyping			Cck-cre or Crh-cre genotyping	
	Tempe-rature	Time		Tempe-rature	Time
Heated lid	105°C	During all procedure		105°C	During all procedure
Initial denatu-ration	94°C	3 min		94°C	2 min
35 cycles	94°C	30 sec.	30 cycles	94°C	20 sec
	58°C	30 sec.		59.5°C	30 sec
	72°C	1 min.		72°C	30 sec
Final elongation	72°C	5 min.		72°C	10 min
Final hold	4°C	Until removal		4°C	Until removal

PCR products were separated by acrylamide gel electrophoresis (200 V for 40 min) using a DNA ladder as reference (O'GeneRuler Express DNA ladder, SM1563, Thermo Scientific). Vglut2-cre genotypes were determined with the presence of a band of ~500 base pairs (bp), while Cck-cre or Crh-cre genotypes were identified with a band of ~200 bp corresponding to *Cre* expression. Absence of any band meant WT genotype.

4.3. Viral vector production

For tracing purposes, CRE-dependent, EF1α-promoter-driven pAAV synaptophysin-green fluorescent protein (Syn-GFP) plasmid was used (Carter et al., 2013). For chemogenetic purposes, CRE-dependent, human synapsin-promoter-driven pAAV hM4Di-mCherry plasmid was employed (Addgene plasmid #44362; http://n2t.net/addgene:44362; RRID:Addgene_44362). For optogenetic approaches, CRE-dependent, EF1α-promoter-driven pAAV EYFP (Addgene plasmid #27056; http://n2t.net/addgene:27056; RRID:Addgene_27056) or ChR2-YFP (Addgene plasmid #100056; http://n2t.net/addgene:100056; RRID:Addgene_100056) plasmid were used. For genetic identification of neuronal subsets, EF1α-promotor-driven pAAV RiboTag plasmid was used (Sanz et al., 2015).

Recombinant adeno-associated viral vectors (AAV) were then produced in human embryonic kidney (HEK293T) cells, with anterograde, neurotrophic type 1 (AAV1) coat proteins and packaging on-purpose specific genes. Purification was achieved by several sucrose and CsCl gradient centrifugations and a final

re-suspension in 1x Hanks Balanced Saline Solution (HBSS) at 2 x 10^9 viral genomes/µL of viral titer. AAVs were aliquoted and stored at -80°C until stereotaxic injection (Quintana et al., 2012; Sanz et al., 2015).

4.4. Stereotaxic surgery

All surgeries were performed under aseptic conditions. Animal anaesthesia was induced with 5% isoflurane/O_2 and maintained with 1-1.5%/O_2. Thereupon, analgesia (5 mg kg^{-1} ketoprofen; Orudis 100 mg; Sanofi-aventis, S.A) and ocular protective gel (Viscotears®, Bausch + Lomb España S.A.) were applied. Mice were then placed over a heating pad equipped in a robot-operated, 3-dimensional (stereotaxic) frame (NEUROSTAR) for intracerebral viral delivery. Normalization of stereotaxic coordinates was applied to reduce inter-individual variability through a correction factor (Bregma-Lambda/4.21) in light of the Paxinos and Franklin's Mouse Brain Atlas (Paxinos & Franklin, 2007). After small craniotomy, intracranial AAV injections were unilaterally (right side) or bilaterally delivered into the VN (antero-posterior (AP), –5.65 mm; medio-lateral (ML), ± 0.90 mm; dorso-ventral (DV), –4.60 mm from bregma, creating a small pocket from –4.60 to –4.70 mm) at a constant rate of 0.1 µL/min for 3.5-4.0 min (0.35-0.40 µL per injection site) using a 32G blunt needle (7803-04, Hamilton) coupled to a 5 µL-Hamilton syringe (7634-01). After the infusion, the needle was maintained in place during 6 min to allow proper diffusion. Subsequent needle withdrawal

was performed at 1 mm/min, to ensure minimal off-target viral leakage.

4.4.1. Cell type-specific neuronal tracing

For tracing purposes, Vglut2-cre and Cck-cre mice were infused into the right VN with AAV1-EF1α-DIO-Synaptophysin-GFP, an anterograde viral vector encoding, in a CRE-dependent manner, a synapse-directed, GFP-fluorescent fused synaptophysin protein (Syn-GFP) (Carter et al., 2013). Animals were euthanized by CO_2 overdose 3 weeks after surgery for subsequent histological procedures.

4.4.2. Chemogenetics

Vglut2-cre, Cck-cre and Crh-cre mice were bilaterally infused in the VN with 0.35µL (0.70µL in total) of AAV1-hSyn-DIO-hM4Di-mCherry (from now on, $VGLUT2^{VN}$ DREADDs, CCK^{VN} DREADDs or CRH^{VN} DREADDs mice, respectively). CNO or vehicle (Veh) were prepared as follows. 10 mg of dried CNO (TO-4936/10 MG, Tocris) was dissolved in 100 µL of dimethyl sulfoxide (DMSO) and then aliquoted and stored at -20°C (stock solution). On the day of the experiment, a 1:1000 dilution of stock CNO solution was prepared in saline solution, achieving a working solution of 1mg CNO mL^{-1} with 0.1% DMSO proportion. On the other hand, Veh working solution consisted in a DMSO 1:1000 dilution in saline solution. The prepared CNO or Veh were administered via intraperitoneal (i.p.) injection 35 min prior to rotational or control

stimulation (see section 4.5. Rotations paradigm) on the basis of 10uL g^{-1} animal weight of the respective working solution.

4.4.3. Optogenetics

Vglut2-cre and Cck-cre mice were infused in the right VN with 0.4 µL AAV1-EF1α-DIO-ChR2-YFP (ChR2, activation groups) or AAV1-EF1α-DIO-eYFP (YFP, control groups). Then, a multimode mono fiber optic-containing cannula (200 µm fiber core diameter, 0.22 numeric aperture; 2.5 mm ferrule diameter; model SF270-10 or custom-made, Thorlabs) was implanted over the right VN of Vglut2-cre or Cck-cre mice (from now on, $VGLUT2^{VN}$ optoVN or CCK^{VN} optoVN mice, respectively) or over the right PBN of Cck-cre animals (CCK^{VN} optoPBN mice) (AP, –4.65 mm; ML, +1.70 mm; DV, -3.00 mm). Only one cannula was implanted per mouse. Cannula was fixed to the exposed skull with a layer of adhesive cement (Super-Bond C&B, Sun Medical) and dental acrylic cement (Rebaron Pink Powder 100 g and Rebaron Self-Curing Acrylic for Direct Rebasin Liquid 100 g, GC Corporation) until covering half of the ferrule. Skin was affixed to the cement with tissue adhesive (Vetbond, 3M). Blue 473-nm laser light was produced by a DPSS Laser System (LRS-0473-GFM-00100-05 Laserglow) and driven by a fiber optic patch-cord (200 µm core diameter, 0.22 numeric aperture; FT030 protection unless otherwise stated, Thorlabs). Light intensity was set at 10 mW measured by a photometer (PM160T, Thorlabs) at the tip of a non-implanted fiber optic cannula attached to the patch-cord. To deliver illumination to the right VN (in case of Vglut2-cre or Cck-

cre mice) or right PBN (in case of Cck-cre mice), the patch-cord was connected to the implanted fiber optic-containing cannula through a ceramic sleeve. A pulse generator (33500B Series Trueform, Keysight) was used to adjust laser output to deliver 40 Hz, 10-ms, pulse trains during 5 min to all optogenetic mice.

4.4.4. RiboTag-mediated genetic identification of neuronal subsets

For genetic identification of neuronal subsets, Vglut2-cre mice were bilaterally infused in the VN with 0.4 µL of AAV1-DIO-RiboTag (Sanz et al., 2015). Animals were euthanized by CO_2 overdose 3 weeks after surgery for subsequent RiboTag-related procedures as described in section 4.8. RiboTag assay.

4.5. Rotation paradigm

During the 2 consecutive days prior to each rotation-related stimulation, animals were daily habituated to 4 min of physical restriction using a 50-mL Falcon tube per animal coupled to a custom-made rotary device (up to 2 animals per device), without applying any rotation yet (from now on, this will be referred as rotary-device habituation). Afterwards, rotational or control stimuli were applied, consisting on receiving 4 min at 75 rpm (every 1 minute: 55 sec @ 75 rpm, 5 sec of deceleration and full stop; radius: 10.5 cm) or 4 min at 0 rpm, respectively, unless otherwise stated. For chemogenetics experiments, rotational stimulus was applied to both CNO and Veh groups.

4.6. Behavioral assays

Each animal was subjected to every test as follows, in order of increasing stressfulness: first, all of them to open-field test, then food intake test or CTA, or conversely CTA or intake for counterbalancing, and finally telemetric temperature sensor implantation and temperature monitoring. In case of animals subjected to surgeries, a post-surgical recovery was allowed for at least 3 weeks prior any behavioral test. Detailed behavioral procedures are addressed below.

4.6.1. Open-field test

The open-field (OF) consisted in a non-covered, white methacrylate box (56 x 36.5 x 31 cm) that allows for video-recording during animal OF exposition.

For rotation-based experiments, to first establish a rotation stimulus, mice were subjected to different intensities and durations, including 2min@130rpm+3min@75rpm, 4min@75rpm, 4min@65rpm, 2min@65rpm, compared to a control, 4min@0rpm group and then placed in OF during 60 min. Other cohorts were individually exposed for 5 min to the OF (pre-spin OF test), then they were removed to be set in the rotary device for receiving rotational (4min@75rpm) or control stimulation. Finally, individual mice were re-exposed to the OF (post-spin OF test) for 60 min to register changes between “spin” vs. “no-spin” animals.

For chemogenetic assays, VGLUT2^{VN} DREADDs, CCK^{VN} DREADDs or CRH^{VN} DREADDs mice were subjected to pre- and

post-spin OF tests following the same procedure as in rotation-based experiments except for the i.p. injection of CNO or Veh 30 min before the pre-spin OF (5 min). Immediately after rotational stimulus, at 35 min after injection, the post-spin OF (60 min) was run. Two weeks after, the same procedure (excluding habituations) was repeated inverting the injection of CNO or Veh, therefore each animal was its own control.

For optogenetic assays, VGLUT2^{VN} optoVN, CCK^{VN} optoVN or CCK^{VN} optoPBN mice, on the day of experiment, were plugged to a fiber optic patch-cord and immediately after subjected to 60 min of a single OF test, comprising 5 min of pre-laser period, 5 min of laser period and 50 min of post-laser period.

Afterwards, video-tracking detection is applied to all video-recordings using Ethovision XT 11.5 Software (Noldus Information Technology) for quantifying spontaneous ambulatory activity.

4.6.2. Appetite-suppression test

Animals were individually placed in a metabolic cage (Oxyletpro-Physiocage with an LE1335 top, Panlab) enabling real-time quantification of food and water intakes. Mice were allowed 2-4 days for cage habituation, with *ad libitum* access for normal-chow diet (unless otherwise stated) and water. Prior to each session, all animals underwent overnight food deprivation, coinciding food re-exposition with the onset of dark cycle. Two sessions of stimulation were applied on every animal, with 48h of rest between them, to obtain technical replicates, except for DREADDs-injected

animals, where the injection of CNO or Veh was inverted each session, being each animal its own control.

For rotation-based experiments, WT mice were subjected to rotational or control stimulus –during this period mice are removed from metabolic cage and cannot eat– followed by 90 min of post-stimulation period.

For chemogenetics experiments, *Vglut2*-VN DREADDs mice were injected i.p. with either CNO or Veh and 35 min after. Subsequently, rotational stimulation was applied and animals were placed back in the metabolic cage for an additional 90-min period. The same protocol was re-run in another session after 48h, switching the injection of Veh or CNO for each animal.

As for optogenetic experiments, VGLUT2^{VN} optoVN, CCK^{VN} optoVN and CCK^{VN} optoPBN mice were subjected in both two sessions to the following protocol: at least 1 h before stimulation, animals were plugged to the fiber optic patch-cord without FT030 protection, to reduce movement restrictions. Then, normal-chow was presented and laser stimulation was applied following a final post-laser period of 85 min. Water intake was also monitored on the same basis only in VGLUT2^{VN} optoVN mice. In other VGLUT2^{VN} optoVN cohorts, chocolate-flavoured, highly-palatable liquid diet (ENSURE Nutrivigor, Abbott) was first exposed during the cage habituation period and in the subsequent experimental sessions, while maintaining normal-chow diet.

Food and water intake were expressed in bins of 5 min of cumulative intake using the Metabolism software version v3.0.00 (Panlab). Specific details for each experiment are provided below.

4.6.3. Surgical implantation of telemetry devices and temperature monitoring

Analgesia and ocular protective gel were provided to all animals as in the stereotaxic surgery. Right after, anesthetized mice (isoflurane 5% induction, 1.5% maintenance) were aseptically implanted into the peritoneum with telemetric temperature transmitters (15.5mm x 6.5mm, G2 E-Mitter, STARR Life Sciences Corp.). Animals were allowed to recover for 2 weeks in their home cages. Afterwards, cages were placed on telemetry receivers (ER4000 Energizer/Receiver, STARR Life Sciences Corp.). Body core temperature was monitored using the VitalView software version 5.0 (STARR Life Sciences Corp.) in unrestrained conditions (unless otherwise stated) under controlled ambient temperature (22°C). Temperature data was expressed in bins of 5 min and normalized from the bin prior to stimulation. All recordings started when animals were resting. Specific details for every experiment are provided below.

For rotational-based experiments, resting WT animals were individually monitored for 25 min, then they were inserted into the rotary device for 15 min followed by the 4 min rotational or control stimulation. Afterwards, mice were monitored for additional 66 min (70 min from stimulus onset).

For chemogenetic experiments, VGLUT2^{VN} DREADDs, CCK^{VN} DREADDs and CRH^{VN} DREADDs mice were subjected to two experimental sessions separated with 24h for rest. Each session comprises the same features as in rotational experiments, except for injecting CNO or Veh 35 min before the rotational stimulation

and applying that rotational stimulus to all DREADDs animals. In the second session, the compound injected was switched for each animal, to make each animal its own control.

For optogenetic experiments, resting VGLUT2^{VN} optoVN, CCK^{VN} optoVN and CCK^{VN} optoPBN mice were individually monitored for 25 min, then they were subjected to handling during 10 min to initially synchronize body temperature physiology, 5 min of resting followed by 5 min of laser stimulation. Finally, mice were monitored for additional 65 min (70 min from laser onset). Additionally, VGLUT2^{VN} optoVN mice were inserted in 50-mL Falcon tubes (1 animal per tube) to ensure physical movement restriction while allowing for fiber optic patch-cord plugging. The protocol applied was 5 min of temperature monitoring followed by physical restrain and a subsequent 5 min pre-laser period, then 5 min laser period and finally 15 min post-laser period.

4.6.4. Conditioned taste aversion test

For the CTA test, a two bottle-based protocol was used (Chen et al., 2018). Animals were individually placed on a custom cage with angular ports for two liquid-containing bottles. *Ad libitum* water access was provided for 2 days of habituation. Next, animals were habituated for 3 days (D1, D2 and D3) to restricted access for both water-containing bottles: 30 min access in the morning, 30-60 min in the afternoon. After that, in the days D4 and D6, conditioning sessions in the morning were applied using high-preference 5%-sucrose water solution only in one out of two bottles, allowing the animal to choose, and pairing it with specific stimulus (see below

for specific conditioning-session details). D5 and D7 were resting sessions, maintaining the restriction as in D1, D2 and D3. The test day, D8, was repeated as in the conditioning sessions, except for no stimulation or i.p. injection were applied. To measure whether aversive learning (avoidance of high-preference solution) had taken place, sucrose preference value was calculated using the following formula:

$$\text{Sucrose preference} = \frac{\text{Sucrose solution consumption}}{\text{Total liquid consumption}}$$

A value of 1 means maximum sucrose preference and 0, minimum sucrose preference, where values inferior than 0.5 are considered as CTA establishment. During two bottle expositions, biased animals showing strong preference for one bottle regardless of its content were discarded from the study.

For rotational experiments, WT mice were subjected to rotary-device habituation in the 2 consecutive days (D2 and D3) before the first conditioning session. In the D4 and D6, right after exposure to 5%-sucrose water solution, mice were subjected to rotational or control stimulus.

For chemogenetic experiments, *Vglut2*-VN DREADDs animals were subjected to the same protocol as for rotation-based experiments, except for applying, in both conditioning sessions, injection of CNO or Veh 5 min before starting each 30-min sucrose solution exposition and, right after, rotational stimulations for all mice.

As for optogenetic experiments, VGLUT2^{VN} optoVN, CCK^{VN} optoVN and CCK^{VN} optoPBN mice were connected to the fiber optic patch-cord in the D4 and D6, right after finishing the 30 min sucrose solution vs. water exposition and then a 5 min laser stimulus was delivered.

4.7. Histology

4.7.1. Immunohistochemistry

Mouse brains were freshly dissected following euthanasia by CO_2 overdose and fixed overnight at 4°C, 4% paraformaldehyde (PFA) in 1X phosphate-buffered saline (PBS tablets, 524650-1EA; EMD Millipore, USA). After fixation, brains were cryoprotected using 30%-sucrose, 1X-PBS solution during 24h and stored at -80°C. 30 µm-thick coronal sections were obtained on a cryostat (-21°C chamber, -19°C brain) and free-floating stored at -20°C in anti-freezing solution of 1X PBS:ethylene glycol:glycerol 0.75:1:0.75 (ethylene glycol, Sigma 102466; glycerol, Sigma G7757/G5516). To start the free-floating immunohistochemistry procedure, sections were washed at RT 3 times for 5 min in 0.1%-Triton X, 1X PBS solution and blocked with 10% normal donkey serum (NDS) in 1X PBS. For all sections, primary antibodies were incubated overnight in 1%-NDS, 1X PBS solution at 4°C, with soft agitations to reduce nonspecific antibody attachments. After washing at RT in 0.1%-Triton X, 1X-PBS solution 3 times for 5 min, secondary antibodies conjugated to select fluorophores were incubated in 1%-NDS, 1X PBS solution for 1 h at RT with soft agitations. Sections were washed in 1X PBS and dropwise-

distilled water and mounted on a crystal slide (Superfrost Plus, Thermo Scientific) with DAPI Fluoromount-G™ (Cat. # 17984-24, Electron Microscopy Sciences) to label cell nuclei. pH was maintained at 7.2-7.4 for the entire procedure.

For connectomic experiments, brain sections were stained with anti-GFP primary antibody (chicken polyclonal, 1:2000, ab13970, Abcam) and green-labelled secondary antibody (goat polyclonal anti-chicken, AlexaFluor 488, 1:500, ab150169, Abcam).

For chemogenetic brain sections, anti-mCherry primary antibody (rabbit polyclonal, 1:2000, ab167453, Abcam) and red fluorophore-conjugated secondary antibody (donkey anti-rabbit, AlexaFluor 555, 1:500, A31572, Invitrogen) were used.

For optogenetic brain sections, anti-GFP and anti-GFAP primary antibodies (respectively, chicken polyclonal, 1:2000, ab13970, Abcam; rabbit polyclonal, 1:1000, PA1-10019, Invitrogen) were used and conjugated to, respectively, green and red fluorophore-conjugated secondary antibodies (respectively, goat polyclonal anti-chicken, AlexaFluor 488, 1:500, ab150169, Abcam; donkey polyclonal anti-rabbit, AlexaFluor 594, 1:500, A21207, Invitrogen).

4.8. RiboTag assay

Punches obtained from the VN of Vglut2-cre mice expressing a virally-delivered RiboTag construct in Vglut2-VN neurons were pooled, homogenized and centrifuged in 1 mL of buffer following published methods (Sanz et al., 2009). 800 µL from the resulting cleared lysate was incubated with 4 µL of anti-HA antibody (MMS-

101R, 2–3 mg/ml; Covance) during 4 h at 4°C, while the remaining 200 µL of lysate were kept as input sample (I). Subsequently after incubation, 300 µl of protein A/G magnetic beads (Thermo Scientific) was added and incubated with rotation overnight at 4°C. A high salt buffer was used for washing the immunoprecipitates (IPs). Then, RNA extractions from I and IPs were performed as previously described(Sanz et al., 2019).

4.8.1. Microarray analysis

Comparative IPs vs. I analyses were executed from RNA (10 ng) previously amplified using the Ovation Pico SL WTA system (NuGEN). Sufficient amplification quality of the resulting cDNA was checked by qPCR analysis using the QuantiTect kit (Qiagen) prior biotinylation as described in the EncoreIL biotinilation kit (NuGEN). Quantification and product size distribution of the biotinylinated cDNA was determined by using 2100 Bioanalyzer system with the RNA 6000 Nano chips (Agilent Technologies). 750 ng of biotinylated cDNA was hybridized to MouseRef-8 v2 expression beadchips (Illumina) at 48°C for 16 h. Subsequent washing and analyses were performed following the manufacturer's instructions. Signal was measured by using a BeadArray Reader (Illumina).

4.9. Statistics

For behavioral tests (except pre-spin OF and CTA tests), two-way ANOVA tests and Sidak's multiple comparisons test were applied

by using GraphPad software (Prism 6 for Windows), with rotation or treatment/stimulation as parameters. Data differences associated to P-values inferior than 0.05 were considered statistically significant.

Regarding the pre-spin OF and CTA tests, 2 groups were compared, where the fixed effect was the rotational vs. control stimulation or CNO vs. Veh hM4Di-mediated neuronal inhibition. With one independent factor —the fixed effect—, 2-group datasets were analyzed through unpaired (in case of rotational experiments) or paired (chemogenetics experiments) parametric t tests, to determine two-tailed P-values. With 95% confidence level, data differences associated to P-values inferior than 0.05 were considered statistically significant.

Differencial expression analyses were obtained through the GenomeStudio data analysis software (Illumina), by applying average normalization, the Illumina custom error model and testing corrections (the Benjamini and Hochberg false discovery rates). A differential score of >13 ($p < 0.05$) was established for transcript.

5. RESULTS

5.1. VGLUT2^{VN} neurons are necessary to elicit MS-related autonomic regulation

5.1.1. Rotational stimulus induces MS-like signs in mice

To assess the necessity of VGLUT2^{VN} neurons in provoking MS-like responses, first it was required to establish a physiological model capable of inducing MS. To that end, a custom-designed rotary device was employed, to which WT mice were previously habituated (Fig. 7A).

Since a reduction in ambulatory activity is a clear hallmark of MS (Fuller et al., 2002; Money, 1970; Nalivaiko, 2018; Ngampramuan et al., 2014), we first performed an Open Field test (OF) to evaluate spontaneous locomotion in mice. Different modalities for increasing rotational intensities and duration were tested in OF. First, groups subjected to 65 rpm either during 2 or 4 min showed 33% of resilient animals. Subsequently, we could identify that a 4 min at 75 rpm combination was sufficient to induce a decrease in spontaneous ambulatory activity in all tested animals, while showing a recovery after 20 to 25 minutes after the spin. Finally, animals receiving a 2-min rotation at 130 rpm followed by a 3-min rotation at 75 rpm showed a robust decrease in ambulatory activity, consistently lasting for well over 1h. On the other hand, animals placed in the rotation device for 4 minutes without any rotational input showed normal locomotion in the OF, indicating that the hypolocomotive behavior was due to the rotational stimulation rather than a unspecific lack of exploratory behavior

(Fig. 7B). Hence, a 4-min, 75 rpm paradigm (spin) was selected for further testing to evaluate other MS-like responses.

Once the rotation paradigm had been established, in different cohorts, normal ambulatory activity in both WT groups was verified through a 5-min OF test before the use of the device (Fig. 7C). After spin, animals were re-exposed to the same OF for an additional 60-min period, revealing again the significant long-lasting decrease in ambulatory activity, consistent with MS (Fig. 7D).

Subsequently, since appetite suppression is a typical response of MS (Abe et al., 2010; Fuller et al., 2002; Money, 1970; Nalivaiko, 2018; Ngampramuan et al., 2014), food-deprived mice were exposed to rotational or control stimulations. Indeed, a significant decrease in food intake, with total food-intake suppression during 35 min, was observed after spin stimulation when compared to controls (Fig. 7E).

Finally, loss of body core temperature is a classical MS response (Fuller et al., 2002; Money, 1970; Murakami et al., 2002; Nalivaiko, 2018; Ngampramuan et al., 2014). Consistently, a sustained and significant reduction in body core temperature resulted after rotation compared to controls (no-spin), with a maximum difference among groups of 4°C after ~17.5 min from rotation onset (Fig. 7F).

Overall, these results highlight that our physiological rotational model can induce MS-like responses.

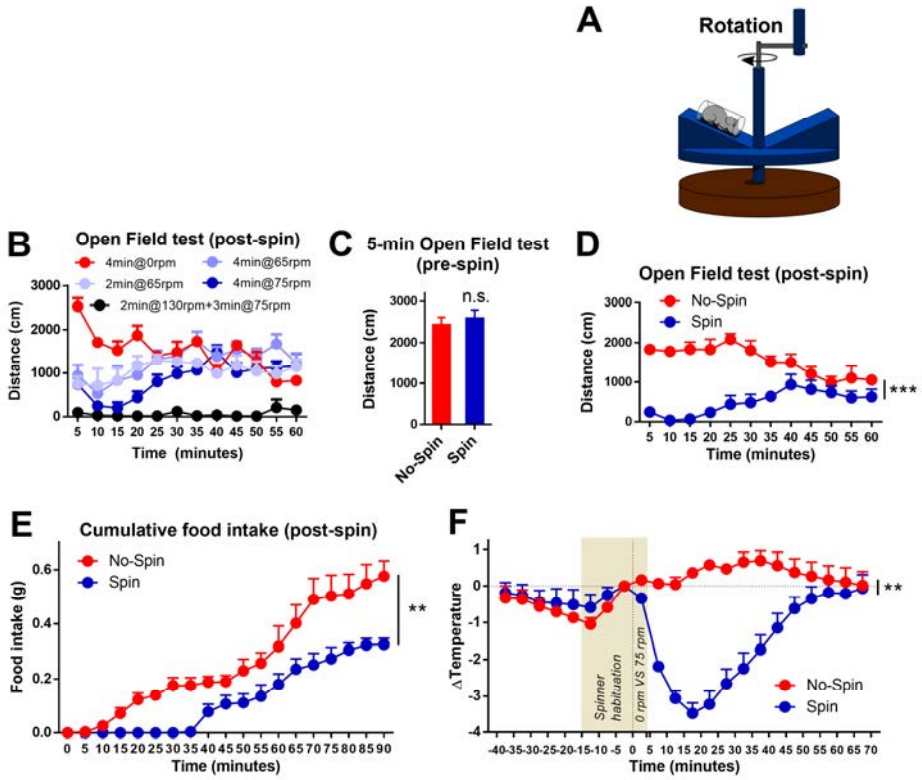

Fig. 7. – A physiological rotation-based model of MS. A) WT mice were subjected to rotational stimulus using a custom-made rotary device, radius 10.5 cm. B) Trials of different modalities of rotational intensities and durations leading to the establishment of 4 periods of 55 sec@75 rpm plus 5 sec@0 rpm up to a total of 4 min as the most robust rotational stimulation (Spin from now onwards) when compared to the 4 min@0 rpm of the No-Spin, control group (2min@130rpm+3min@75rpm group n=2; 4min@75rpm group n=6; 4min@65rpm n=6; 4min@0rpm group n=6; 2min@65rpm group n=6; two-way ANOVA, P-value<0.001). C) Spontaneous ambulatory activity of WT mice was assessed before spin or control stimulation through a 5-min Open Field test (Spin group n=6; No-Spin group n=6; t test, P-value>0.05). D) Traveled distance during 1 h of Open Field test after spin or control stimulation (Spin group n=6; No-Spin group n=6; two-way ANOVA, P-value<0.001). E) Cumulative food intake after spin or control stimulation in food-deprived animals (Spin group n=6; No-Spin group n=6; two-way ANOVA, P-value<0.01). F) Body temperature before and after spin or control stimulation (Spin group n=5; No-Spin group n=5; two-way ANOVA, P-value<0.01).

5.1.2. Chemogenetic inhibition of VGLUT2^{VN} neurons prevents MS-like autonomic responses

Since excitatory neurons are the main neuronal source in the VN (Erö et al., 2018) and neurochemically-characterized, glutamatergic VN neurons are activated after provocative motion (Cai et al., 2007), we moved then to assess the necessity of genetically-defined glutamatergic VN neurons in eliciting MS autonomic responses. Specifically, *Vglut2* (*Slc17a6*) neuronal marker was selected due to its expression in the VN (Ng et al., 2009) and the availability of a *Vglut2*^{iCre} mouse line (Borgius et al., 2010).

To test whether VGLUT2^{VN} neurons are necessary in eliciting MS-like autonomic responses, we expressed the inhibiting DREADD hM4Di-mCherry bilaterally in the VN. Subsequently, animals received either CNO or Veh i.p. and were exposed to our validated physiological provocative stimulation during hM4Di-mediated, VGLUT2^{VN} neuronal inhibition (Fig. 8A), under several behavioral tests. Correct targeting of VGLUT2^{VN} neurons expressing hM4Di-mCherry was verified after finishing all tests by IHC for red signal amplification with anti-mCherry antibody (Fig. 8B).

Targeted inhibition of VGLUT2^{VN} neurons did not induce significant effects on locomotion prior to spin stimulation (Fig. 8C). However, inhibition of VGLUT2^{VN} neurons prevented spin-induced decreases in ambulatory activity (Fig. 8D), appetite suppression (Fig. 8E) and almost completely prevented MS-related decrease in body temperature (Fig. 8F). Noteworthy, there is an initial decrease in body temperature in hM4Di-injected mice (Fig. 8F),

suggesting that other VN neuronal populations may be involved in the early spin-induced drop in body temperature. Hence, these results suggest that VGLUT2^{VN} neurons are necessary to promote the development MS-like autonomic responses elicited by rotational stimulation.

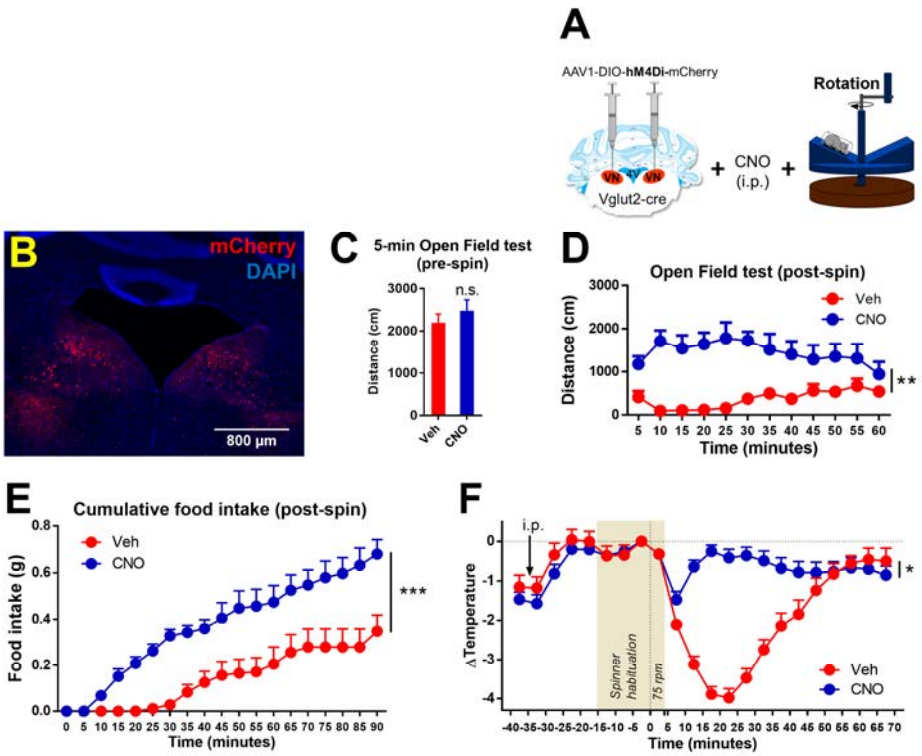

Fig. 8. – Restricted DREADDs-mediated bilateral inhibition of VGLUT2^{VN} neurons prevents MS-like autonomic regulation. A) Vglut2-cre mice were bilaterally injected in the VN with AAV1 encoding hM4Di-mCherry in a CRE-dependent manner. Subsequently, mice were injected with CNO or Veh (i.p.) and subjected to rotational stimulus under different behavioral tests. B) Fluorescence images revealing red-labelled, hM4Di-mCherry-expressing VGLUT2^{VN} neurons. Endogenous signal was amplified using anti-mCherry IHC (scale bar: 800 µm). C) Total distance in a 5-min Open Field test after CNO or Veh i.p. injection, before rotational stimulation (CNO group n=10; Veh group n=10; t test,

P-value>0.05). D) Total distance traveled in a 60-min Open Field test after spin stimulation (CNO group n=10; Veh group n=10; two-way ANOVA, P-value<0.01). E) Food intake after spin stimulation in food-deprived mice (CNO group n=7; Veh group n=7; two-way ANOVA, P-value<0.001). F) Body temperature during CNO or Veh i.p. injection and spin stimulation (CNO group n=4; Veh group n=4; two-way ANOVA, P-value<0.05).

5.2. Optogenetic activation of VGLUT2^{VN} neurons is sufficient to induce MS-like autonomic regulation

Nauseogenic responses can be obtained after unilateral inner ear caloric stimulation (Lidvall, 1962). Analogously, to test whether VGLUT2^{VN} neuronal activation is sufficient to induce MS-like autonomic responses, we optogenetically induced a unilateral VN stimulation in VGLUT2^{VN} neurons. To that end, Vglut2-cre mice received a unilateral injection of AAV1 expressing a CRE-dependent ChR2-YFP (photoactivation) or YFP construct (control) in the right VN. Subsequently, a fiber optic-containing cannula was implanted in the same coordinates (Fig. 9A). 3 weeks post-surgery were allowed to sufficiently express ChR2 prior any behavioral test. After finishing all behavioral tests, proper viral targeting and fiber optic tip placement were respectively analyzed through IHC with anti-GFP antibody to amplify ChR2-YFP green signal and anti-GFAP antibody (against red-labelled secondary antibody) to reveal fiber optic-associated inflammatory trace (Fig. 9B).

As described in the previous sections, a battery of MS-relevant tests was applied. To mimic the reported physiological firing rate of VN neurons (Lin et al., 1993; Waespe et al., 1979), a 5-min, 40Hz-optogenetic stimulation pattern was selected.

Photoactivation lead to a significant decrease in spontaneous ambulatory activity in the ChR2 group compared to YFP controls, consistent with the results obtained after rotational stimulus (Fig. 9C). Furthermore, ingestion of low-palatable, regular chow as well water intakes after optogenetic VGLUT2^{VN} activation was significantly decreased, both intakes tipically completely suppressed during for the first 30 min from laser onset (Fig. 9D and E). Noteworthy, a normal feeding pattern was observed after presentation of highly-palatable, chocolate-flavoured drink to a separate cohort of laser-stimulated ChR2, compared to YFP-injected mice (Fig. 9F), thus ruling out physical inability to feeding but rather a lack of motivational drive to eat regular chow or water. Finally, temperature changes were monitored during handling and photostimulation, showing a significant decrease, with a maximum of 3°C drop after 17.5 min from laser onset (Fig. 9G). To rule out that optogenetic-induced loss of body core temperature was due to a reduction in ambulatory activity in ChR2 group, an additional optogenetic stimulation was applied under physical restrain. After laser application in physically-restrained mice, body temperature was increased in YFP-injected mice, likely due to restrain-induced stress responses. On the other hand, ChR2-injected mice still showed a significant loss of body temperature coincident with photostimulation (Fig. 9H), ruling out the ambulatory activity contribution in post-stimulus thermal differences. Therefore, these results highlight a role of VGLUT2^{VN} neurons in MS neurobiological regulation.

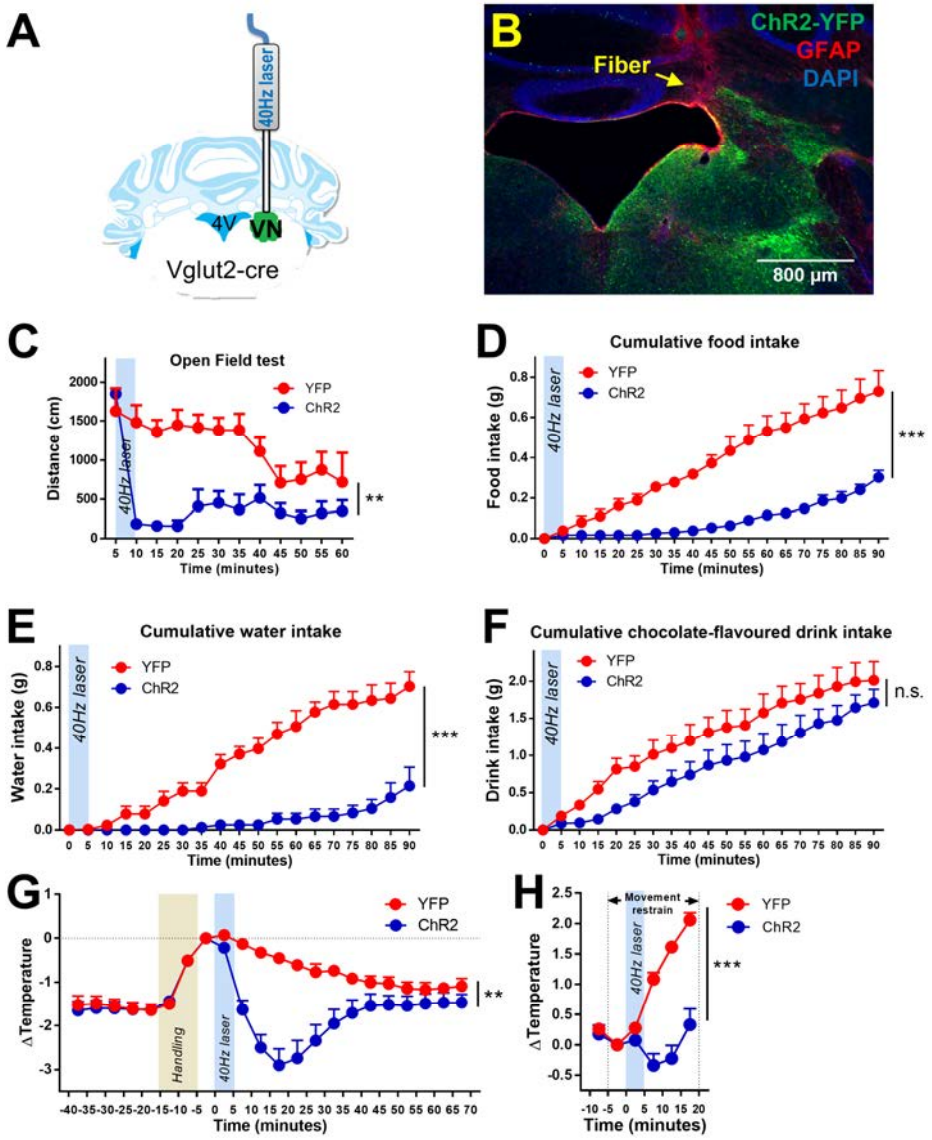

Fig. 9. – Restricted optogenetic activation of VGLUT2^{VN} neurons induces MS-like autonomic responses. A) Vglut2-cre mice were unilaterally injected in the right VN with AAV1 encoding ChR2-YFP or YFP in a CRE-dependent manner, followed by fiber optic implantation over the right VN to deliver a 40 Hz, 10 ms, 10 mW, 5 min, 473 nm light pulses under different behavioral approaches. B) Fluorescence microscopy image showing VGLUT2^{VN} neuronal targeting and fiber optic tip placement by anti-GFP (green), anti-GFAP (red) and DAPI (blue) IHC

(scale bar: 800 µm). C) Open Field test showing traveled distance before and after laser stimulation (ChR2 group n=7; YFP group n=5; two-way ANOVA, P-value<0.01). D) Normal-chow food intake from laser onset in 24-h-fasted animals (ChR2 group n=6; YFP group n=6; two-way ANOVA, P-value<0.001). E) Water intake from laser onset in 24-h-fasted mice (ChR2 group n=6; YFP group n=6; two-way ANOVA, P-value<0.001). F) Highly-palatable, chocolate-flavoured drink intake from laser onset in food-deprived animals (ChR2 group n=6; YFP group n=6; two-way ANOVA, P-value>0.05). G) Freely-moving, telemetric monitoring of body core temperature before handling and before and after laser stimulation (ChR2 group n=8; YFP group n=8; two-way ANOVA, P-value<0.01). H) Telemetric monitoring of body core temperature before and after movement restriction and photostimulation (ChR2 group n=5; YFP group n=5; two-way ANOVA, P-value<0.001).

5.3. Identification of a *Cck*-expressing VGLUT2^{VN} subpopulation

To identify genetically-defined VGLUT2^{VN} neuron subpopulations, we took advantage of the RiboTag approach (Sanz et al., 2009), a molecular profiling approach that allows the cell type-specific immunoisolation of polysome-associated transcripts (Fig. 10A). Vglut2-cre mice were bilaterally injected in the VN with an AAV1 expressing the RiboTag construct, that allows the expression, in a CRE-dependent manner, of a *Rpl22* ribosomal subunit with a human influenza hemagglutinin HA tag (Sanz et al., 2019, 2015). 3 weeks after the injection, animals were euthanized, and the VN were homogenized. Subsequent immunoprecipitation (IP) and purification of ribosome-bound transcripts was achieved taking advantage of the hemagglutinin (HA) tag selectively expressed in the ribosomes of VGLUT2^{VN} neurons. The identification of markers for different VGLUT2^{VN} neuron subpopulations was

accomplished by performing differential expression analysis (microarray) in RNA samples extracted from the RiboTag immunoprecipiates (IP; containing polysome-associated mRNAs from VGLUT2^{VN} neurons) and the input (I) of the immunoprecipitation (containing RNA from all the different cell types in the VN). Differential microarray analysis confirmed specific enrichment for *Slc17a6* (VGLUT2), and depletion for inhibitory neuron (*Gad2*) and non-neuronal markers (*Cnp*, *Gfap*) in the RiboTag IPs, and revealed significant enrichment for candidate VGLUT2^{VN} neuron subpopulation markers such as *Cck*, *Crh*, *Adcyap1*, *Gal*, *Coch*, *Cbln1*, *Cbln2* and *Cbln3* (Fig 10B).

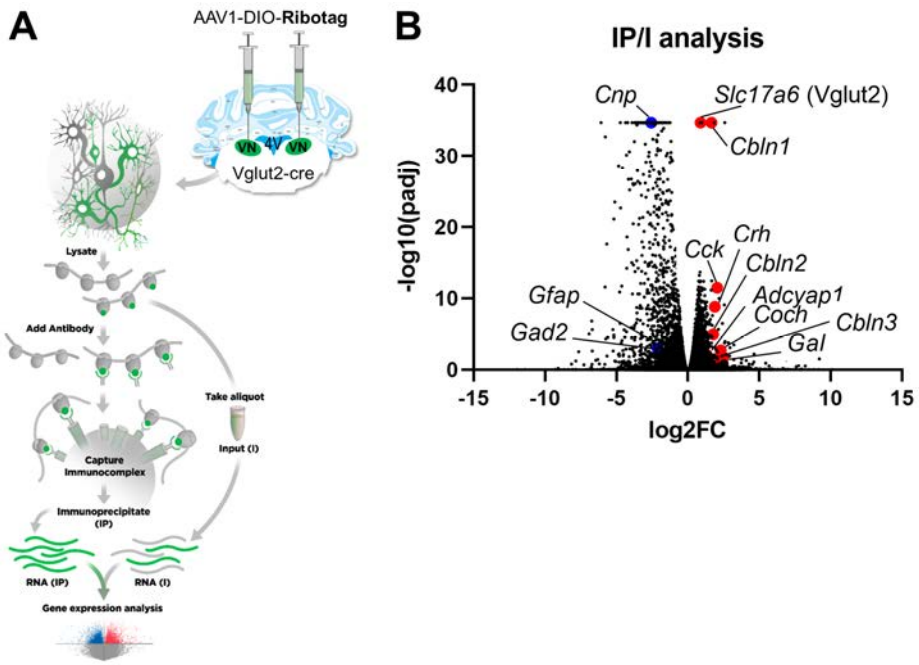

Fig. 10. – Identification of enriched transcripts in VGLUT2^{VN} neurons by RiboTag-based array. A) Vglut2-cre mice (n=3) are bilaterally injected in the VN with AAV expressing a CRE-dependent Ribotag construct, followed by immunoprecipitation of ribosome-bound

transcripts using anti-HA antibody-attached magnetic beads and subsequent gene expression analyses. B) Differential microarray analysis revealed significant enrichment for candidate VGLUT2^{VN} neuron subpopulation markers such as *Cck*, *Crh*, *Adcyap1*, *Gal*, *Coch*, *Cbln1*, *Cbln2* and *Cbln3*, while confirmed specific enrichment for *Slc17a6* (VGLUT2), and confirming depletion for inhibitory neuron (*Gad2*) and non-neuronal markers (*Cnp*, *Gfap*) in the RiboTag IPs.

5.4. CCK^{VN} neuron activation is sufficient to induce MS-like autonomic responses

Among the enriched genes found in VGLUT2^{VN} neurons, brainstem *Cck* expression was found to be highly restricted to the VN region (Ng et al., 2009). Interestingly, CCK has been shown to be involved in nausogenic responses (Feinle et al., 2000; Pilichiewicz et al., 2006). Thus, we took advantage of a commercialy-available Cck-cre mouse line (Taniguchi et al., 2011) to characterize the role of CCK^{VN} neurons in MS. To this end, we applied the same optogenetic approach as in section 5.2, using Cck-cre mice instead of Vglut2-cre mice (Fig. 11A). After behavioral testing, animals were euthanized and histologically processed, confirming correct targeting of CCK^{VN} neurons, as well as proper fiber optic placement (Fig. 11B). Also, absence of somatic labeling in neighboring CCK-positive areas such as the NTS was checked (Fig. 11C).

Behaviorally, optogenetic activation of CCK^{VN} neurons led to a significant and prolonged decrease in spontaneous ambulatory activity in the OF test in the ChR2 group compared to the control animals (Fig. 11D). Similarly, food intake was significantly decreased after photostimulation of CCK^{VN} neurons, showing a

complete intake suppression during 35 min, while control animals engaged in feeding almost immediately (Fig. 11E). Along the same lines, CCK^{VN} optogenetic stimulation lead to an overt body core temperature drop, reaching a significant decrease of ~4.5°C drop after 22.5 min from light onset, in stark contrast with control mice (Fig. 11F). In global, these results demonstrate that CCK^{VN} neurons are key in controlling MS-like autonomic alteration.

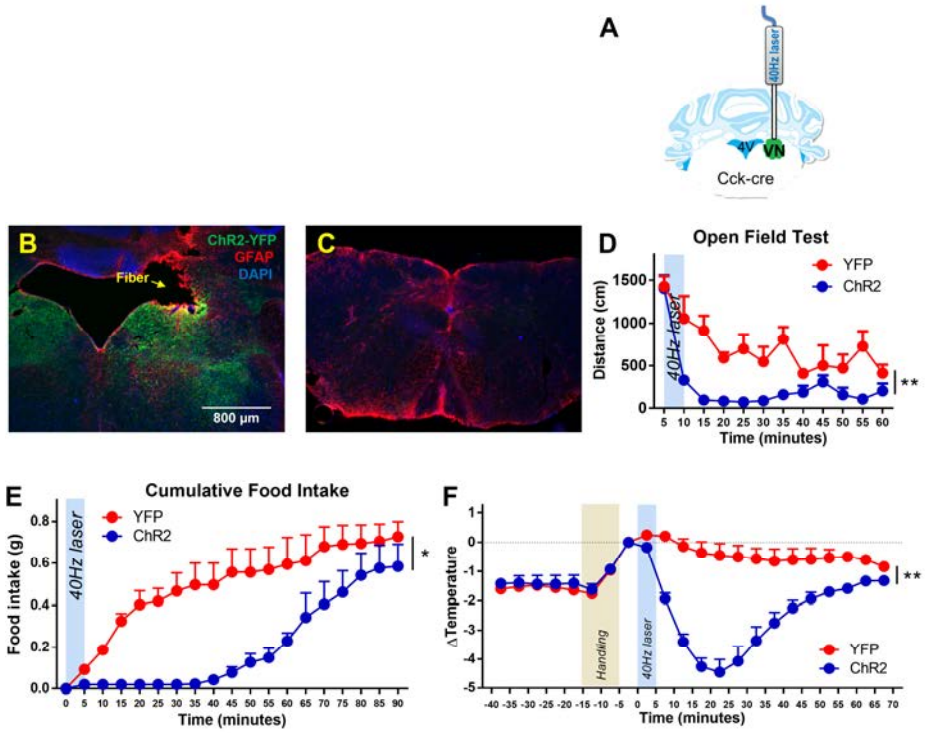

Fig. 11. – Restricted optogenetic activation of CCK^{VN} neurons induces MS-like autonomic responses. A) Cck-cre mice were unilaterally injected in the right VN with AAV1 encoding in a CRE-dependent manner ChR2-YFP or YFP followed by a fiber optic implantation over the right VN to deliver a 5 min, 40 Hz, 10 mW, 10 ms, 473 nm laser stimulation under several freely-moving behavioral tests. B) and C) Fluorescence microscopy images showing either green-

labelled, ChR2-YFP-expressing CCK^{VN} neurons, or absence of CCK^{VN} positive somas in NTS, respectively, after signal amplification by anti-GFP IHC and fiber optic tip placement over the VN by anti-GFAP (red) IHC and DAPI (blue) staining (scale bar: 800 µm). D) Open Field test showing traveled distance before and after photostimulation (ChR2 group n=4; YFP group n=4; two-way ANOVA, P-value<0.01). E) Normal-chow food intake in 24-h-fasted animals before and after light stimulation (ChR2 group n=4; YFP group n=4; two-way ANOVA, P-value<0.05). F) Monitoring of body core temperature along handling and laser stimulation (ChR2 group n=4; YFP group n=4; two-way ANOVA, P-value<0.01).

5.5. $VGLUT2^{VN}$ and CCK^{VN} neurons send dense projections to the PBN

Since optogenetic activation of $VGLUT2^{VN}$ or CCK^{VN} neurons elicited similar behavioral responses, we hypothesized that common projection areas between the two populations would underlie the MS-like responses. Thus, to elucidate the genetically-defined vestibular circuits involved in these responses, Vglut2-cre and Cck-cre mice received a unilateral injection of an AAV1 expressing a CRE-dependent Synaptophysin-GFP construct in the right VN (Fig. 12A and D). Taking advantage of the synaptic tropism of the labeling, we could identify bothunilateral or contralateral projection sites for each neuronal population. VN targeting was confirmed in both *Cre*-expressing lines (Fig. 12B and E). Among the different targeting areas, dense $VGLUT2^{VN}$ - and CCK^{VN} terminals were found in the ipsilateral PBN (Fig. 11C and F), with much less intense contralateral PBN projections (data not shown). In detail, $VGLUT2^{VN}$ projections widely targeted the medial, external-medial, external-lateral, ventral-lateral, central-

lateral parts of the PBN, while CCK^{VN} terminals targeted only the external-lateral and external-medial parts of the PBN. These results indicate the existence of a *Vglut2*- and *Cck*-expressing vestibulo-parabrachial ($CCK^{VN \rightarrow PBN}$) circuit potentially relevant in MS, highlighting the external-lateral and external-medial parts of the PBN.

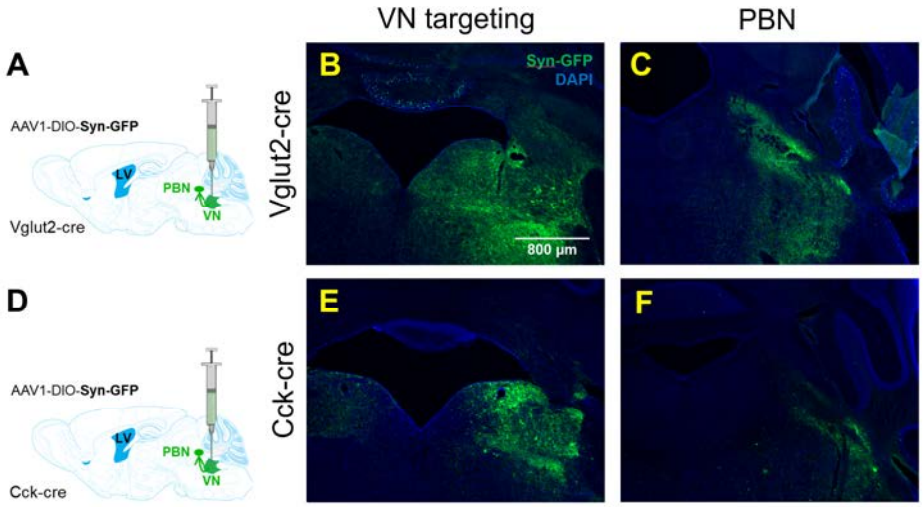

Fig. 12. – $VGLUT2^{VN}$ and CCK^{VN} neurons send dense projections to the ipsilateral PBN. A) Vglut2-cre mice (n=3) were unilaterally injected in the right VN with AAV1 encoding a CRE-dependent Synaptophysin-GFP (AAV-DIO-SynGFP) construct. B and C) Fluorescent microscopy images, respectively showing VN targeting in $VGLUT2^{VN}$ neurons, and $VGLUT2^{VN}$ terminals in the PBN (scale bar: 800 µm). D) Cck-cre mice (n=3) were unilaterally injected in the right VN with AAV1-DIO-SynGFP. E) and F) Fluorescent microscopy images respectively showing VN targeting in CCK^{VN} neurons, and CCK^{VN} terminals in the external-lateral and external-medial parts of the PBN.

5.6. $CCK^{VN→PBN}$ circuit stimulation does not mediate MS-related autonomic responses

To ascertain whether the *Cck*-expressing vestibulo-parabrachial ($CCK^{VN→PBN}$) circuit plays a role in MS-like autonomic regulation, we took advantage of the optogenetic technology to activate CCK^{VN} axon terminals in the PBN by placing the fiber optic tip over the PBN in CCK^{VN} ChR2-expressing neurons (Fig. 13A). After behavioral testing, animals were euthanized and brains were histologically processed by IHC to verify correct ChR2 targeting to the VN and successful location of the fiber optic tip over the PBN (Fig. 13B). We revealed the presence of CCK^{VN} terminals in the NTS, with absence of positive somas, in agreement with our observations in $VGLUT2^{VN}$ and CCK^{VN} connectomic mice (data not shown).

Behaviorally, optogenetic stimulation of $CCK^{VN->PBN}$ fibers did not lead to significant differences in locomotion, food intake and body temperature (Fig. 13D, E and F), revealing that the $CCK^{VN→PBN}$ circuit does not play a role in MS-related autonomic regulation. Nevertheless, significant variability was observed in the autonomic responses, especially for appetite suppression and hypothermia. Thus, further characterization is needed to fully elucidate the involvement of the $CCK^{VN→PBN}$ circuit in MS-like autonomic regulation.

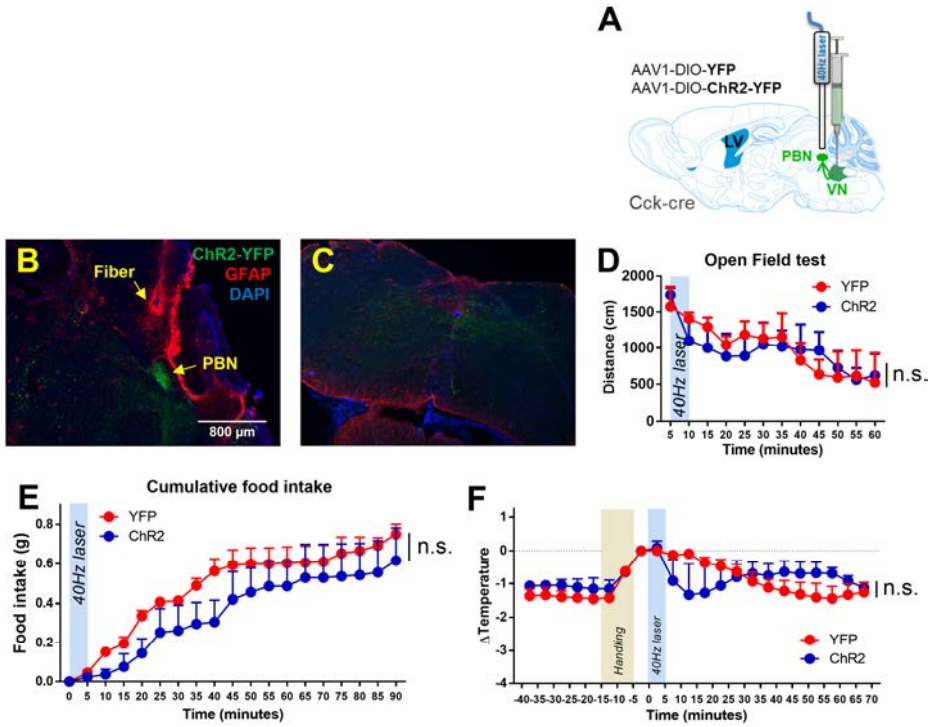

Fig. 13. – Targeted optogenetic activation of the CCK$^{VN→PBN}$ circuit does not induce MS-like autonomic responses. A) Cck-cre mice were subjected to unilateral infusion in the right VN of AAV1 expressing ChR2-YFP or YFP in a CRE-dependent manner and a subsequent fiber optic implantation over the PBN to pursue further behavioral paradigms. B) and C) Fluorescence images of, respectively, a PBN-containing or NTS-containing brain slice subjected to IHC with anti-GFP, anti-GFAP and stained with DAPI, revealing the position of the fiber optic tip over the PBN and presence of CCK^{VN} projections in the NTS (scale bar: 800 µm). D) Locomotor activity in the open field test before and after laser stimulation (ChR2 group n=4; YFP group n=4; two-way ANOVA, P-value>0.05). E) Food intake in food-deprived mice after photostimulation (ChR2 group n=3; YFP group n=3; two-way ANOVA, P-value>0.05). F) Body temperature monitoring during handling and optogenetic stimulation (ChR2 group n=3; YFP group n=4; two-way ANOVA, P-value>0.05).

5.7. A $CCK^{VN \rightarrow PBN}$ circuit stimulation mediates MS-like CTA response

MS is well known to induce a robust conditioned taste aversion (Braun & McIntosh, 1973). Thus, MS has been proposed to be an accidental byproduct of the toxic defense system (Treisman, 1977). Since the PBN has been reported to be required in aversive learning (Agüero et al., 1993) and in particular in MS-like CTA acquisition (Gallo et al., 1999), we aimed at unravelling whether the $CCK^{VN \rightarrow PBN}$ circuit mediates the MS-like CTA establishment. To that end, we adapted a two-bottle-based CTA test developed by the laboratory of Dr. Richard Palmiter (Chen et al., 2018), applying two conditioning sessions pairing a 5%-sucrose solution, in one out of two bottles, to our different scientific paradigms. Mice were habituated to the two-bottle setting prior to all CTA experiments (Fig. 14A).

After pairing the 5%-sucrose solution with rotational or control stimulus, we observed significant differences in the preference of sucrose, with control animals preferring sucrose solution while rotated animals developed an avoidance response to the taste (Fig. 14B), in agreement with the described role of MS establishing a CTA (Braun & McIntosh, 1973).

Strikingly, hM4Di-mediated, $VGLUT2^{VN}$ inhibition prevented rotational stimulus-related CTA acquisition, as the CNO-injected group showed high sucrose preference whereas the Veh-injected group developed an intense sucrose avoidance response (Fig. 14C). Thus, these results reveal that $VGLUT2^{VN}$ neurons are necessary to develop MS-like CTA.

Conversely, pairing of the 5%-sucrose solution to optogenetic activation of VGLUT2^{VN} neurons did not result in significant differences in ChR2 vs. YFP groups (Fig. 14D), revealing that VGLUT2^{VN} neurons are not sufficient to elicit MS-like CTA.

Strikingly, restricted optogenetic activation of the CCK^{VN} subpopulation was sufficient to significantly decrease the sucrose preference when compared to controls (Fig. 14E), indicating that CCK^{VN} neurons are involved in MS-like CTA.

Finally, a targeted optogenetic activation of the CCK$^{VN \rightarrow PBN}$ circuit was also sufficient to elicit a significant decrease of sucrose preference vs. controls (Fig. 14F).

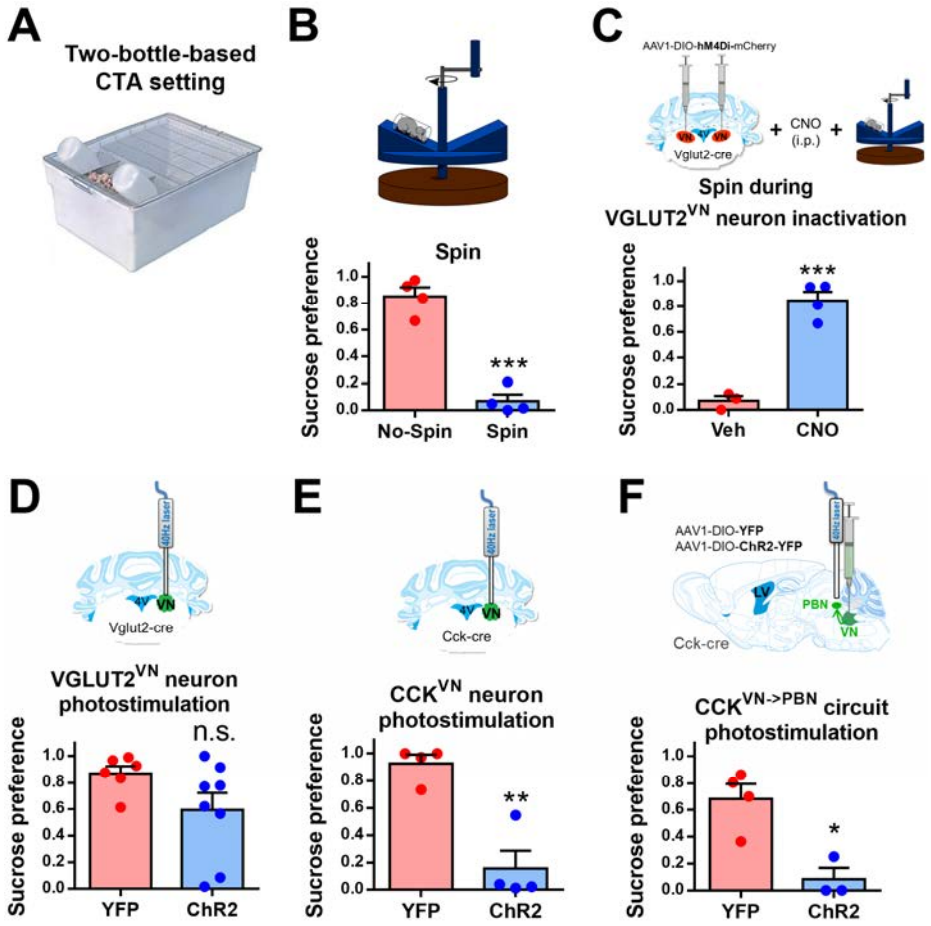

Fig. 14. – Photoactivation of the CCK$^{VN→PBN}$ circuit induces MS-like CTA response. A) Mice were exposed to a two-bottle-based test pairing 5%-sucrose solution to several stimuli or inhibition to functionally characterize the neurobiological regulation of CTA. Evaluation of the establishment of a CTA response after either B) rotational stimulus (Spin group n=4; Spin group n=4; t test, P-value<0.001), C) rotational stimulus under DREADDs-mediated VGLUT2^{VN} neuronal inhibition (hM4Di+CNO group n=4; hM4Di+Veh group n=3; t test, P-value<0.001), D) optogenetic activation of VGLUT2^{VN} neurons (ChR2 group n=8; YFP group n=6; t test, P-value>0.05), E) optogenetic activation of CCK^{VN} neurons (ChR2 group n=4; YFP group n=4; t test, P-value<0.01) or F) targeted optogenetic activation of the CCK$^{VN→PBN}$ circuit (ChR2 group n=3; YFP group n=4; t test, P-value<0.05).

5.8. CCK^{VN} neuron inactivation leads to MS-like autonomic alterations

Our experiments with CCK^{VN} optogenetic activation haves revealed the involvement of this neuronal population in the development of MS-like autonomic responses and MS-related aversive learning. However, whether the activation of these neurons is necessary to these response remains unknown. To this end, we pursued chemogenetic hM4Di-mediated, CCK^{VN} inhibition.

Cck-cre mice expressing bilaterally hM4Di-mCherry in CCK^{VN} neurons —validated by IHC after the tests (Fig. 15A)— were subjected to either CNO or Veh i.p. administrations. 30 min after, a 5-min locomotion period was evaluated in the open field test. Strikingly, CNO-treated group already showed a significant decrease in pre-spin ambulatory activity (Fig. 15B), suggesting CCK^{VN} inhibition *per se* is sufficient to induce locomotor effects. Subsequently, a rotational stimulus was applied to both CNO and Veh groups and a 60 min Open Field test resulted in an additional significant decrease in spontaneous ambulatory activity in the CNO group, with complete loss in the willingness to move, whereas Veh animals were able to recover (Fig. 15C). Body core temperature was also measured after CNO or Veh i.p. injection. In a similar fashion than locomotion, 10 min after injection, temperature started to decrease in the CNO-injected group, yielding significant differences of more than 4°C with Veh-injected mice (Fig. 15D).

Temperature was also separately measured after CNO or Veh injections followed by spinner habituation and rotation stimulus

time periods. In this experiment, temperature again started to drop in CNO animals before spin, again up to approximately 4°C compared to Veh animals. After spin, both groups experienced an additional temperature decrease, revealing an additive effect of rotational stimulation, which suggests that other neurons besides the CCK^{VN} population participate in MS-related temperature response (Fig. 15E).

These results further highlight the requirement of normal CCK^{VN} neuron functioning in MS-like autonomic control, suggesting a key role of these neurons in regulating the conflict in the vestibular system.

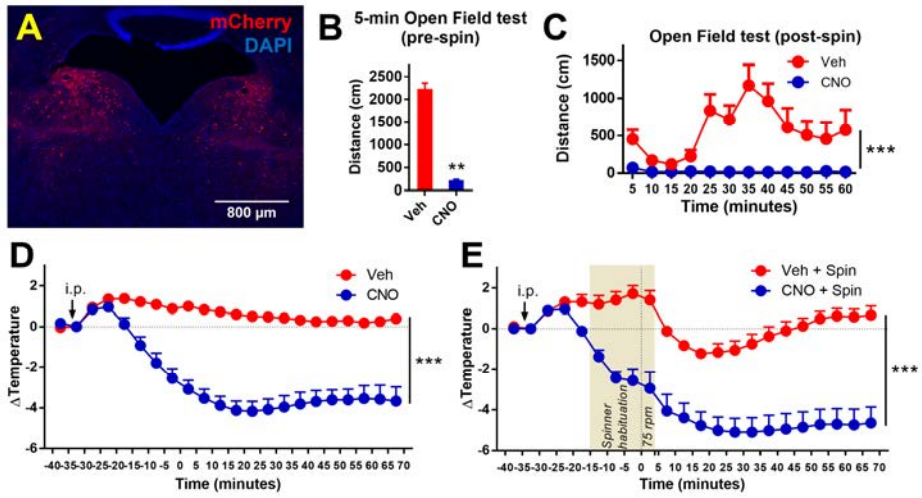

Fig. 15. – Restricted, DREADDs-mediated inhibition of Cck-VN neurons leads to MS-like autonomic responses. Cck-cre mice were subjected to bilateral infusion in the right VN of AAV1 encoding a hM4Di-mCherry construct in a CRE-dependent manner. A) Fluorescent microscopy image of mCherry staining of CCK^{VN}, hM4Di-mCherry-labelled neurons (scale bar: 800 µm). B) 5-min Open Field test before rotational stimulus under the effects of hM4Di-mediated, CNO-triggered, CCK^{VN} neuronal inhibition compared to Veh group (CNO n=4; Veh group

n=4; t test, P-value<0.01). C) 60-min Open Field test after spin stimulation during CCK^{VN} neuronal inhibition (CNO n=4; Veh group n=4; two-way ANOVA, P-value<0.001). D) Body core temperature assessment after CNO or Veh i.p. injection (CNO n=4; Veh group n=4; two-way ANOVA, P-value<0.001). E) Body core temperature monitoring along CNO or Veh i.p. injection and spin stimulation (CNO n=4; Veh group n=4; two-way ANOVA, P-value<0.001).

5.9. CRH^{VN} neurons are not necessary to induce MS-like autonomic responses

Our previous results indicated the synergistic effect of other neuronal populations to the MS-like autonomic responses. Therefore, given the existence of a CRH^{VN} glutamatergic population (Kodama et al., 2012), and our RiboTag results as seen in section 5.3), we carried out a similar paradigm after CRH^{VN} neuronal inhibition. To that end, Crh-cre mice were bilaterally injected in the VN with the same AAV1 encoding hM4Di-mCherry in a CRE-dependent fashion. Both pre-spin 5-min and post-spin 60-min Open Field tests described no significant changes between CNO vs. Veh groups as for ambulatory activity (Fig. 16A and B), indicating CRH^{VN} neurons are not necessary to regulate MS-like decreases in ambulatory activity. Likewise, body core temperature curves match in both CNO and Veh animals (Fig. 16C), indicating CRH^{VN} neurons are not necessary either for controlling the MS-like decrease in body temperature.

In global, DREADDs-mediated CRH^{VN} inhibition serves as an experimental control reinforcing the major role of CCK^{VN} neurons in the neurobiological regulation of, at least, MS-like autonomic functions.

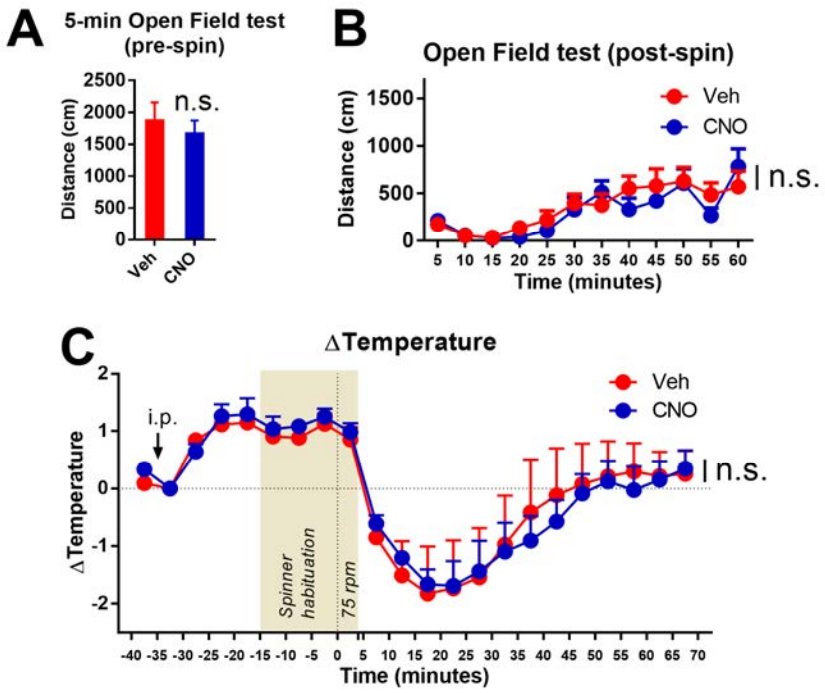

Fig. 16. – Restricted, DREADDs-mediated inhibition of CRH^{VN} neurons does not elicit MS-like responses. Crh-cre mice were subjected to bilateral infusion in the right VN of AAV1 encoding a hM4Di-mCherry construct in a CRE-dependent manner. A) Locomotor activity in a 5-min Open Field test before rotational stimulus under the effects of hM4Di-mediated, CNO-triggered, CRH^{VN} neuronal inhibition compared to Veh controls (CNO n=9; Veh group n=9; t test, P-value>0.05). B) Locomotor activity in a 60-min Open Field test after spin stimulation during CRH^{VN} neuronal inhibition (CNO n=9; Veh group n=9; two-way ANOVA, P-value>0.05). C) Body core temperature measurements along CNO or Veh i.p. administration and spin stimulation (CNO n=4; Veh group n=4; two-way ANOVA, P-value>0.05).

6. DISCUSSION

The vestibular system is classically associated to body balance control, a process that requires the integration of sensory information from proprioception, vision, and vestibular inner ear organs (Money, 1970; Reason, 1978; Treisman, 1977). Alterations of this system can provoke MS, which involves a malaise characterized by hypolocomotion, hypophagia, hypothermia (Money, 1970) and the establishment of a conditioned aversion to novel flavors presented coincidentally (Braun & McIntosh, 1973), mirroring toxic-induced nausea (Treisman, 1977). It is accepted that MS develops with the occurrence of neural mismatches, a conflict between present sensory input and memory retrieved from past, similar motions (Reason, 1978). However, the neurobiological regulation of MS is still poorly understood.

6.1. The crucial role of VGLUT2^{VN} neurons in MS-related autonomic responses and aversive learning

Currently accepted theories posit that the vestibular inner ear organs provide a major input for the subsequent computing comparisons between present sensory input (integrated input including vestibular, visual and proprioceptive information) and memory recalled from similar motion situations experienced in the past (Oman, 1991; Reason, 1978). At the anatomical level, it is known that VN neurons receive input from the vestibular inner ear organs through the VIII cranial nerve and that MS-eliciting provocative motion activates VN neurons (Murakami et al., 2002),

highlighting the relevance of these brainstem regions. Past studies showed that mouse models lacking components of the vestibular inner ear organs, namely the vestibular hair cells (Murakami et al., 2002) or macular otoconia (Fuller et al., 2002), exhibited resilience to MS. Noteworthy, vestibular inner ear input is necessary for the susceptibility of MS and conversely, vestibular stimulations are sufficient to elicit MS (Money, 1970). Thus, the role of the vestibular system in MS is well established in the literature. However, the vestibular-mediated neurobiology of MS has not been well characterized.

The CNS is thought to compute an MS-triggering sensory conflict signal analogously to “toxic shock”, that is, eliciting malaise and nausea (Treisman, 1977). Toxic-related nausea involves the development of malaise appearing after toxic ingestion, leading to autonomic alterations and aversive learning for future avoidance of spoiled food, in the form of a CTA response even hours after ingestion (Bernstein, 1978). As previously stated, these toxic shock-like responses are also observed as a consequence of MS-eliciting provocative motion (Braun & McIntosh, 1973). This analogy is suggested by attributing a role of neurotoxin detector to the vestibular system, since it is a system continuously involved in body orientation in a highly-sensitive manner (Treisman, 1977). In line with this, hallucinogens such as phencyclidine cause activation of at least the LVN (Nabatame et al., 1986). Also, the use of cis-platin, an anti-cancer agent including toxic properties, leads to alteration of the vestibular system, specifically at damaging vestibular hair cells (Ding et al., 2018), while vestibular hair cell loss *in vivo* is known to cause MS-like signs (Murakami et

al., 2002). Thus, in an evolutionary context, MS-alterations could represent a proxy for toxic-induced balance mismatches, and hence, vomiting observed in humans would be a response to evacuate toxics, while nausea would be more oriented either towards immediate defense (appetite suppression to avoid additional toxic ingestion; hypolocomotion and hypothermia to minimize the metabolic rate to fight against already ingested vestibular-affecting neurotoxins) and towards learning avoidance of future risking situations (CTA response). However, despite the relevance of the vestibular system and in particular VN neurons in MS, the genetic identification of MS-controlling VN neurons and the source of the MS-triggering conflict signal in the CNS are lacking.

The physiological correlates for studying MS are a challenge under discussion in the scientific community. The dual nature of MS, that includes nausea (a subjective experience) and vomiting (a reflex), has contributed to the issue. Although MS is highly conserved across animal species, including humans, monkeys, horses, codfish, sheeps, some birds, rats, musk shrews, mice, excluding guinea pigs, rabbits and lower invertebrates (Lychakov, 2012; Ngampramuan et al., 2014; Treisman, 1977; Wei et al., 2011), vomiting cannot be used as a readout of MS in rodent preclinical models since rodents are unable to vomit. Nevertheless, the use of animals susceptible to vomiting, such as musk shrew (Ngampramuan et al., 2014) is not useful either as a readout of nausea, since it is recently becoming accepted that nausea and vomiting represent distinct entities from the neurophysiological and pharmacotherapeutical point of view.

Furthermore, nausea is classically been considered the "neglected symptom", since current therapies are targeted to relieve vomiting or regulate gastrointestinal motility (Horn, 2008; Hornby, 2001; Ngampramuan et al., 2014; Singh et al., 2016). On the other hand, a lack of standardization of MS physiological correlates across experimental designs and differences among animal species including humans have classically hindered the progression in understanding MS neurobiology. Fortunately, mice are susceptible to develop MS-like autonomic alteration and aversive learning (Braun & McIntosh, 1973; Fuller et al., 2002; Murakami et al., 2002; Nalivaiko, 2018), which represent a great advantage due to the existence of well-developed techniques for untangling the *in vivo* involvement of cell type-specific neural substrates and circuitry governing behavioral responses. In conclusion, since the use of vomiting is not suitable for studying nausea, there is a need of standardization of physiological correlates of nausea to study the neurobiology of MS that can be addressed in mice.

Despite the complexity in the study of nausea, different correlates have been studied to provide significant breakthroughs in the characterization of MS. Locomotion, food intake and thermoregulation are consolidated, excellent autonomic MS correlates for preclinical studies in rodents, presenting a characteristic hypolocomotion, hypophagia and hypothermia (Fuller et al., 2002). The thermoregulatory response observed in MS has been pointed as very specific for MS and toxic shock, characterized by hypothermia despite the stressfulness inherent to provocative motion, highly conserved across multiple species

including humans, mice, rats and musk shrews (Nalivaiko, 2018; Nalivaiko et al., 2014; Ngampramuan et al., 2014). It is believed that hypothermia —along with hypolocomotion and hypophagia— may be crucial for survival under intoxications, since it reduces tissue O_2 demand, as seen after LPS (a component of infective, gram-negative bacteria) intoxication (Romanovsky et al., 1997), which would explain the existence of this response in MS under the Treisman's toxic shock evolutionary theory (Treisman, 1977). Furthermore, in agreement with the accepted etiological MS theories, the CTA response is established as an excellent behavioral readout for nausea, albeit its usefulness to evaluate unconditioned responses like the MS-induced autonomic regulation is limited. For studying MS, it is thus needed a behavioral approach addressing multiple MS correlates, since individually they are not sufficient to unravel the neural substrates and circuitry governing MS-related nausea and ultimately to find better anti-MS drugs. Therefore, and to shed light on a genetically-defined vestibular MS circuit, it was critical to establish a robust physiological rotational mouse model enabling the induction and the assessment of physiological correlates of MS.

Rotational models are classically used in the study of the MS (Abe et al., 2010; Fuller et al., 2002; Murakami et al., 2002; Nalivaiko, 2018), since rotations remarkably affect the semicircular canals, which are thought to present a more prominent nauseogenic role and project strongly to the MVN (Paxinos et al., 2012; Previc, 1993, 2018; Watson et al., 2012). However, although these studies have significantly contributed to the study of the MS role of the vestibular system, they used a variety of duration for MS-

inducing stimulus, such as 8 consecutive weeks (Fuller et al., 2002) or 10-40 min (Nalivaiko, 2018). Since MS signs has been reported in mice just after 4 min from stimulus onset (Nalivaiko, 2018), in the present PhD Thesis we have developed a physiological rotational mouse model involving 4 min of by implementing a state-of-the-art technological physiological and behavioral setting enabling for the first time real-time resolution for assessing MS-relevant unconditioned (autonomic) readouts, including locomotion, food intake, thermoregulation, and on the other hand, aversive learning. To this aim, we first built a custom-made rotary device and established the intensity and duration for animal rotations by applying several combinations assessed under OF tests, since they are an excellent and straightforward readout to assess MS-like decrease in ambulatory activity or unwillingness to move.

Hence, we established a stimulus that produced a robust, long-lasting decrease in spontaneous ambulatory locomotion in WT mice when compared to controls, in agreement with past studies showing that WT mice subjected to provocative motion at 2G for 8 weeks developed hypolocomotion (Fuller et al., 2002). Then, our next aim was to expand the model to other established MS-like autonomic and aversive responses in mice, namely appetite suppression and loss of core body temperature (Abe et al., 2010; Fuller et al., 2002; Murakami et al., 2002; Ngampramuan et al., 2014). In agreement with a nauseogenic environment (Money, 1970), the application of this rotational stimulus to specifically-designed behavioral paradigms yielded long-lasting hypophagia and hypothermia accompanying the drop in spontaneous

ambulatory activity. Thus, the observed results can be attributed to a clear MS experience and therefore we consider our model validated to achieve further functionally-relevant interrogations, establishing for the first time robust, real-time methodologies for evaluating the autonomic biomarkers of MS-related nausea. However, as mentioned, since the vomiting reflex is not present in all of these species and since vomiting is assumed to be governed under different circuitries (Horn, 2008; Hornby, 2001; Singh et al., 2016), mouse models present intrinsic limitations. Nevertheless, since MS and its downstream responses are evolutionary conserved across animal species (Lychakov, 2012; Ngampramuan et al., 2014; Treisman, 1977; Wei et al., 2011), our methodologies demonstrate that mice constitute a good preclinical model for further characterizing the role of genetically-identified neural substrates and circuitries in MS.

Excitatory neurons represent the main neuronal source of the VN (Erö et al., 2018). Furthermore, provocative motion activates neurochemically-characterized glutamatergic VN neurons (Cai et al., 2007). Thus, taking into account the predominance of *Slc17a6* (VGLUT2) expression in excitatory hindbrain neurons (Herzog et al., 2001; Kodama et al., 2012) we chose to use a mouse genetics approach to target this neuronal population. First, we considered that a bilateral loss of function approach was required to interrogate the necessity of specific components in the vestibular system. Since unilateral vestibular alterations such as unilateral vestibular loss or caloric stimulations are nauseogenic (Lidvall, 1962), we assumed that a unilateral VN neuronal inhibition would probably trigger an MS-eliciting conflict signal due to vestibular

imbalance rather than revealing the proper function of specific neurons. Consistently, past studies assessing the necessity of specific components of the vestibular system have only been bilaterally targeted, at vestibular inner ear components. For instance, (1) vestibular hair cell loss of function in mice prevents MS-like hypothermic response and abolishment of immediate-early gene *Fos* expression in MVN, PBN, amygdala, paraventricular hypothalamus and locus coeruleus (Murakami et al., 2002), (2) loss of macular otoconia in mice protects from MS-like hypothermia and slightly ameliorates both MS-associated hypolocomotion and hypophagia (Fuller et al., 2002), and (3) bilateral labyrinthectomy in rats induces resistance to MS (Ossenkopp et al., 1994). On the other hand, to achieve sufficient, cell type-specific bilateral neuronal targeting, we opted for a chemogenetic approach since it allows wider neuronal targeting than optogenetics while providing a more sustained neuronal inhibition with the advantage of avoiding fiber optic implantation, which would be incompatible with our physiological rotational model because of the use of fiber optic cables. Hence, to test whether VGLUT2^{VN} neurons are necessary in eliciting MS, we applied a Cre-loxP-dependent chemogenetic approach (Atasoy et al., 2008; Lee & Saito, 1998; Schnütgen et al., 2003; Sternberg & Hamilton, 1981) to inhibit this neuronal population in the context of MS. This represents the first time, to our knowledge, that an *in vivo,* targeted neuronal interrogation approach with cell-type specificity, has been applied to VN neurons for studying MS.

Strikingly, after subjecting these animals to our physiological rotational model under different behavioral tests, we observed a

prevention of MS-related hypolocomotion, hypophagia, hypothermia due to bilateral VGLUT2^{VN} neuronal inhibition, revealing that VGLUT2^{VN} neurons are necessary in MS-like autonomic responses. Hence, our results are in agreement with past studies highlighting the necessity of intact bilateral vestibular inner ear organs to enable MS susceptibility (James, 1881; Money, 1970), since bilateral loss of vestibular function, as happens in bilateral labyrinthectomy, abolishes MS (Ossenkopp et al., 1994). Additionally, these inhibition-related observations further validate our physiological mouse model of MS for additional neuronal interrogation approaches.

In agreement with our results targeting the MVN, recent studies (Previc, 2018) have highlighted the more prominent nauseogenic role of the semicircular canal, sending inputs mainly to the MVN and SVN, as opposed to the otoliths, sending inputs mainly to the LVN and DVN (Previc, 1993). Also, the role of the MVN has been highlighted in another study in rats subjected to provocative motion under the effects of ketanserin administration, a serotonin (5-HT) antagonist that presents anti-MS properties, as evidenced by a significant prevention, after provocative motion, of the MS-like decrease in food intake and MS-associated *Fos* expression in the MVN (Abe et al., 2010).

Besides characterizing the necessity of VGLUT2^{VN} neurons in MS, we continued our characterization by behaviorally addressing the sufficiency of VGLUT2^{VN} neuronal stimulation in eliciting these MS responses. To do so, we applied for the first time in MS field an optogenetic approach activating unilaterally and restrictively

VGLUT2^{VN} neurons in *in vivo* settings. A unilateral approach is sufficient to interrogate the involvement of specific components in the vestibular system, as it is widely known with the nauseogenic studies of vestibular inner ear caloric stimulation (Lidvall, 1962). On the other hand, an optogenetic approach was required to address the sufficiency of specific vestibular neurons or circuits, since a timely-restricted stimulation was necessary to reveal the post-MS recovery while containing the severity of the stimulation in terms of animal well-being. Thus, our results showed that optogenetic activation of VGLUT2^{VN} neurons produced significant and long-lasting decreases in ambulatory activity, food intake and body core temperature. Interestingly, the decrease in food intake, obtained using normal-palatable diet, was not present when using in other cohorts highly-palatable, liquid chocolate drink. Moreover, water intake showed a significant and long-lasting decrease during the normal-palatable diet food intake experiment. Taken together, these results importantly rule out physical impairment for the MS-related hypolocomotion and hypophagia by revealing a relevant motivational component mediating MS. On the other hand, to evaluate the possible contribution to loss of body core temperature due to hypolocomotion, we applied physical-restrain conditions in an additional experiment. We observed the persistence of loss of temperature despite physical restriction, ruling out the contribution of hypolocomotion in temperature reduction. The hypothermic signature observed after optogenetic VGLUT2^{VN} stimulation (3°C) reproduces the one provoked by physiological rotation stimulation (3.5-4°C), with a swift decrease during around 20 min, despite the stressfulness of the rotation.

This signature has been reported as specific for MS across animal species (Nalivaiko, 2018; Nalivaiko et al., 2014; Ngampramuan et al., 2014).

In global, our observations suggest that VGLUT2^{VN} neurons are either encoding the MS-eliciting conflict signal aroused upon discordances between present sensory inputs and sensory memory retrieved from similar past situations, or alternatively these neurons are necessary neural substrates of a larger neural system devoted to the computation of the MS-eliciting mismatch signal. Thus, our results unravel for the first time with genetically-defined resolution a role for excitatory VN neurons controlling MS.

6.2. Identification of VGLUT2 (*Slc17a6*)-expressing vestibular neuronal subpopulations

Excitatory *Vglut2*-expressing neurons constitute a vast population in the VN (Erö et al., 2018; Ng et al., 2009), that is organized specialized subsets mediating specific functions yet to be characterized (Kodama et al., 2012). Therefore, we hypothesized it is likely that a concerted contribution of different VGLUT2^{VN} subpopulations drive MS responses. Thus, to dive into the heterogenous diversity of VGLUT2^{VN} neurons for identifying distinct subpopulations, we relied on the RiboTag technology (Sanz et al., 2019, 2015), based on the viral-mediated expression of an Rpl22 ribosomal subunit with a human influenza hemagglutinin HA tag in a CRE-dependent manner (Sanz et al., 2019) to perform a cell-type specific translational profiling in this neuronal population.

By microarray-based differential expression analysis we could provide a comprehensive list of the genes specifically enriched in VGLUT2^{VN}. As expected, *Slc17a6* was among the enriched genes. On the other hand, markers for inhibitory neurons (*Gad1*, *Gad2*) or non-neuronal markers such as *Gfap* and *Cnp*, for astrocytes and oligodendrocytes, respectively, were depleted, thus validating this approach. Among the enriched genes, thus suggestive of glutamatergic markers, we could identify *Cck* (encoding cholecystokinin), *Crh* (encoding corticotropin-releasing hormone), *Adcyap1* (encoding pituitary adenylate cyclase-activating peptide or PACAP), *Gal* (encoding a precursor of galanin and galanin message-associated peptide or GMAP), *Cbln1* (encoding cerebellin 1 precursor), *Cbln2* (encoding cerebellin 2 precursor), *Cbln3* (encoding cerebellin 3 precursor), and *Coch* (cochlin). Among them, according to previous ISH reports, *Cbln1*, *Cbln2, Cbln3* and *Gal* are not restricted to the VN (Ng et al., 2009).

These results are partly in agreement with a previous study addressing the single-cell transcript profiling of VOR-relevant MVN cells using single-cell qRT-PCR, that identified six functionally-relevant categories of main MVN cells types by quantitative profiling analysis of genes encoding 40 ion channels, 5 neurotransmitters and 14 marker gene candidates (Kodama et al., 2012). This study, identified 3 excitatory subpopulations genetically defined as *Crh/Slc17a6*, *Vglut1* (*Slc17a7*, a glutamatergic marker encoding the vesicular glutamate transporter 1)*,* or *Adcyap1,* thus in agreement with our results. However, we could not find *Slc17a7* expression in VGLUT2^{VN} by

microarray. Nevertheless, *Vglut1* expression in the VN is anecdotal (Ng et al., 2009), likely requiring extensive amplification to be detected, thus explaining the difference between the two studies. In line with this unpublished RiboTag-RNAseq studies from our lab suggest VGLUT2^{VN} neurons physiologically co-express *Vglut1* (Prada-Dacasa, in preparation).

Interestingly, Kodama et al., (2012) identified *Cck* expression in both excitatory and inhibitory cell types. Furthermore, in contrast to our results, *Coch* gene was suggested to be a marker for inhibitory neurons rather than in VGLUT2^{VN}. Different possibilities may account for these discrepancies. First, as the authors report, a potential pitfall in their approach is RNA contaminations in the cell-suspension solution during their cell culture harvest (Kodama et al., 2012). Furthemore, the reporter mouse lines used are not restricted to one neurochemical profile, being mixed GABA-glycinergic and glutamatergic-glycinergic (Kodama et al., 2012) thus likely confounding the molecular profile found.

Secondly, these genes show a remarkable anatomical distribution (Kodama et al., 2012). Furthermore, while our RiboTag results point at a predominant VGLUT2/CCK-positive population, the presence of a CCK-positive/VGLUT2-negative population cannot be ruled out. Therefore, it is plausible that differences in sampling may contribute to the observed differences. To this end, a subsequent *in situ* hybridization is undergoing in our laboratory (Urpi-Badell, unpublished observations) to validate the co-expression of *Vglut2* (and *Gad2*) with each one of our relevant markers of VN neurons (*Crh*, *Cck*, *Adcyap1*).

6.3. Characterization of the role of VGLUT2 (*Slc17a6*)-expressing vestibular subpopulations

Our results have revealed genetically-defined, VGLUT2^{VN} subpopulations, such as CCK^{VN}, CRH^{VN} or ADCYAP1^{VN} thus encouraging us towards the characterization of their *in vivo* role in MS. *Cck*, *Crh* and *Adcyap1* all show restricted VN expression (Ng et al., 2009). Among them, CCK is a known anorexigenic gastrointestinal hormone whose presence in plasma is increased along with apolipoprotein AIV (Apo AIV) upon lipid ingestion to regulate satiation (Lo et al., 2014). CCK can be secreted by intestinal endocrine cells, but also they act in the CNS as neuropeptides. Increased plasmatic CCK in conjunction with increased insulin levels –a typical situation occurring during or after meals– can synergistically facilitate insulin interaction with the blood brain barrier (expressing CCK receptors) leading to boosted insulin transport into the brain, contributing to satiation (May, Liu, Woods, & Begg, 2016). Interestingly, CCK has already been linked to lipid-induced nausea in humans, showing a certain correlation between duodenal lipid dose, plasmatic CCK and nausea (Feinle et al., 2000; Pilichiewicz et al., 2006). However, the CCK-related mechanisms mediating MS have not been clarified yet.

6.3.1. The pivotal role of CCK^{VN} neurons in MS regulation

Here, we show that restricted optogenetic activation of CCK^{VN} neurons elicits a decrease in MS-like ambulatory activity, temperature, food intake and the establishment of a CTA

response, similar to rotational and VGLUT2^{VN} optogenetic stimulations, revealing that CCK^{VN} neuronal activation is sufficient to elicit MS-like autonomic responses and aversive learning. Despite past reports linking CCK with nausea (Feinle et al., 2000; Pilichiewicz et al., 2006), we cannot rule out whether the neurotransmission is mediated CCK itself or a different neurotransmitter, such as glutamate. Thus, a local administration of CCK, or CCK antagonist combined with our physiological rotational model of MS, could be applied in the VN to clarify the CCK role in MS.

Strikingly, a DREADDs-mediated, restricted inhibition of CCK^{VN} neurons (with i.p.-administered CNO) before and after rotational stimulation resulted in significant decreases in MS-like ambulatory activity and temperature, even without rotational stimulus. Further analyses are required to inquire about the role of CCK^{VN} inhibition in eliciting MS-like appetite suppression and aversive learning. However, our data clearly show that alterations in the firing rate of these neurons exert a pivotal role in controlling MS-like autonomic responses and likely aversive learning. In this regard, MVN neurons show endogenous, spontaneous pacemaker activity under tight, tonic modulation of both excitatory and inhibitory neurotransmitters, mediated by kynurenate-sensitive glutamate receptors and bicuculline-sensitive $GABA_A$ receptors (Lin et al., 1993). Furthermore, restoration of MVN neurons pacemaking activity has been associated with recovery from laberynthectomy (Ris, Capron, Vibert, Vidal, & Godaux, 2001), hence suggesting that these endogenous rhythmic discharges are pivotal in controlling MS responses. In this regard our histological

validations show that we are targeting the MVN. Thus, it is tempting to speculate that CCK^{VN} neurons may be one of the contributors to this pacemaker activity and that increases or decreases of this rhythmic firing rate lead to MS-like symptoms, a hypothesis that could be revealed with subsequent electrophysiological approaches.

6.4. Diving into the MS-relevant vestibular circuitry

Our results so far had indicated that CCK^{VN} neurons are crucial in MS autonomic regulation. Thus, to further dissect the *Cck*-expressing vestibular circuit controlling the action of CCK^{VN} neurons in MS. In this regard it has been described that intraperitoneal administration of CCK can induce both appetite suppression and *Fos* expression in the paraventricular nucleus, hypothalamic arcuate nucleus, NTS (Lo et al., 2014) and PBN (Essner et al., 2017). Interestingly, neurochemically-characterized, glutamatergic VN neurons project both to the NTS and the PBN, all three nuclei showing *Fos* expression after provocative motion (Cai et al., 2007). Hence, we addressed the identification of the genetically-defined connectomes of $VGLUT2^{VN}$ and CCK^{VN} neurons. By unilaterally expressing Synaptophysin-GFP, a fluorescent protein with axon terminal tropism, with cell-type specificity in $VGLUT2^{VN}$ neurons or CCK^{VN} neurons, we revealed fluorescent signal from both $VGLUT2^{VN}$ and CCK^{VN} neurons in the PBN and NTS (NTS data not shown). Thus, both $VGLUT2^{VN}$ and CCK^{VN} populations project both to the PBN and the NTS, in agreement with previous anatomical reports of

vestibulo-parabrachial and vestibulo-solitary projections (Balaban, 1996; Balaban & Beryozkin, 1994; Cai et al., 2007).

Recently, it has been shown that optogenetic activation of *CamK2a*-expressing neurons the ipsilateral MVN of anesthetized mice in combination with functional magnetic resonance imaging (fMRI) leads to activation in visual, somatosensory, motor and auditory thalamic nuclei along with their associated sensorimotor cortices, and also in high-order cortices and hippocampal regions (Leong et al., 2019). These results, in conjunction with our data, highlight the role of excitatory vestibular neurons as a major sensory mediator in the vestibular system.

The PBN and NTS have been proposed to be common vestibulo-autonomic pathways, highlighting the hypothesis of a evolutionarily conserved vestibulo-autonomic system in mammals (Porter & Balaban, 1997). Consistently, vagal afferent nerves terminating in the NTS cause satiation through CCK 1 receptors (CCK-1R) triggered by Apo AIV and CCK, as demonstrated by the fact that CCK knockout (KO) mice were not susceptible to Apo AIV-mediated appetite suppression, and the milder Apo AIV-induced appetite suppression due to lorglumide (CCK-1R antagonist) administration (Lo et al., 2012). Furthermore, Apo AIV KO mice showed increased sensibility to CCK, whereas CCK and/or Apo AIV satiating effects are milder when CCK-1R antagonists are used either peripherally or locally around the NTS, indicating that CCK-1R in the NTS is key for Apo AIV-induced appetite suppression (Lo et al., 2014). Together, it is evidenced that vagal CCK signaling and an NTS-associated circuitry are

required for CCK-1R activation, revealing the key role of the vagal CCK system in mediating both CCK-induced and Apo AIV-related appetite suppression after high-fat ingestion (Lo et al., 2014). Noteworthy, an excitatory *Cck*-expressing solitary-parabrachial circuit has been shown to mediate appetite suppression (Roman, Derkach, & Palmiter, 2016). Therefore, it is highly likely that a potential *Cck*-expressing vestibulo-solitary circuit may mediate the MS-related appetite suppression.

On the other hand, the PBN is a brain region known to be required in malaise, appetite suppression, lethargy, anxiety (Campos et al., 2017), thermoregulation (Geerling et al., 2016) and CTA (Carter et al., 2015), all typical features present in MS-associated nausea (Money, 1970). As previously discussed, the hypothermic signature has been reported as specific for MS across animal species (Nalivaiko, 2018; Nalivaiko et al., 2014; Ngampramuan et al., 2014). Since we speculate that this hypothermia resembles a transient, orchestrated torpor behavior, known to be mediated by medial and lateral preoptic area neurons (Hrvatin et al., 2020), and since torpor involves decreased metabolic activity, it may fit in the protective feature of the evolutionary theory of MS (Knott, 2015; Takahashi M. et al., 2020; Treisman, 1977). Interestingly, in mice the PBN is known to be activated in warm and cold ambient temperature, with some of these activated PBN neurons sending projections to the preoptic area (Geerling et al., 2016). Thus, these PBN neurons may relay the VN-mediated hypothermia observed in MS. Furthermore, the PBN has been suggested as a center for vertigo and panic association, in line with clinical reports

correlating panic disorder-related and agoraphobia-related anxiety with space and motion malaise (Jacob et al., 1996).

Hence, both the NTS and the PBN, pose potential interests in the dissection of the vestibulo-autonomic connectome. However, since the NTS has been classically associated with vomiting (Horn, 2008; Hornby, 2001; Singh et al., 2016) —which is not useful as a proxy of MS and is not present in rodents, as previously discussed—, we decided to focus on the vestibulo-parabrachial circuit as a potential candidate for MS-elicited nausea.

6.4.1. Dissection of a $CCK^{VN \rightarrow PBN}$ circuit controlling MS-triggered aversive learning

Taking advantage of optogenetic technology that allows the expression of ChR2 in axon terminals, we addressed the role of the $CCK^{VN \rightarrow PBN}$ pathway by localized stimulation of the parabrachial terminals of CCK^{VN} neurons, *in vivo* settings. $CCK^{VN \rightarrow PBN}$ stimulation did not affect the ambulatory activity, food intake and temperature of the mice, suggesting that the $CCK^{VN \rightarrow PBN}$ circuit does not mediate in MS-like autonomic regulation. Histological validations confirmed the restricted stereotaxic targeting for ChR2 expression in the VN of $CCK^{VN \rightarrow PBN}$ optoPBN mice, thus excluding the possibility of off-target stimulation of solitary-parabrachial terminals. However, we observed significant variability between stimulated animals. Hence, since the PBN has been reported to be involved in both appetite suppression (Carter et al., 2013) and thermoregulation

(Geerling et al., 2016), further characterization of the $CCK^{VN \rightarrow PBN}$ circuit is needed to definitively rule out its autonomic involvement.

As mentioned, the PBN is a brain region known to be involved, among others, in malaise (Campos et al., 2017) and CTA (Carter et al., 2015), classical hallmarks in MS (Braun & McIntosh, 1973; Treisman, 1977). Consistently, MS-evoking rotations can establish a CTA (Braun & McIntosh, 1973) while conversely lesions in the PBN lead to the prevention of MS-related CTA establishment by provocative rotations (Gallo et al., 1999), strongly supporting that the PBN sustains MS-triggered CTA.

Hence, we adjusted previously established two-bottle-based CTA methodologies (Chen et al., 2018) by pairing a 5%-sucrose solution to fit in two conditioning sessions to our different experimental paradigms. First of all, rotational stimulus was sufficient to develop a CTA response to the 5%-sucrose solution whereas restricted chemogenetic inhibition of $VGLUT2^{VN}$ neurons prevented MS-like CTA, revealing that $VGLUT2^{VN}$ neurons are necessary to establish an MS-like CTA, further validating our physiological rotational model. On the other hand, photoactivation of $VGLUT2^{VN}$ neurons was not sufficient to elicit an MS-like CTA response. While puzzling, these results may point out at functional variability between $VGLUT2^{VN}$ neurons, with different subpopulations of $VGLUT2^{VN}$ neurons are mediating opposing effects on CTA. While speculative, this could easily be achieved by means of a $VGLUT2^{VN}$-receiving interneuronal inhibitory microcircuitry at the PBN preventing the establishment of MS-like CTA.

Noteworthy, optogenetic activation of CCK^{VN} neurons was sufficient to establish a clear CTA response, revealing that CCK^{VN} neurons are involved in MS-like CTA. In this regard, targeted optogenetic activation of $CCK^{VN \rightarrow PBN}$ fibers was sufficient to mimic CCK^{VN} MS-like CTA response. Although previous anatomic studies showed that the PBN and the VN are bidirectionally connected (Balaban, 1996, 2004), and that the PBN is necessary for developing an MS-like CTA (Braun & McIntosh, 1973), a VN role in CTA had not been described. Thus, we have established for the first time a physiologic link between MS-like CTA, VN and PBN, by dissecting a genetically-defined, functionally-relevant vestibulo-parabrachial CCK-expressing circuit crucially controlling selectively MS-triggered aversive learning, providing novel evidence for explaining the resemblance of MS with intoxications, probably by conveying the MS-eliciting conflict signal hypothetically produced in the VN (C. M. Oman, 1990; Treisman, 1977).

In line with this, calcitonin gene-related peptide (*Calca*)-expressing PBN neurons are activated in intoxication situations, namely by systemic administration of lithium chloride (LiCl), an exogenous substance that induces gastric discomfort, or lipopolysaccharide (LPS), an inflammation-inducing component of the bacterial wall, but also by CCK (Essner et al., 2017). Additionally, it has been reported that optogenetic activation of *Calca*-expressing neurons in the external lateral part of the PBN (PBel) is sufficient to elicit a CTA in absence of anorexigenic substances like CCK, whereas silencing of *Calca*-expressing PBel neurons ameliorates LiCl-induced CTA, revealing that these

neurons are involved in the neurobiological regulation of CTA via conveying the required gastrointestinal distress input (Carter et al., 2015). Recent studies have revealed that *Calca*-expressing PBN neurons are not only crucial for eliciting CTA but also for retaining and expressing CTA-related aversive memories (Chen et al., 2018). Thus, the necessity of the PBN for eliciting CTA has already been clearly defined. However, the genetic identification of PBN neurons mediating specifically MS-triggered CTA and a genetically-defined, vestibulo-parabrachial circuit functionally linking MS responses with the Treisman's toxic theory of MS (Treisman, 1977) has not been untangled yet.

While the role of CCK in MS has just begun to be associated, as discussed before, we cannot rule out whether CCK or a different neurotransmitter is mediating, such as glutamate. Noteworthy, a *Cck*-expressing, solitary-parabrachial circuit playing a role in aversive behavior have been previously identified and demonstrated to be excitatory (Roman et al., 2016). However, although the activation of CCK^{NTS} neurons has been reported to be sufficient to induce CTA, the targeted activation of *Cck*-expressing solitary-parabrachial ($CCK^{NTS \rightarrow PBN}$) circuit resulted in aversive contextual avoidance but was not sufficient to induce CTA, suggesting *Calca*-expressing PBN neurons require additional, simultaneous excitatory inputs to be sufficiently activated to induce CTA (Roman, Sloat, & Palmiter, 2017). Hence, we speculate that in MS or intoxication situations the VN may be required to recruit sufficient activation of *Calca*-expressing PBN neurons, through a combination of both a $CCK^{VN \rightarrow PBN}$ and a putative genetically-undefined excitatory vestibulo-solitary

pathway (downstream relaying through the $CCK^{NTS \rightarrow PBN}$ circuit) to elicit not only MS-related or visceral malaise-associated CTA, but also MS-related autonomic responses. However, as previously discussed, NTS has been classically associated with vomiting, which is not present in rodents and therefore cannot be used for studying MS in preclinical models, which finally encouraged us to dissect the role of the vestibulo-parabrachial circuit in MS-elicited CTA.

6.5. A novel, genetically-defined model for vestibular-mediated neurobiological regulation of MS

Taking into consideration all of our observations, I propose the following model for neurobiological regulation of MS (Fig. 16). First, we have revealed that glutamatergic vestibular neurons sustain MS-related autonomic and aversive responses. The specific DREADDs-mediated inhibition of $VGLUT2^{VN}$ neurons in our physiological rotational model demonstrated the necessity of these neurons in enabling MS susceptibility. Even *de visum*, a normal animal behavior was evident despite the MS-triggering provocative motion. We infer that $VGLUT2^{VN}$ neurons are necessary for producing an MS-like conflict, although other nuclei are expected to be contribute in conflict processing. In this sense, the vestibular system is assumed to be governed under the influence of the cerebellum, to refine head position and trunk rotation movements (Watson et al., 2010), with specific influences to the MVN through inputs from the ipsilateral nodulus, uvula,

flocculus and paraflocculus, with a putative projection from the contralateral fastigial nucleus (Highstein et al., 2006).

On the other hand, specific optogenetic activation of VGLUT2^{VN} neurons was sufficient to induce MS-associated autonomic responses but not for the CTA response, which we attribute to the existence of distinct circuits for selectively controlling these responses, with a local inhibitory microcircuitry impeding MS-like CTA establishment. Noteworthy, we revealed a motivational component in MS that somehow override MS-like appetite suppression in presence of highly-palatable, motivating food. Interestingly, it has been reported that the specific stimulation of inhibiting, agouti-related protein (*Agrp*)-expressing hypothalamic terminals in the PBN rescue CCK-induced or LiCl-induced, but not LPS-induced, appetite suppression, suggesting *Agrp*-expressing hypothalamic neurons are sufficient in the homeostatic regulation of feeding by selectively increasing food intake in noninflammatory-related appetite suppression and inhibiting the activity of anorexigenic *Calca*-expressing PBN neurons (Essner et al., 2017). We speculate that this hypothalamic pathway may contribute to the MS-like appetite suppression amelioration.

Furthermore, our results have also established a pivotal role for CCK^{VN} neurons in controlling MS, since both specific DREADDs-mediated silencing and optogenetic-mediated activation elicit MS responses. We attribute this *in vivo* role to a highly precise pacemaker activity that when sufficiently altered either physiologically or under chemogenetic or optogenetic manipulations, triggers MS. This pacemaker activity has been

long reported in MVN neurons and still today is debated for MS etiological theories (Lin et al., 1993; Oman et al., 2014). Subsequent electrophysiological analyses are undergoing to untangle whether $CCK^{VN \rightarrow PBN}$ neurons present such pacemaker activity. Thus, it represents the first time an MS-inducing conflict can be directly elicited through several cell type-specific neuronal manipulations. On the other hand, DREADDs-mediated, restricted inhibition of *Crh*-VN neurons did not elicit or prevented MS-like hypolocomotion or hypothermia while optogenetic activation seems to be sufficient to induce MS-like hypolocomotion, hypophagia and hypothermia (ongoing experiments, data not shown). Therefore, we conclude that *Crh*-VN neurons are mediating MS although they are not necessary for MS and thus we believe they are hierarchically upstream from CCK^{VN} neurons.

The role of $ADCYAP1^{VN}$ neurons has not been interrogated yet. However, the recent availability of an *Adcyap1*^{Cre} mouse line enables this approach as future direction. *Adcyap1* has been clearly associated to the excitatory Vglut2 marker in the MVN (Kodama et al., 2012). Consistently with our Ribotag results and our context of MS, there are previous reports linking CRH with PACAP (encoded by *Adcyap1*). PACAP or pituitary adenylate cyclase-activating polypeptide presents neuromodulatory properties, and it is known that CRH and PACAP cooperate to increase anxiety-like behavior and anorexia in the bed nucleus of the stria terminalis (BNST) (Hammack et al., 2010; Meloni et al., 2016). In line with this, CCK is also expected to play a role in the HPA axis. The paraventricular thalamic nucleus is a brain region that expresses *Fos* during chronically-induced stress. *Cck*-

expressing projections from the lateral PBN, dorsal raphe and periaqueductal gray to the paraventricular thalamic nucleus have been identified acting through CCK-B receptor with a role in chronically-induced but not naive stress, which highlights that chronic stress promote the activation of an additional circuitry for the HPA regulation of stress (Bhatnagar et al., 2000). Although the stressful feature is not included in our model, this promising background enable the future inclusion of the stress field in MS.

Our Ribotag approach robustly identified *Cck*, *Crh* and *Adcyap1* as genes enriched in VGLUT2^{VN} neurons. However, ISH analysis will further validate the co-expression of these markers with *Vglut2* as well as inhibitory markers such as *Gad2*, since CCK^{VN} neurons have been associated with excitatory and inhibitory markers (Kodama et al., 2012). Conversely, performing a Ribotag approach in CCK^{VN} neurons instead of VGLUT2^{VN} neurons will further contribute to the genetic identification of CCK^{VN} neuronal subsets, paving the way to additional, more restricted *in vivo* characterization of specific CCK^{VN} subpopulations in controlling select MS-like responses. Since the vestibular circuit is expected to be highly intertwined, further characterization of GABAergic VN neurons needs to be addressed to complement our model.

As commented before, VGLUT2^{VN} optogenetic activation was not sufficient for eliciting this CTA response while VGLUT2^{VN} silencing prevented it. On the other hand, CCK^{VN} neurons triggers both MS-like autonomic and CTA responses. And strikingly, we dissected a CCK$^{VN \rightarrow PBN}$ circuit selectively eliciting MS-like CTA. Hence, we believe a local microcircuitry is inhibiting the CTA response when

optogenetically activating VGLUT2^{VN} neurons, with opposing neurons rendering null CTA response.

As a final future direction, we propose to assess the MS-relevant role for a putative *Cck*-expressing vestibulo-solitary (CCK$^{VN \rightarrow NTS}$) pathway.

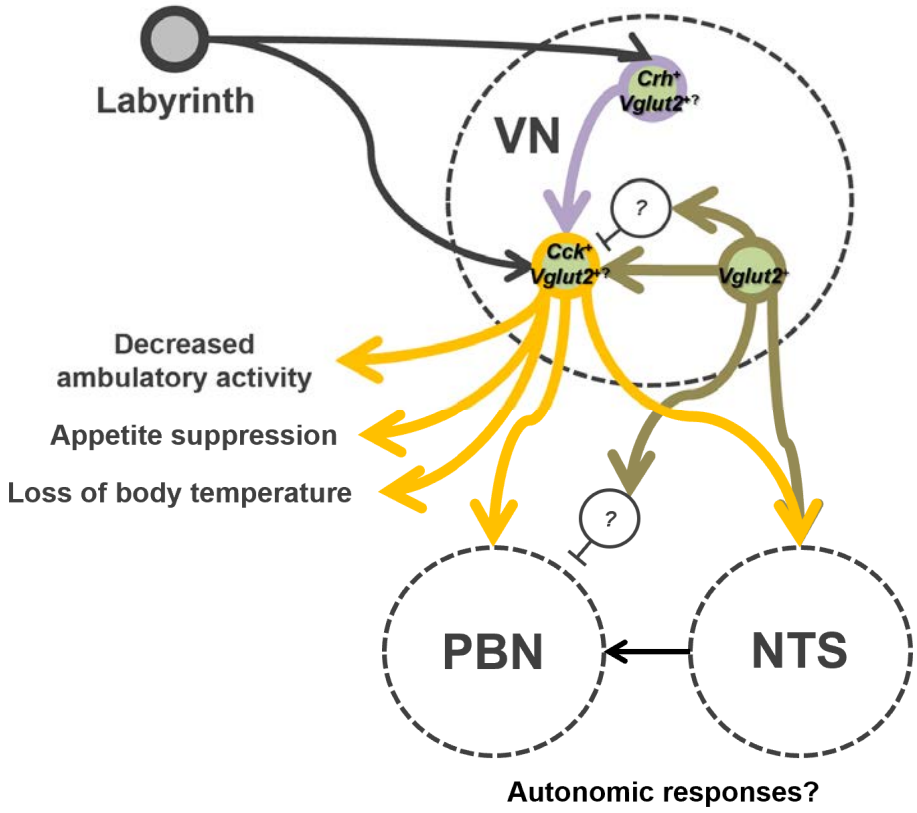

Fig. 16. — A genetically-defined model for vestibular-mediated neurobiological MS regulation.

7. CONCLUSIONS

In light of the results obtained in this PhD Thesis, we can conclude that:

1. Glutamatergic, VGLUT2^{VN} neurons sustain motion sickness-related autonomic regulation and aversive learning, specifically, MS-like hypolocomotion, hypophagia, hypothermia and CTA, as demonstrated by the following facts:

    - Restricted chemogenetic inhibition of VGLUT2^{VN} neurons prevents MS-like autonomic and aversive responses, namely prevention of MS-like hypolocomotion, hypophagia, hypothermia and CTA.

    - Restricted optogenetic activation of VGLUT2^{VN} neurons is sufficient to induce MS-like autonomic responses including hypolocomotion, hypophagia and hypothermia, unlike the aversive response CTA.

2. CCK^{VN}, CRH^{VN} and ADCYAP1^{VN} neurons constitute VGLUT2^{VN} neuronal subpopulations.

3. CCK^{VN} neurons present a pivotal role in controlling, at least, MS-like autonomic regulation, as evidenced by the facts that:

- Restricted optogenetic activation of CCK^{VN} neurons induces MS-like hypolocomotion, hypophagia, hypothermia and CTA.

- Restricted chemogenetic inhibition of CCK^{VN} neurons induces at least MS-like hypolocomotion and hypothermia. Further characterization is needed for elucidating the involvement of CCK^{VN} neuron inhibition in MS-like hypophagia and CTA.

4. Both $VGLUT2^{VN}$ and CCK^{VN} neurons project to the PBN, mainly ipsilaterally.

5. A $CCK^{VN \rightarrow PBN}$ circuit controls MS-like CTA. Further characterization is needed to determine the involvement of this circuit in MS-like autonomic regulation.

6. CRH^{VN} neurons are not necessary to establish MS-like hypolocomotion or hypothermia.

8. REFERENCES

Abe, C., Tanaka, K., Iwata, C., & Morita, H. (2010). Vestibular-mediated increase in central serotonin plays an important role in hypergravity-induced hypophagia in rats. *Journal of Applied Physiology*, *109*(6), 1635–1643. https://doi.org/10.1152/japplphysiol.00515.2010

Agüero, A., Arnedo, M., Gallo, M., & Puerto, A. (1993). The functional relevance of the lateral parabrachial nucleus in lithium chloride-induced aversion learning. *Pharmacology, Biochemistry, and Behavior*, *45*(4), 973–978. https://doi.org/doi:10.1016/0091-3057(93)90150-r

Alexander, G. M., Rogan, S. C., Abbas, A. I., Armbruster, B. N., Pei, Y., Allen, J. A., … Roth, B. L. (2009). Remote Control of Neuronal Activity in Transgenic Mice Expressing Evolved G Protein-Coupled Receptors. *Neuron*, *63*(1), 27–39. https://doi.org/10.1016/j.neuron.2009.06.014

Alhadeff, A. L., Holland, R. A., Nelson, A., Grill, H. J., & De Jonghe, B. C. (2015). Glutamate receptors in the central nucleus of the amygdala mediate cisplatin-induced malaise and energy balance dysregulation through direct hindbrain projections. *Journal of Neuroscience*, *35*(31), 11094–11104. https://doi.org/10.1523/JNEUROSCI.0440-15.2015

Armbruster, B. N., Li, X., Pausch, M. H., Herlitze, S., & Roth, B. L. (2007). Evolving the lock to fit the key to create a family of G protein-coupled receptors potently activated by an inert ligand. *Proceedings of the National Academy of Sciences*, *104*(12), 5163–5168. https://doi.org/10.1073/pnas.0700293104

Atasoy, D., Aponte, Y., Su, H. H., & Sternson, S. M. (2008). A FLEX

switch targets Channelrhodopsin-2 to multiple cell types for imaging and long-range circuit mapping. *The Journal of Neuroscience : The Official Journal of the Society for Neuroscience*, *28*(28), 7025–7030. https://doi.org/10.1523/JNEUROSCI.1954-08.2008

Bagnall, M. W., Stevens, R. J., & Du Lac, S. (2007). Transgenic mouse lines subdivide medial vestibular nucleus neurons into discrete, neurochemically distinct populations. *Journal of Neuroscience*, *27*(9), 2318–2330. https://doi.org/10.1523/JNEUROSCI.4322-06.2007

Balaban, C.D. (2016). Neurotransmitters in the vestibular system. In *Handbook of clinical neurology* (Vol. 137, pp. 41–55). https://doi.org/10.1016/B978-0-444-63437-5.00003-0

Balaban, C D. (1996). Vestibular nucleus projections to the parabrachial nucleus in rabbits: implications for vestibular influences on the autonomic nervous system. *Experimental Brain Research*, *108*(3), 367–381. https://doi.org/doi:10.1007/BF00227260

Balaban, C D. (2004). Projections from the parabrachial nucleus to the vestibular nuclei: potential substrates for autonomic and limbic influences on vestibular responses. *Brain Research*, *996*(1), 126–137. https://doi.org/10.1016/j.brainres.2003.10.026

Balaban, C D, & Beryozkin, G. (1994). Vestibular nucleus projections to nucleus tractus solitarius and the dorsal motor nucleus of the vagus nerve: potential substrates for vestibulo-autonomic interactions. *Experimental Brain Research*, *98*(2), 200–212. https://doi.org/10.1007/bf00228409

Balaban, Carey D. (2003). Vestibular nucleus projections to the

Edinger-Westphal and anteromedian nuclei of rabbits. *Brain Research*, *963*(1–2), 121–131. https://doi.org/10.1016/S0006-8993(02)03955-0

Barnes, C. A. (1988, January 1). Spatial learning and memory processes: the search for their neurobiological mechanisms in the rat. *Trends in Neurosciences*, Vol. 11, pp. 163–169. https://doi.org/10.1016/0166-2236(88)90143-9

Bernstein, I. L. (1978). Learned taste aversions in children receiving chemotherapy. *Science*, *200*(4347), 1302–1303. https://doi.org/10.1126/science.663613

Bertolini, G., & Straumann, D. (2016). Moving in a Moving World: A Review on Vestibular Motion Sickness. *Frontiers in Neurology*, *7*, 14. https://doi.org/10.3389/fneur.2016.00014

Bhatnagar, S., Viau, V., Chu, A., Soriano, L., Meijer, O. C., & Dallman, M. F. (2000). A cholecystokinin-mediated pathway to the paraventricular thalamus is recruited in chronically stressed rats and regulates hypothalamic-pituitary- adrenal function. *Journal of Neuroscience*, *20*(14), 5564–5573. https://doi.org/10.1523/jneurosci.20-14-05564.2000

Borgius, L., Restrepo, C. E., Leao, R. N., Saleh, N., & Kiehn, O. (2010). A transgenic mouse line for molecular genetic analysis of excitatory glutamatergic neurons. *Molecular and Cellular Neuroscience*, *45*(3), 245–257. https://doi.org/10.1016/j.mcn.2010.06.016

Boyden, E. S., Zhang, F., Bamberg, E., Nagel, G., & Deisseroth, K. (2005). Millisecond-timescale, genetically targeted optical control of neural activity. *Nature Neuroscience*, *8*(9), 1263–1268. https://doi.org/10.1038/nn1525

Brand, J. J., & Perry, W. L. M. (1966). Drugs used in motion sickness. A critical review of the methods available for the study of drugs of potential value in its treatment and of the information which has been derived by these methods. *Pharmacological Reviews*, *18*(1), 895–924.

Braun, J. J., & McIntosh, H. (1973). Learned taste aversions induced by rotational stimulation. *Physiological Psychology*, *1*(4), 301–304. https://doi.org/10.3758/BF03326928

Cai, Y.-L., Ma, W.-L., Li, M., Guo, J.-S., Li, Y.-Q., Wang, L.-G., & Wang, W.-Z. (2007). Glutamatergic vestibular neurons express Fos after vestibular stimulation and project to the NTS and the PBN in rats. *Neuroscience Letters*, *417*(2), 132–137. https://doi.org/10.1016/j.neulet.2007.01.079

Campos, C. A., Bowen, A. J., Han, S., Wisse, B. E., Palmiter, R. D., & Schwartz, M. W. (2017). Cancer-induced anorexia and malaise are mediated by CGRP neurons in the parabrachial nucleus. *Nature Neuroscience*, *20*(7), 934–942. https://doi.org/10.1038/nn.4574

Carter, M. E., Han, S., & Palmiter, R. D. (2015). Parabrachial Calcitonin Gene-Related Peptide Neurons Mediate Conditioned Taste Aversion. *Journal of Neuroscience*, *35*(11), 4582–4586. https://doi.org/10.1523/JNEUROSCI.3729-14.2015

Carter, Matthew E., Soden, M. E., Zweifel, L. S., & Palmiter, R. D. (2013). Genetic identification of a neural circuit that suppresses appetite. *Nature*, *503*(7474), 111–114. https://doi.org/10.1038/nature12596

Carter, Matthew E, Han, S., & Palmiter, R. D. (2015). Parabrachial calcitonin gene-related peptide neurons mediate conditioned taste

aversion. *The Journal of Neuroscience : The Official Journal of the Society for Neuroscience*, *35*(11), 4582–4586. https://doi.org/10.1523/JNEUROSCI.3729-14.2015

Carter, Matthew E, Soden, M. E., Zweifel, L. S., & Palmiter, R. D. (2013). Genetic identification of a neural circuit that suppresses appetite. *Nature*, *503*(7474), 111–114. https://doi.org/10.1038/nature12596

Chen, J. Y., Campos, C. A., Jarvie, B. C., & Palmiter, R. D. (2018). Parabrachial CGRP Neurons Establish and Sustain Aversive Taste Memories. *Neuron*, *100*(4), 891-899.e5. https://doi.org/10.1016/j.neuron.2018.09.032

Deisseroth, K. (2011). Optogenetics. *Nature Methods*, *8*(1), 26–29. https://doi.org/10.1038/nmeth.f.324

Di Maio, M., Bria, E., Banna, G. L., Puglisi, F., Garassino, M. C., Lorusso, D., & Perrone, F. (2013, February). Prevention of chemotherapy-induced nausea and vomiting and the role of neurokinin 1 inhibitors: from guidelines to clinical practice in solid tumors. *Anti-Cancer Drugs*, Vol. 24, pp. 99–111. https://doi.org/10.1097/CAD.0b013e328359d7ba

Dieterich, M., Bense, S., Stephan, T., Brandt, T., Schwaiger, M., & Bartenstein, P. (2005). Medial Vestibular Nucleus Lesions in Wallenberg's Syndrome Cause Decreased Activity of the Contralateral Vestibular Cortex. *Annals of the New York Academy of Sciences*, *1039*(1), 368–383. https://doi.org/10.1196/annals.1325.035

Ding, D., Jiang, H., Zhang, J., Xu, X., Qi, W., Shi, H., … Salvi, R. (2018). Cisplatin-induced vestibular hair cell lesion-less damage at high doses. *Journal of Otology*, *13*(4), 115–121.

https://doi.org/10.1016/j.joto.2018.08.002

Eliasen, A., Dalhoff, K., Mathiasen, R., Schmiegelow, K., Rechnitzer, C., Schelde, A. B., … Brok, J. (2020, May 1). Pharmacogenetics of antiemetics for chemotherapy-induced nausea and vomiting: A systematic review and meta-analysis. *Critical Reviews in Oncology/Hematology*, Vol. 149, p. 102939. https://doi.org/10.1016/j.critrevonc.2020.102939

Erö, C., Gewaltig, M.-O., Keller, D., & Markram, H. (2018). A Cell Atlas for the Mouse Brain. *Frontiers in Neuroinformatics*, *12*, 84. https://doi.org/10.3389/fninf.2018.00084

Essner, R. A., Smith, A. G., Jamnik, A. A., Ryba, A. R., Trutner, Z. D., & Carter, M. E. (2017). AgRP Neurons Can Increase Food Intake during Conditions of Appetite Suppression and Inhibit Anorexigenic Parabrachial Neurons. *The Journal of Neuroscience : The Official Journal of the Society for Neuroscience*, *37*(36), 8678–8687. https://doi.org/10.1523/JNEUROSCI.0798-17.2017

Feinle, C., Grundy, D., Otto, B., & Fried, M. (2000). Relationship between increasing duodenal lipid doses, gastric perception, and plasma hormone levels in humans. *American Journal of Physiology - Regulatory Integrative and Comparative Physiology*, *278*(5 47-5). https://doi.org/10.1152/ajpregu.2000.278.5.r1217

Fenno, L., Yizhar, O., & Deisseroth, K. (2011). The development and application of optogenetics. *Annual Review of Neuroscience*, *34*, 389–412. https://doi.org/10.1146/annurev-neuro-061010-113817

Foote, S. L., Berridge, C. W., Adams, L. M., & Pineda, J. A. (1991). Electrophysiological evidence for the involvement of the locus coeruleus in alerting, orienting, and attending. *Progress in Brain*

Research, *88*, 521–532. https://doi.org/10.1016/s0079-6123(08)63831-5

Foubert, J., & Vaessen, G. (2005). Nausea: The neglected symptom? *European Journal of Oncology Nursing*, *9*(1), 21–32. https://doi.org/10.1016/j.ejon.2004.03.006

Fuller, P. M., Jones, T. A., Jones, S. M., & Fuller, C. A. (2002). Neurovestibular modulation of circadian and homeostatic regulation: vestibulohypothalamic connection? *Proceedings of the National Academy of Sciences of the United States of America*, *99*(24), 15723–15728. https://doi.org/10.1073/pnas.242251499

Gallo, M., Marquez, S. L., Ballesteros, M. A., & Maldonado, A. (1999). Functional blockade of the parabrachial area by tetrodotoxin disrupts the acquisition of conditioned taste aversion induced by motion-sickness in rats. *Neuroscience Letters*, *265*(1), 57–60. https://doi.org/doi:10.1016/s0304-3940(99)00209-8

Geerling, J. C., Kim, M., Mahoney, C. E., Abbott, S. B. G., Agostinelli, L. J., Garfield, A. S., … Scammell, T. E. (2016). Genetic identity of thermosensory relay neurons in the lateral parabrachial nucleus. *American Journal of Physiology. Regulatory, Integrative and Comparative Physiology*, *310*(1), R41-54. https://doi.org/10.1152/ajpregu.00094.2015

Gomez, J. L., Bonaventura, J., Lesniak, W., Mathews, W. B., Sysa-Shah, P., Rodriguez, L. A., … Michaelides, M. (2017). Chemogenetics revealed: DREADD occupancy and activation via converted clozapine. *Science (New York, N.Y.)*, *357*(6350), 503–507. https://doi.org/10.1126/science.aan2475

Gradinaru, V., Thompson, K. R., & Deisseroth, K. (2008). eNpHR: a Natronomonas halorhodopsin enhanced for optogenetic

applications. *Brain Cell Biology*, *36*(1–4), 129–139. https://doi.org/10.1007/s11068-008-9027-6

Gradinaru, V., Zhang, F., Ramakrishnan, C., Mattis, J., Prakash, R., Diester, I., … Deisseroth, K. (2010). Molecular and Cellular Approaches for Diversifying and Extending Optogenetics. *Cell*, *141*(1), 154–165. https://doi.org/10.1016/j.cell.2010.02.037

Graybiel, A., & Knepton, J. (1976). Sopite syndrome: a sometimes sole manifestation of motion sickness. *Aviation, Space, and Environmental Medicine*, *47*(8), 873–882.

Graybiel, A., Wood, C. D., Knepton, J., Hoche, J. P., & Perkins, G. F. (1975). Human assay of antimotion sickness drugs. *Aviation, Space, and Environmental Medicine*, *46*(9), 1107–1118.

Graybiel, A., Wood, C. D., Miller, E. F., & Cramer, D. B. (1968). Diagnostic criteria for grading the severity of acute motion sickness. *Aerospace Medicine*, *39*(5), 453–455. Retrieved from http://www.ncbi.nlm.nih.gov/pubmed/5648730

Hammack, S. E., Roman, C. W., Lezak, K. R., Kocho-Shellenberg, M., Grimmig, B., Falls, W. A., … May, V. (2010, November). Roles for pituitary adenylate cyclase-activating peptide (PACAP) expression and signaling in the bed nucleus of the stria terminalis (BNST) in mediating the behavioral consequences of chronic stress. *Journal of Molecular Neuroscience*, Vol. 42, pp. 327–340. https://doi.org/10.1007/s12031-010-9364-7

Hasselmo, M. E., Anderson, B. P., & Bower, J. M. (1992). Cholinergic modulation of cortical associative memory function. *Journal of Neurophysiology*, *67*(5), 1230–1246. https://doi.org/10.1152/jn.1992.67.5.1230

Hasselmo, Michael E., & Bower, J. M. (1993). Acetylcholine and

memory. *Trends in Neurosciences*, Vol. 16, pp. 218–222. https://doi.org/10.1016/0166-2236(93)90159-J

Haupts, U., Tittor, J., Bamberg, E., & Oesterhelt, D. (1997). General concept for ion translocation by halobacterial retinal proteins: The isomerization/switch/transfer (IST) model. *Biochemistry*, *36*(1), 2–7. https://doi.org/10.1021/bi962014g

Held, R. (1961). Exposure-history as a factor in maintaining stability of perception and coordination. *The Journal of Nervous and Mental Disease*, *132*, 26–32. Retrieved from http://www.ncbi.nlm.nih.gov/pubmed/13713070

Herbert, H., Moga, M. M., & Saper, C. B. (1990). Connections of the parabrachial nucleus with the nucleus of the solitary tract and the medullary reticular formation in the rat. *The Journal of Comparative Neurology*, *293*(4), 540–580. https://doi.org/10.1002/cne.902930404

Herzog, E., Bellenchi, G. C., Gras, C., Bernard, V., Ravassard, P., Bedet, C., … El Mestikawy, S. (2001). The existence of a second vesicular glutamate transporter specifies subpopulations of glutamatergic neurons. *The Journal of Neuroscience : The Official Journal of the Society for Neuroscience*, *21*(22). https://doi.org/10.1523/jneurosci.21-22-j0001.2001

Highstein, S. M., & Holstein, G. R. (2006). The Anatomy of the vestibular nuclei. In *Progress in brain research* (Vol. 151, pp. 157–203). https://doi.org/10.1016/S0079-6123(05)51006-9

Horii, A., Takeda, N., Matsunaga, T., Yamatodani, A., Mochizuki, T., Okakura- Mochizuki, K., & Wada, H. (1993). Effect of unilateral vestibular stimulation on histamine release from the hypothalamus of rats in vivo. *Journal of Neurophysiology*, *70*(5),

1822–1826. https://doi.org/10.1152/jn.1993.70.5.1822

Horii, A., Takeda, N., Mochizuki, T., Okakura-Mochizuki, K., Yamamoto, Y., & Yamatodani, A. (1994). Effects of vestibular stimulation on acetylcholine release from rat hippocampus: An in vivo microdialysis study. *Journal of Neurophysiology*, *72*(2), 605–611. https://doi.org/10.1152/jn.1994.72.2.605

Horn, C. C. (2008). Why is the neurobiology of nausea and vomiting so important? *Appetite*, *50*(2–3), 430–434. https://doi.org/10.1016/j.appet.2007.09.015

Hornby, P. J. (2001). Central neurocircuitry associated with emesis. *American Journal of Medicine*, *111*(8 suppl. 1), 106–112. https://doi.org/10.1016/s0002-9343(01)00849-x

Hrvatin, S., Sun, S., Wilcox, O. F., Yao, H., Lavin-Peter, A. J., Cicconet, M., … Greenberg, M. E. (2020). Neurons that regulate mouse torpor. *Nature*, 1–7. https://doi.org/10.1038/s41586-020-2387-5

Irwin, J. A. (1881). The pathology of sea-sickness. *The Lancet*, *118*(3039), 907–909. https://doi.org/10.1016/S0140-6736(02)38129-7

Jacob, R. G., Furman, J. M., Durrant, J. D., & Turner, S. M. (1996). Panic, agoraphobia, and vestibular dysfunction. *American Journal of Psychiatry*, *153*(4), 503–512. https://doi.org/10.1176/ajp.153.4.503

James W. (1881). The sense of dizziness in deaf-mutes. https://doi.org/10.1093/mind/os-VI.23.412.

Kaufman, G. D., Anderson, J. H., & Beitz, A. J. (1992). Fos-defined activity in rat brainstem following centripetal acceleration. *The*

Journal of Neuroscience : The Official Journal of the Society for Neuroscience, *12*(11), 4489–4500. https://doi.org/10.1523/JNEUROSCI.12-11-04489.1992

Knott, G. (2015, February 12). Neurodegeneration: Cold shock protects the brain. *Nature*, Vol. 518, pp. 177–178. https://doi.org/10.1038/nature14195

Kodama, T., Guerrero, S., Shin, M., Moghadam, S., Faulstich, M., & du Lac, S. (2012). Neuronal classification and marker gene identification via single-cell expression profiling of brainstem vestibular neurons subserving cerebellar learning. *Journal of Neuroscience*, *32*(23), 7819–7831. https://doi.org/10.1523/JNEUROSCI.0543-12.2012

Kohl, R. L. (1983). Sensory conflict theory of space motion sickness: an anatomical location for the neuroconflict. *Aviation, Space, and Environmental Medicine*, *54*(5), 464–465.

Kohl, R. L., Calkins, D. S., & Mandell, A. J. (1986). Arousal and stability: the effects of five new sympathomimetic drugs suggest a new principle for the prevention of space motion sickness. *Aviation, Space, and Environmental Medicine*, *57*(2), 137–143.

Kohl, R. L., & Homick, J. L. (1983). Motion sickness: a modulatory role for the central cholinergic nervous system. *Neuroscience and Biobehavioral Reviews*, *7*(1), 73–85. https://doi.org/10.1016/0149-7634(83)90008-8

Lee, G., & Saito, I. (1998). Role of nucleotide sequences of loxP spacer region in Cre-mediated recombination. *Gene*, *216*(1), 55–65. https://doi.org/10.1016/s0378-1119(98)00325-4

Leong, A. T. L., Gu, Y., Chan, Y. S., Zheng, H., Dong, C. M., Chan, R. W., … Wu, E. X. (2019). Optogenetic fMRI interrogation of brain-

wide central vestibular pathways. *Proceedings of the National Academy of Sciences of the United States of America*, *116*(20), 10122–10129. https://doi.org/10.1073/pnas.1812453116

Lidvall, H. F. (1962). Mechanisms of Motion Sickness as Reflected in the Vertigo and Nystagmus Responses to Repeated Caloric Stimuli. *Acta Oto-Laryngologica*, *55*(1–6), 527–536. https://doi.org/10.3109/00016486209127388

Lin, Y., & Carpenter, D. O. (1993). Medial vestibular neurons are endogenous pacemakers whose discharge is modulated by neurotransmitters. *Cellular and Molecular Neurobiology*, *13*(6), 601–613. https://doi.org/10.1007/BF00711560

Lo, C. C., Davidson, W. S., Hibbard, S. K., Georgievsky, M., Lee, A., Tso, P., & Woods, S. C. (2014). Intraperitoneal cck and fourth-intraventricular apo aiv require both peripheral and nts cck1r to reduce food intake in male rats. *Endocrinology*, *155*(5), 1700–1707. https://doi.org/10.1210/en.2013-1846

Lo, C. C., Langhans, W., Georgievsky, M., Arnold, M., Caldwell, J. L., Cheng, S., … Tso, P. (2012). Apolipoprotein AIV requires cholecystokinin and vagal nerves to suppress food intake. *Endocrinology*, *153*(12), 5857–5865. https://doi.org/10.1210/en.2012-1427

Lychakov, D. V. (2012). Motion sickness in lower vertebrates: studies under conditions of weightlessness and under land conditions. *Zhurnal Evoliutsionnoi Biokhimii i Fiziologii*, *48*(6), 613–631. Retrieved from http://www.ncbi.nlm.nih.gov/pubmed/23401973

May, A. A., Liu, M., Woods, S. C., & Begg, D. P. (2016). CCK increases the transport of insulin into the brain. *Physiology and Behavior*, *165*, 392–397.

https://doi.org/10.1016/j.physbeh.2016.08.025

Mehler, W. R. (1983). Observations on the Connectivity of the Parvicellular Reticular Formation with Respect to a Vomiting Center. *Brain, Behavior and Evolution*, *23*(1–2), 63–80. https://doi.org/10.1159/000121489

Meloni, E. G., Venkataraman, A., Donahue, R. J., & Carlezon, W. A. (2016). Bi-directional effects of pituitary adenylate cyclase-activating polypeptide (PACAP) on fear-related behavior and c-Fos expression after fear conditioning in rats. *Psychoneuroendocrinology*, *64*, 12–21. https://doi.org/10.1016/j.psyneuen.2015.11.003

Moga, M. M., Herbert, H., Hurley, K. M., Yasui, Y., Gray, T. S., & Saper, C. B. (1990). Organization of cortical, basal forebrain, and hypothalamic afferents to the parabrachial nucleus in the rat. *The Journal of Comparative Neurology*, *295*(4), 624–661. https://doi.org/10.1002/cne.902950408

Money, K. E. (1970). Motion sickness. *Physiological Reviews*, *50*(1), 1–39. https://doi.org/10.1152/physrev.1970.50.1.1

Morita, M., Takeda, N., Hasegawa, S., Yamatodani, A., Wada, H., Sakai, S. I., … Matsunaga, T. (1990). Effects of anti-cholinergic and cholinergic drugs on habituation to motion in rats. *Acta Oto-Laryngologica*, *110*(3–4), 196–202. https://doi.org/10.3109/00016489009122537

Morita, M., Takeda, N., Kubo, T., & Matsunaga, T. (1988). Pica as an index of motion sickness in rats. *ORL*, *50*(3), 188–192. https://doi.org/10.1159/000275989

Murakami, D. M., Erkman, L., Hermanson, O., Rosenfeld, M. G., & Fuller, C. A. (2002). Evidence for vestibular regulation of

autonomic functions in a mouse genetic model. *Proceedings of the National Academy of Sciences*, *99*(26), 17078–17082. https://doi.org/10.1073/PNAS.252652299

Nabatame, H., Sasa, M., Ohno, Y., Takaori, S., Nabatame, H., & Kameyama, M. (1986). Activation of Lateral Vestibular Nucleus Neurons by Iontophoretically Applied Phencyclidine. *The Japanese Journal of Pharmacology*, *42*(1), 117–122. https://doi.org/10.1254/jjp.42.117

Nalivaiko, E. (2018). Thermoregulation and nausea. In *Handbook of clinical neurology* (Vol. 156, pp. 445–456). https://doi.org/10.1016/B978-0-444-63912-7.00027-8

Nalivaiko, E., Rudd, J. A., & So, R. H. (2014). Motion sickness, nausea and thermoregulation: The “toxic” hypothesis. *Temperature: Multidisciplinary Biomedical Journal*, *1*(3), 164. https://doi.org/10.4161/23328940.2014.982047

Navari, R. M. (2013, March). Management of chemotherapy-induced nausea and vomiting: Focus on newer agents and new uses for older agents. *Drugs*, Vol. 73, pp. 249–262. https://doi.org/10.1007/s40265-013-0019-1

Ng, L., Bernard, A., Lau, C., Overly, C. C., Dong, H.-W., Kuan, C., … Hawrylycz, M. (2009). An anatomic gene expression atlas of the adult mouse brain. *Nature Neuroscience*, *12*(3), 356–362. https://doi.org/10.1038/nn.2281

Ngampramuan, S., Cerri, M., Del Vecchio, F., Corrigan, J. J., Kamphee, A., Dragic, A. S., … Nalivaiko, E. (2014). Thermoregulatory correlates of nausea in rats and musk shrews. *Oncotarget*, *5*(6), 1565–1575. https://doi.org/10.18632/oncotarget.1732

Nishiike, S., Nakamura, S., Arakawa, S., Takeda, N., & Kubo, T. (1996). GABAergic inhibitory response of locus coeruleus neurons to caloric vestibular stimulation in rats. *Brain Research*, *712*(1), 84–94. https://doi.org/10.1016/0006-8993(95)01485-3

Oman, C. (1991). Sensory conflict in motion sickness: an Observer Theory approach. *Pictorial Communication in Virtual and Real Environments*, 362–376. Retrieved from https://ci.nii.ac.jp/naid/10007443135

Oman, C. M. (1990). Motion sickness: a synthesis and evaluation of the sensory conflict theory. *Canadian Journal of Physiology and Pharmacology*, *68*(2), 294–303. https://doi.org/10.1139/y90-044

Oman, C. M., & Cullen, K. E. (2014). Brainstem processing of vestibular sensory exafference: implications for motion sickness etiology. *Experimental Brain Research*, *232*(8), 2483–2492. https://doi.org/10.1007/s00221-014-3973-2

Ossenkopp, K. P. (1983). Area postrema lesions in rats enhance the magnitude of body rotation-induced conditioned taste aversions. *Behavioral and Neural Biology*, *38*(1), 82–96. https://doi.org/10.1016/s0163-1047(83)90414-4

Ossenkopp, K. P., Rabi, Y. J., Eckel, L. A., & Hargreaves, E. L. (1994). Reductions in body temperature and spontaneous activity in rats exposed to horizontal rotation: abolition following chemical labyrinthectomy. *Physiology & Behavior*, *56*(2), 319–324. https://doi.org/10.1016/0031-9384(94)90201-1

Pan, L., Qi, R., Wang, J., Zhou, W., Liu, J., & Cai, Y. (2016). Evidence for a role of orexin/hypocretin system in vestibular lesion-induced locomotor abnormalities in rats. *Frontiers in Neuroscience*, *10*(JUL). https://doi.org/10.3389/fnins.2016.00355

Pavlov, I. P. (2010). Conditioned reflexes: An investigation of the physiological activity of the cerebral cortex. *Annals of Neurosciences*, *17*(3), 136. https://doi.org/10.5214/ans.0972-7531.1017309

Paxinos, G., & Franklin, K. B. J. (2007). *The mouse brain in stereotaxic coordinates* (3rd ed.). Elsevier.

Paxinos, G., Xu-Feng, H., Sengul, G., & Watson, C. (2012). Organization of Brainstem Nuclei. *The Human Nervous System*, 260–327. https://doi.org/10.1016/B978-0-12-374236-0.10008-2

Pilichiewicz, A. N., Little, T. J., Brennan, I. M., Meyer, J. H., Wishart, J. M., Otto, B., … Feinle-Bisset, C. (2006). Effects of load, and duration, of duodenal lipid on antropyloroduodenal motility, plasma CCK and PYY, and energy intake in healthy men. *American Journal of Physiology - Regulatory Integrative and Comparative Physiology*, *290*(3). https://doi.org/10.1152/ajpregu.00606.2005

Porter, J. D., & Balaban, C. D. (1997). Connections between the vestibular nuclei and brain stem regions that mediate autonomic function in the rat. *Journal of Vestibular Research : Equilibrium & Orientation*, *7*(1), 63–76. Retrieved from http://www.ncbi.nlm.nih.gov/pubmed/9057160

Previc, F. H. (1993). Do the organs of the labyrinth differentially influence the sympathetic and parasympathetic systems? *Neuroscience and Biobehavioral Reviews*, *17*(4), 397–404. https://doi.org/10.1016/s0149-7634(05)80116-2

Previc, F. H. (2018). Intravestibular Balance and Motion Sickness. *Aerospace Medicine and Human Performance*, *89*(2), 130–140. https://doi.org/10.3357/AMHP.4946.2018

Quintana, A., Zanella, S., Koch, H., Kruse, S. E., Lee, D., Ramirez, J. M., & Palmiter, R. D. (2012). Fatal breathing dysfunction in a mouse model of Leigh syndrome. *The Journal of Clinical Investigation*, *122*(7), 2359–2368. https://doi.org/10.1172/JCI62923

Reason, J. T. (1978). Motion Sickness Adaptation: A Neural Mismatch Model. *Journal of the Royal Society of Medicine*, *71*(11), 819–829. https://doi.org/10.1177/014107687807101109

Reason, J. T., & Brand, J. J. (1975). *Motion sickness*. Academic Press.

Ris, L., Capron, B., Vibert, N., Vidal, P. P., & Godaux, E. (2001). Modification of the pacemaker activity of vestibular neurons in brainstem slices during vestibular compensation in the guinea pig. *European Journal of Neuroscience*, *13*(12), 2234–2240. https://doi.org/10.1046/j.0953-816X.2001.01603.x

Roman, C. W., Derkach, V. A., & Palmiter, R. D. (2016). Genetically and functionally defined NTS to PBN brain circuits mediating anorexia. *Nature Communications*, *7*. https://doi.org/10.1038/ncomms11905

Roman, C. W., Sloat, S. R., & Palmiter, R. D. (2017). A tale of two circuits: CCKNTS neuron stimulation controls appetite and induces opposing motivational states by projections to distinct brain regions. *Neuroscience*, *358*, 316–324. https://doi.org/10.1016/j.neuroscience.2017.06.049

Romanovsky, A. A., Shido, O., Sakurada, S., Sugimoto, N., & Nagasaka, T. (1997). Endotoxin shock-associated hypothermia. How and why does it occur? *Annals of the New York Academy of Sciences*, *813*, 733–737. https://doi.org/10.1111/j.1749-6632.1997.tb51775.x

Roth, B. L. (2016). DREADDs for Neuroscientists. *Neuron*, *89*(4), 683–694. https://doi.org/10.1016/j.neuron.2016.01.040

Sanz, E., Yang, L., Su, T., Morris, D. R., McKnight, G. S., & Amieux, P. S. (2009). Cell-type-specific isolation of ribosome-associated mRNA from complex tissues. *Proceedings of the National Academy of Sciences*, *106*(33), 13939–13944. https://doi.org/10.1073/pnas.0907143106

Sanz, Elisenda, Bean, J. C., Carey, D. P., Quintana, A., & McKnight, G. S. (2019). RiboTag: Ribosomal Tagging Strategy to Analyze Cell-Type-Specific mRNA Expression In Vivo. *Current Protocols in Neuroscience*, *88*(1). https://doi.org/10.1002/cpns.77

Sanz, Elisenda, Quintana, A., Deem, J. D., Steiner, R. A., Palmiter, R. D., & McKnight, G. S. (2015). Fertility-regulating kiss1 neurons arise from hypothalamic pomc-expressing progenitors. *Journal of Neuroscience*, *35*(14), 5549–5556. https://doi.org/10.1523/JNEUROSCI.3614-14.2015

Schnütgen, F., Doerflinger, N., Calléja, C., Wendling, O., Chambon, P., & Ghyselinck, N. B. (2003). A directional strategy for monitoring Cre-mediated recombination at the cellular level in the mouse. *Nature Biotechnology*, *21*(5), 562–565. https://doi.org/10.1038/nbt811

Schwartz, R. D. (1986). Autoradiographic distribution of high affinity muscarinic and nicotinic cholinergic receptors labeled with [3H]acetylcholine in rat brain. *Life Sciences*, *38*(23), 2111–2119. https://doi.org/10.1016/0024-3205(86)90210-9

Sharma, A. K., Spudich, J. L., & Doolittle, W. F. (2006, November). Microbial rhodopsins: functional versatility and genetic mobility. *Trends in Microbiology*, Vol. 14, pp. 463–469.

https://doi.org/10.1016/j.tim.2006.09.006

Shichida, Y., & Yamashita, T. (2003). Diversity of visual pigments from the viewpoint of G protein activation - Comparison with other G protein-coupled receptors. *Photochemical and Photobiological Sciences*, Vol. 2, pp. 1237–1246. https://doi.org/10.1039/b300434a

Shin, M., Moghadam, S. H., Sekirnjak, C., Bagnall, M. W., Kolkman, K. E., Jacobs, R., … du Lac, S. (2011). Multiple types of cerebellar target neurons and their circuitry in the vestibule-ocular reflex. *Journal of Neuroscience*, *31*(30), 10776–10786. https://doi.org/10.1523/JNEUROSCI.0768-11.2011

Sillitoe, R. V., & Fu, Y. (2012). Cerebellum. *The Mouse Nervous System*, 360–397. https://doi.org/10.1016/B978-0-12-369497-3.10011-1

Singh, P., Yoon, S. S., & Kuo, B. (2016). Nausea: A review of pathophysiology and therapeutics. *Therapeutic Advances in Gastroenterology*, Vol. 9, pp. 98–112. https://doi.org/10.1177/1756283X15618131

Spudich, J. L. (2006, November). The multitalented microbial sensory rhodopsins. *Trends in Microbiology*, Vol. 14, pp. 480–487. https://doi.org/10.1016/j.tim.2006.09.005

Steinbusch, H. W. M. (1991). Distribution of Histaminergic Neurons and Fibers in Rat Brain. *Acta Oto-Laryngologica*, *111*(sup479), 12–23. https://doi.org/10.3109/00016489109121144

Sternberg, N., & Hamilton, D. (1981). Bacteriophage P1 site-specific recombination. *Journal of Molecular Biology*, *150*(4), 467–486. https://doi.org/10.1016/0022-2836(81)90375-2

Takahashi M., T., Sunagawa A., G., Soya, S., Abe, M., Sakurai, K., Ishikawa, K., … Sakurai, T. (2020). A discrete neuronal circuit induces a hibernation-like state in rodents. *Nature*, 1–6. https://doi.org/10.1038/s41586-020-2163-6

Takeda, N, Morita, M., Horii, A., Nishiike, S., Kitahara, T., & Uno, A. (2001). Neural mechanisms of motion sickness. *The Journal of Medical Investigation : JMI*, *48*(1–2), 44–59.

Takeda, Noriaki, Hasegawa, S., Morita, M., & Matsunaga, T. (1993). Pica in rats is analogous to emesis: An animal model in emesis research. *Pharmacology, Biochemistry and Behavior*, *45*(4), 817–821. https://doi.org/10.1016/0091-3057(93)90126-E

Taniguchi, H., He, M., Wu, P., Kim, S., Paik, R., Sugino, K., … Huang, Z. J. (2011). A Resource of Cre Driver Lines for Genetic Targeting of GABAergic Neurons in Cerebral Cortex. *Neuron*, *71*(6), 995–1013. https://doi.org/10.1016/j.neuron.2011.07.026

Treisman, M. (1977). Motion sickness: an evolutionary hypothesis. *Science*, *197*(4302), 493–495. https://doi.org/10.1126/science.301659

Urban, D. J., & Roth, B. L. (2015). DREADDs (Designer Receptors Exclusively Activated by Designer Drugs): Chemogenetic Tools with Therapeutic Utility. *Annual Review of Pharmacology and Toxicology*, *55*(1), 399–417. https://doi.org/10.1146/annurev-pharmtox-010814-124803

Vardy, E., Robinson, J. E., Li, C., Olsen, R. H. J., DiBerto, J. F., Giguere, P. M., … Roth, B. L. (2015). A New DREADD Facilitates the Multiplexed Chemogenetic Interrogation of Behavior. *Neuron*, *86*(4), 936–946. https://doi.org/10.1016/j.neuron.2015.03.065

Vlasov, K., Van Dort, C. J., & Solt, K. (2018). Optogenetics and

Chemogenetics. In *Methods in enzymology* (Vol. 603, pp. 181–196). https://doi.org/10.1016/bs.mie.2018.01.022

von Holst, E. (1954). Relations between the central Nervous System and the peripheral organs. *The British Journal of Animal Behaviour*, *2*(3), 89–94. https://doi.org/10.1016/S0950-5601(54)80044-X

Waespe, W., & Henn, V. (1979). The velocity response of vestibular nucleus neurons during vestibular, visual, and combined angular acceleration. *Experimental Brain Research*, *37*(2), 337–347. https://doi.org/10.1007/BF00237718

Watson, C., Kirkcaldie, M., Paxinos, G., Watson, C., Kirkcaldie, M., & Paxinos, G. (2010). Gathering information–the sensory systems. *The Brain*, 75–96. https://doi.org/10.1016/B978-0-12-373889-9.50006-1

Watson, C., Paxinos, G., & Puelles, L. (2012). The Mouse Nervous System. In *The Mouse Nervous System*. https://doi.org/10.1016/C2009-0-00185-8

Weerts, Aurélie P., Putcha, L., Hoag, S. W., Hallgren, E., Van Ombergen, A., Van de Heyning, P. H., & Wuyts, F. L. (2015). Intranasal scopolamine affects the semicircular canals centrally and peripherally. *Journal of Applied Physiology*, *119*(3), 213–218. https://doi.org/10.1152/japplphysiol.00149.2015

Weerts, Aurelie P., Vanspauwen, R., Fransen, E., Jorens, P. G., Van de Heyning, P. H., & Wuyts, F. L. (2013). Baclofen affects the semicircular canals but not the otoliths in humans. *Acta Oto-Laryngologica*, *133*(8), 846–852. https://doi.org/10.3109/00016489.2013.782615

Wei, X., Wang, Z.-B., Zhang, L.-C., Liu, W.-Y., Su, D.-F., & Li, L.

(2011). Verification of motion sickness index in mice. *CNS Neuroscience & Therapeutics*, *17*(6), 790–792. https://doi.org/10.1111/j.1755-5949.2011.00272.x

Wood, C. D., & Graybiel, A. (1970). A theory of motion sickness based on pharmacological reactions. *Clinical Pharmacology & Therapeutics*, *11*(5), 621–629. https://doi.org/10.1002/cpt1970115621

Yates, B. J., Holmes, M. J., & Jian, B. J. (2000). Adaptive plasticity in vestibular influences on cardiovascular control. *Brain Research Bulletin*, *53*(1), 3–9. https://doi.org/10.1016/s0361-9230(00)00302-6

Yates, B. J., & Miller, A. D. (1994). Properties of sympathetic reflexes elicited by natural vestibular stimulation: implications for cardiovascular control. *Journal of Neurophysiology*, *71*(6), 2087–2092. https://doi.org/10.1152/jn.1994.71.6.2087

Zhang, D., Fan, Z., Han, Y., Lv, Y., Li, Y., & Wang, H. (2016). Triple semicircular canal plugging: a novel modality for the treatment of intractable Meniere's disease. *Acta Oto-Laryngologica*, *136*(12), 1230–1235. https://doi.org/10.1080/00016489.2016.1206966

Zhao, S., Cunha, C., Zhang, F., Liu, Q., Gloss, B., Deisseroth, K., … Feng, G. (2008). Improved expression of halorhodopsin for light-induced silencing of neuronal activity. *Brain Cell Biology*, *36*(1–4), 141–154. https://doi.org/10.1007/s11068-008-9034-7